Development of recombinant human anti-diphtheria toxin neutralizing antibodies for diphtheria therapy

Von der Fakultät für Lebenswissenschaften

der Technischen Universität Carolo-Wilhelmina zu Braunschweig

zur Erlangung des Grades einer

Doktorin der Naturwissenschaften

(Dr. rer. nat.)

genehmigte

D i s s e r t a t i o n

von Esther Veronika Wenzel

aus Rüsselsheim

1. Referent: apl. Professor Dr. Michael Hust
2. Referent: Professor Dr. Stefan Dübel
eingereicht am: 17.12.2018
mündliche Prüfung (Disputation) am: 01.04.2019

Druckjahr 2019

Vorveröffentlichungen der Dissertation

Teilergebnisse aus dieser Arbeit wurden mit Genehmigung der Fakultät für Lebenswissenschaften, vertreten durch den Mentor der Arbeit, in folgenden Beiträgen vorab veröffentlicht:

Publikationen:

Russo, G., Meier, D., Helmsing, S., **Wenzel, E.**, Oberle, F., Frenzel, A. & Hust, M. Parallelized antibody selection in microtiter plates. Phage Display, Ed: Lim, T.S. & Hust, M. Methods Mol Biol. 1701: 273-284 (2018).

Wenzel, E.V., Roth, K.D.R., Russo, G., Fühner, V., Helmsing, S., Frenzel, A. & Hust, M. Antibody selection in solution using biotinylated antigens. Genotype Phenotype Coupling, Ed: Zielonka, S. & Krah, S. Methods Mol Biol. (under revision).

Tagungsbeiträge:

Esther Wenzel: "Fighting pathogens and toxins with human and human-like recombinant antibodies" (Reston, USA: III International Conference on Vaccines Research and Development; 2017)

Esther V. Wenzel, Paul Stickings, Jeffrey Brown, Thea Sesardic, Androulla Efstratiou, Michael Hust: "Development of recombinant human anti-diphtheria toxin neutralizing antibody for diphtheria therapy" (St, Julian's, Malta: European Scientific Conference on Applied Infectious Disease Epidemiology (ESCAIDE); 2018)

Posterbeiträge:

Esther Wenzel, Stefan Dübel and Michael Hust: "Development of recombinant human anti-diphtheria toxin neutralizing antibody for diphtheria therapy", Naunyn-Schmiedeberg's Arch Pharmacol (2017) 390 (Suppl 1):S1 7 –S101 (Heidelberg, Germany: 2nd German Pharm-Tox Summit; 2017)

Esther V. Wenzel, Paul Stickings, Jeffrey Brown, Thea Sesardic, Androulla Efstratiou, Michael Hust: "Generation of recombinant human anti-diphtheria toxin neutralizing antibody to replace equine sera" Poster 88 (Berlin, Germany, 20th International Congress on In Vitro Toxicology (ESTIV2018); 2018)

Table of Contents

Summary

Diphtheria is an infectious disease caused by toxigenic *Corynebacterium* spp. that produce diphtheria toxin (DT). Diphtheria is a significant health problem in countries with poor immunization coverage or disrupted immunization programs. Even in countries where the disease is well controlled, there is a need to maintain a stockpile of therapeutic diphtheria antitoxin (DAT) for management of sporadic or imported cases. Currently, diphtheria is still treated with equine sera in the same way it was treated more than 100 years ago by Emil von Behring.

Antibodies against DT have been generated from immune and naive human antibody gene libraries by phage display. The panning was performed on unnicked DT once classically with DT immobilized on a microtiterplate and once with biotinylated-DT in panning in solution. Among both panning strategies, 660 monoclonal antibodies were selected. The first screening was either for binding of the antibodies against diphtheria toxin or for neutralization of diphtheria toxin in a cell-based assay. In total, 439 antibodies were further characterized in scFv-Fc format regarding neutralization in a cell-based *in vitro* neutralization assay. In this assay, 290 scFv-Fc antibodies showed neutralization potency. The best 35 neutralizing scFv-Fc were sub-cloned into IgG1 format. Three best neutralizing lead candidates were selected, one against each of the three domains of DT. The IgG targeting the receptor binding domain is ewe372-D4 and has a neutralization potency of 446 IU/mg. ewe375-H4 has a neutralization potency of 20.4 IU/mg and binds the catalytic domain and ewe372-F6 binds the translocation domain with a neutralization potency of 2.25 IU/mg. In comparison, neutralization potency of equine DAT is approximately 50 IU/mg. In this study, seven antibodies with a higher neutralization potency then equine DAT were developed, and they all bind the receptor binding domain of diphtheria toxin. In the next step, experiments in a non-lethal guinea pig model were conducted to test *in vivo* protection potency. Possible prospects include further development and testing of these antibodies for clinical application as therapeutic agents against diphtheria toxin.

Zusammenfassung

Diphtherie ist eine Infektionskrankheit, die durch *Corynebacterium* spp. verursacht wird, die das Diphtherie Toxin (DT) produzieren. Diphtherie ist ein großes Gesundheitsproblem in Ländern mit schlechter Impfrate oder beeinträchtigten Impfprogrammen. Selbst in Ländern, in denen die Krankheit gut kontrolliert wird, ist es notwendig, einen Vorrat an therapeutischem Diphtherie-Antitoxin (DAT) für die Behandlung von sporadisch auftretenden oder importierten Fällen zu halten. Diphtherie wird heutzutage immer noch mit Pferdeseren behandelt, wie es vor mehr als 100 Jahren von Emil von Behring entwickelt wurde.

In dieser Arbeit wurden Antikörper gegen DT aus immun- und naiven- menschlichen Antikörpergenbibliotheken durch Phagen Display erzeugt. Das Panning wurde an nativem DT einmal klassisch mit immobilisiertem DT in einer Mikrotiterplatte und einmal mit biotinyliertem DT mit Panning in Lösung durchgeführt. Insgesamt wurden 660 monoklonale Antikörper selektiert. Das erste Screening erfolgte entweder zur Bindung der Antikörper gegen DT oder zur Neutralisierung von DT in einem zell-basierten Assay. Insgesamt wurden 439 Antikörper im scFv-Fc-Format hinsichtlich der Neutralisation in einem zell-basierten *in vitro* Neutralisationstest weiter charakterisiert. In diesem Assay zeigten 290 scFv-Fc-Antikörper eine Neutralisation. Die besten 35 neutralisierenden scFv-Fc wurden in das IgG1-Format kloniert.

Es wurden die drei best neutralisierendsten Kandidaten ausgewählt, einer gegen jede der drei Domänen von DT. Der Antikörper ewe372-D4 bindet an die Rezeptorbindungsdomäne und neutralisiert mit 446 IU/mg. ewe375-H4 bindet die katalytische Domäne und neutralisiert mit 20,4 IU/mg und ewe372-F6 neutralisiert durch Bindung an die Translokationsdomäne mit 2,25 IU/mg. Das polyklonale DAT (Pferdeserum) neutralisiert mit ca. 50 IU/mg. In dieser Studie wurden sieben Antikörper mit einer höheren Neutralisationsrate als Pferde-DAT entwickelt, die alle die Rezeptorbindungsdomäne des Diphtherie Toxins binden. Anschließend folgen Experimente in einem nicht tödlichen Meerschweinchen Modell, um die Protektion *in vivo* zu testen. Die aus dieser Studie stammenden Antikörper können für die klinische Anwendung als Therapie gegen Diphtherie weiterentwickelt werden.

Abbreviations

%	Percent
°C	Degree Celsius
∞	Infinity
A, mA	Ampere, milli-Ampere
Ab, mAb	Antibody, monoclonal antibody
Ag	Antigen
AP	Alkaline phosphatase
APS	Ammonium persulfate
ATP	Adenosin triphosphate
A_x	Absorption at wavelength of x nm
BCIP	5-bromo-4-chloro-3-indolyl-phosphate
BLAST	Basic local alignment search tool
bp, kb	Basepair, kilobase
BSA	Bovine serum albumine
C-domain	Catalytic domain of diphtheria toxin
C. diphtheriae	*Corynebacterium diphtheriae*
CD	Cluster of differentiation
cDNA	Complementary DNA
CDR	Complementary determining region
cfu	Colony forming units
CH	Constant domain of the heavy chain
CIP	Calf intestine phosphatase
CL	Constant domain of the light chain
CO_2	Carbon dioxide
Conj.	Conjugated
CRM197	Cross Reacting Materials 197, non-toxic mutant of DT
Da, kDa	Dalton, kilodalton
ddH_2O	Water with a conductivity of 0.05 µS
DE	Germany
DMF	Dimethylformamide
DMSO	Dimethyl sulfoxide
DNA	Desoxyribonucleic acid
dNTP	Deoxyribonucleotide triphosphate
DT	Diphtheria toxin
DTd	Diphtheria toxoid
E. coli	*Escherichia coli*

e.g.	*Exampli gratia* (lat.) = for example
EC50	Half maximal effective concentration
EDTA	Ethylenediaminetetraacetic acid
ELISA	Enzyme-linked immunosorbent assay
EMEM	Eagle's minimal essential medium
et al.	*Et alii* (lat.) = and others
EXPI	EXPI293F
Fab	Fragment antigen binding
FACS	Fluorescence-activated cell sorting
Fc	Fragment cristallisable/constant
Fig.	Figure
Fv	Fragment variable
g, mg, µg	Gram, milligram, microgram
gIII	M13 minor coat protein III gene
HAL	Human antibody library
HC	Heavy chain
His	Histidin
HRP	Horseradish peroxidase
i.e.	*Id est* (lat.) = that is to say
Ig	Immunglobulin
IMAC	Immobilized metal ion affinity chromatography
IPTG	Isopropyl-β-D-thiogalactopyranosid
IS	International standard
IU	International unit
KOR	Republic Korea
L, mL, µL	Liter, milliliter, microliter
LB	Lysogeny broth
M, mM, nM	Molar, millimolar, nanomolar
m, mm, µm, nm	Meter, millimeter, micrometer, nanometer
MCD (4x)	Minimal cytopathic dose (4 times)
MED50%	Minimum effective dose 50 %
mRNA	Messenger RNA
MTP	Microtiter plate
MTT	3-(4,5-dimethylthiazol-2-yl)-2,5-diphenyltetrazolium bromide
MWCO	Molecular weight cut-off
NAD	Nicotinamide adenine dinucleotide
OD_x	Optical density at wavelength of x nanometer
PAGE	Polyacrylamide gel electrophoresis

PBMC	Peripheral blood mononuclear cell
PBS	Phosphate buffered saline
PCR	Polymerase chain reaction
PEI	Polyethylenimine
pelB	Pectate lyase B leadersequence
pIII	M13 minor coat protein III
PP	Polypropylene
PVDF	Polyvinylidene fluoride
R-domain	Receptor binding domain of diphtheria toxin
RNA	Ribonucleic acid
rpm	Rounds per minute
RT	Room temperature
s, min, h	Second, minute, hour
scFv	Single-chain variable fragment
SDS	Sodium lauryl sulfate
T-domain	Translocation domain of diphtheria toxin
Tab.	Table
TEMED	N,N,N',N'-Tetramethylethylenediamine
tetR	Tetracycline repressor
TMB	Tetramethylbenzidine
TNT	Toxin neutralization test
U	Units
UK	United Kingdom of Great Britain and Northern Ireland
USA	United States of America
UV	Ultraviolet
V	Volt
V gene	Variable region gene
v/v	Volume per volume
VH	Variable domain of heavy chain
VL	Variable domain of light chain
w/v	Weight per volume
WHO	World Health Organization
wt	Wildtype
YT	Yeast tryptone media
α	Anti
Δ	Delta
κ	Kappa light chain
λ	Phage lambda, wave length, lambda light chain

1 Introduction

Antibodies are proteins postulated first in the 19th century. The German physiologist Emil von Behring experimented with blood serum for the treatment of tetanus and diphtheria (Behring and Kitasato 1890). He found that the serum of immunized animals is protective against tetanus, respectively diphtheria toxin. His conclusion was, that the serum contains anti-toxin substances. This serum therapy was a breakthrough for the treatment of diphtheria, especially children, and was awarded 1901 with the first Nobel Prize in physiology or medicine.

In 1897, Paul Ehrlich published the first immunological concept, the side chain theory. He postulated that chemical receptors were produced by blood cells and that these receptors fitted to entering toxins like a key to a lock (key-lock principle). More than 50 years later, the antibody structure was discovered (Edelman and Gally 1964; Porter 1959).

Antibodies are indispensable molecules for research, therapy and diagnostic. The first therapeutic antibody (Orthoclone Okt3) was approved 1986 (Emmons and Hunsicker 1987) and generated by hybridoma technology (Köhler and Milstein 1975). This method of generating antibodies is really time-consuming, expensive and needs the immunization of animals. An *in vitro* alternative method for antibody generation is antibody phage display. Phage display is a powerful tool which offers a rapid, efficient and relatively inexpensive method for developing antibodies independent of any immune system. The first therapeutic antibody developed by phage display (adalimumab) was approved 2003 (Frenzel, Schirrmann, and Hust 2016). Until now (status autumn 2018), 85 therapeutic antibodies have been approved as drug, eleven of which were discovered by phage display, and the number will increase in the next years.

1.1 Antibody

Antibodies are glycoproteins and also known as immunoglobulins (Ig). They are produced by B cells and are found in the blood plasma and extracellular fluids. Antibodies are Y-shaped molecules and have a variable region with two arms for binding and one of the five constant parts that defines the isotype of the antibody. It exists five isotypes of antibodies:

IgA, IgD, IgE, IgG and IgM. Each of these isotypes have a defined role in the immune system. The predominant isotype in the human serum are IgG antibodies, and they are responsible for the immunity against invading pathogens (Murphy et al. 2009).

IgG consist of four polypeptide chains, two identical light and heavy chains (figure 1). The chains are linked by disulfide bridges. The heavy chain of IgG consists of four different regions with different functions. The variable area (VH) represents the N-terminal part of the heavy chain followed by a constant domain (CH1). Responsible for the flexibility is the hinge area. The C-terminal constant domains (CH2 and CH3) mediate activation of complements or binding of effector cells via their Fc receptors. The light chain consists of two domains: the N terminal variable (VL) and the C-terminal constant part (CL1) (Abbas et al. 2015).

A papain digested IgG antibody results in a Fab-format. When removing the constant part of a Fab the smallest fragment with an antigen binding site is generated, a single chain fragment of a variable part (scFv) (figure 1). Here, a peptide linker is needed to stabilize both fragments because the cystein of the constant part is missing that facilitates the formation of a disulfid bond to covalently bind the two constant parts. To obtain a IgG-like format, a Fc-part can be added to the scFv. This bivalent scFv-Fc antibody format shares many properties with IgG (Jäger et al. 2013). These antibody fragment formats can all be generated recombinantly (F. Breitling and Dübel 1997).

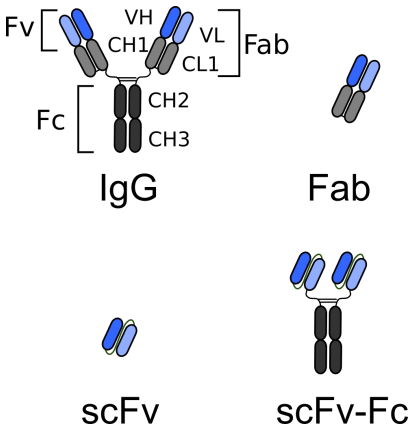

Figure 1: Recombinant antibody formats compared to IgG.

1.2 Antibody phage display technology

Antibody phage display is a key technology to generate antibodies, mainly human antibodies, *in vitro*, independent of the restriction of the immune system (Winter and Milstein 1991). This technology is based on the work of G.P. Smith (Parmley and Smith 1988). The antibody technology was developed independently on three sites in parallel and published 1990/91 by John McCafferty in Cambridge (UK) (McCafferty et al. 1990), by Carlos Barbas III in La Jolla (USA) (Barbas et al. 1991) and by Breitling and Dübel in Heidelberg (DE) (Frank Breitling et al. 1991).

Filamentous phage are used for phage display, because they consist of one circular single strand DNA surrounded by thousands of coat proteins (pVIII). On one side five copies of the protein pVII and pIX are located and on the other side five copies of pIII and pVI. Most common for M13 bacteriophage based systems is the coupling of an antibody fragment to the pIII protein, but also coupling to pVII and pIX are described (Gao et al. 2002; Kwaśnikowski, Kristensen, and Markiewicz 2005). In this pIII system, an antibody-pIII fusion is formed which leads to a coupling of genotype and phenotype (Frank Breitling et al. 1991). For phage display, mainly the single chain fragment variable (scFv) (Hust et al. 2011; Schofield et al. 2007) are used.

When the M13K07 phage is used to package the phagemids, just some particles will carry an antibody-pIII fusion on the surface. The wildtype pIII of M13K07 competes with the fusion-protein pIII encoded on the phagemid. To increase the number of presented antibodies on the phage surface, the so-called hyperphage can be used. Hyperphage is a M13K07ΔpIII phage, where the pIII gene is partial deleted, thus, the phagemid is the only source for functional pIII (Rondot et al. 2001).

1.2.1 Antibody gene libraries

The human germline contains a lot of different genes for the variable region of the heavy and light chain (V gene). The variable region of the heavy chain (VH) locus is on chromosome 14, 1,100 kb long and contains 51 functional VH gene fractions as well as the same number of pseudogenes (Cook and Tomlinson 1995). The variable region of the light chain (VL) locus is on chromosome 22 and at 800 bp 52 V λ genes are located (Frippiat et

al. 1995). All these different VH and VL fused by a short peptide linker are used to develop an antibody gene library.

There are different types of antibody gene libraries, universal and immune libraries. Their usage depends on the scientific or medical application they are constructed for. An immune library is often constructed with the V genes isolated from the blood of infected or immunized volunteers. These libraries are often used in medical research to generate antibodies against a specific target antigen. The isolated V genes are generated with IgG specific primers and contain hypermutations and are affinity matured.

Universal library is a general term to summarize naive, semi-synthetic and synergistic libraries. Universal libraries are developed for isolating antibody fragments that binds to any type of possible antigen. The semi-synthetic library is often constructed with unrearranged V genes from pre B cells (germline cells), where, on the other hand a fully synthetic libraries have a human framework with randomly integrated CDR cassettes. The naive library contains the naive, complete gene repertoire isolated with IgM specific oligonucleotide primer. Often non-immunized volunteers are used to build a naive library (Hust and Dübel 2010).

1.2.2 Panning

The *in vitro* procedure for isolation of these antibody fragments from antibody gene libraries is called panning. During the panning process the antigen can be immobilized to a solid surface such as plastic surfaces with high protein binding capacity like polystyrene microtiter wells (MTPs) (Hust et al. 2002) or magnetic beads (Moghaddam et al. 2003). Another strategy is to select antibodies in solution using biotinylated antigens followed by a pull-down with streptavidin beads (Schütte et al. 2009).

During panning process physical (e.g. temparture), chemical (e.g. pH) and biological (e.g. competitor) parameters are controlled and chosen specifically to bind the wanted antigen. For the selection in solution, the first step is to incubate the antibody phage with the soluble biotinylated antigen before magnetic streptavidin beads are used for the pull-down. A stringent washing is performed subsequently to remove the vast excess of non-binding and weak binding antibody phage. Specifically binding antibodies can be eluted by trypsin

treatment and subsequently used for *E. coli* infection. After adding helperphage, the antigen specific antibody-phage are amplified. This antibody phage can be used for further panning rounds until a significant enrichment of antigen specific antibody phage is achieved. The number of antigen specific antibody phage clones should increase with every panning round.

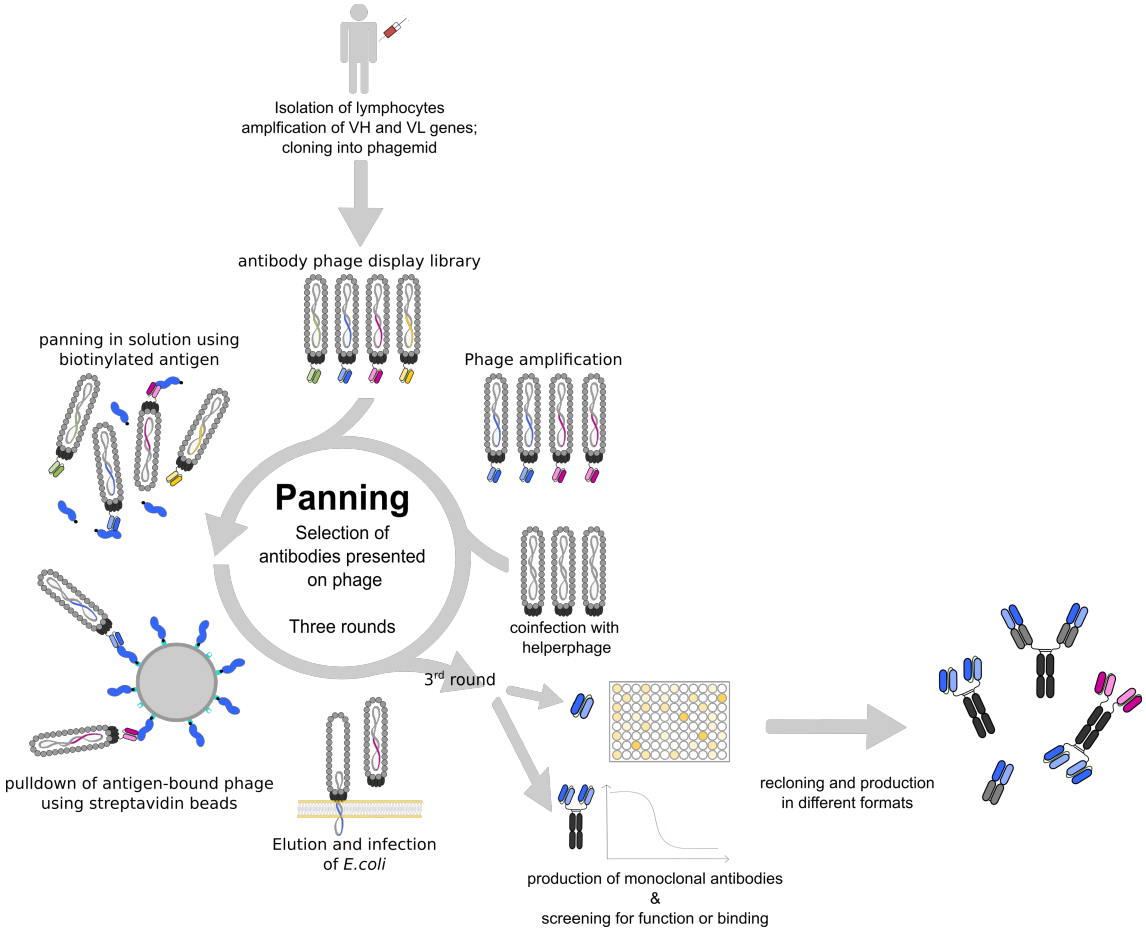

Figure 2: Schematic workflow for panning in solution (adapted from Viola Fühner, TU Bs)

Normally, 2-3 panning rounds are performed to identify monoclonal binding antibody fragments. For screening of monoclonal binders, they are produced as soluble monoclonal antibody fragments. These monoclonal antibodies can be identified by e.g. their binding properties in ELISA (Frenzel et al. 2014) or neutralization properties in cell based neutralization assay. Afterwards, the gene fragments encoding the antibody fragments can be sub-cloned into any other antibody format, e.g. scFv-Fc or IgG (Hust et al. 2011; Hoet et al. 2005; Frenzel et al. 2014; Jäger et al. 2013). A scheme of the selection procedure is given in figure 2.

1.3 Diphtheria

Diphtheria is an infectious disease and mainly caused by a corynebacteriophage bearing *Corynebacterium diphtheriae.* The *C. diphtheriae* is gram-stain-positive, straight or slightly curved rod, frequently swollen at one or both ends (club-shaped), 0.3 – 0.8 µm × 1.0 – 8.0 µm. It is an aerobic bacterium, non spore-forming and non motile. Descriptive cultural types or biovars (= biotypes) of *C. diphtheriae* strains are designated gravis, intermedius, mitis and belfanti. Designations for gravis, intermedius, and mitis were originally given in accordance with the clinical severity of cases from which the different strains were most frequently isolated (Bernard and Funke 2015). The bacterium primarily infects the throat and upper airways. The produced toxin can spread through the bloodstream and affects other organs, such as heart and kidneys. Diphtheria has an acute onset and the main symptoms are sore throat, low fever and swollen glands in the neck. In severe cases, diphtheria toxin may cause myocarditis or peripheral neuropathy. Due to a membrane of dead tissue over the throat and tonsils, swallowing and breathing can be difficult. The disease is spread through direct physical contact or by coughing or sneezing of infected individuals ("WHO | Diphtheria" 2018).

Diphtheria toxin can also be produced by *C. ulcerans* and *C. pseudotuberculosis*. These two stains are less common globally and mostly associated with farm animal contact and dairy products (Sangal et al. 2014; Peel et al. 1997; Mills, Mitchell, and Lim 1997).

1.3.1 Diphtheria toxin

Diphtheria toxin (DT) was the first investigated bacterial protein toxin and has since been the most extensively studied one. Thus, it has served as a model system for the analysis of other protein toxins (Pappenheimer Jr 1977). *Corynebacterium diphtheriae* was identified as the causative agent of diphtheria in 1884 and in 1888 the toxin was first described in the culture medium of *C. diphtheriae* (Roux and Yersin in 1888). The gene for DT is encoded on a corynebacteriophage (Greenfield et al. 1983; Uchida, Gill, and Pappenheimer Jr 1971), and is expressed only under conditions of iron deprivation (Pappenheimer Jr 1977). DT is secreted as a single polypeptide chain of 535 amino acid residues with a molecular weight of 58 kDa (Smith et al. 1980; Kaczorek et al. 1983). Mild trypsinization and

reduction of DT *in vitro* generates two fragments, A and B, which remain covalently attached by an inter-chain disulfide bond (Gill and Pappenheimer 1971). Fragment A contains the enzymatic activity (Collier and Kandel 1971), whereas Fragment B binds the protein to the cell surface receptors and promotes transfer of fragment A to the cytoplasm (Drazin, Kandel, and Collier 1971). DT is composed of three structural domains: the catalytic domain (C) corresponds to fragment A (21 kDa), the transmembrane (T) domain (20 kDa) and receptor binding (R) domain (17 kDa) are included in fragment B (37 kDa) (Figure 3) (Choe et al. 1992).

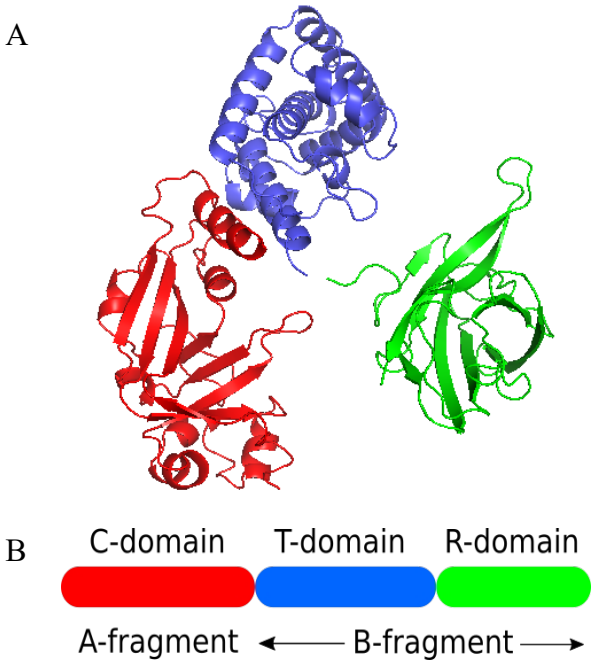

Figure 3: Protein structure of diphtheria toxin with the 3 domains: C-domain (red), T-domain (blue) and R-domain (green). A) crystal structure B) schematic structure.

Diphtheria toxin binds with the receptor binding domain to heparin-binding epidermal growth factor (HP-EGF) on the cell surface of susceptible cells. This binding triggers receptor-mediated endocytosis of the toxin (Dorland, Middlebrook, and Leppla 1979; Morris and Gerstein 1985). Acidic conditions in the endosome leads to a confirmational change and permits the translocation domain of DT to form a channel through the endosomal membrane. Through this channel the C-domain is released into the cytosol

(Draper 1980; Sandvig 1980; Hu and Holmes 1984; Montecucco et al. 1986; Moskaug, Sandvig, and Olsnes 1988; Kagan, Finkelstein, and Colombini 1981). After being delivered into the cytosol, the C-domain catalyzes the NAD^+-dependent ADP-ribosylation of elongation factor 2 (EF-2). EF-2 is the only known substrate for the C-domain in eukaryotic cells and it is involved in protein synthesis (Pappenheimer Jr 1977).

A post-translational modification of a histidine residue in EF-2 (diphthamide) is the known site of action of DT. Here, transfer of an ADP-ribosyl moiety of NAD^+ results in the irreversible arrest of chain elongation during protein synthesis (Collier and Cole 1969). This arrest leads to cell death by apoptosis. (Ratts and Murphy 2012).

DT, especially diphtheria toxoid (DTd), was well studied and characterized and due to its mode of action and immunogenicity. It is a good agent for vaccination. But the detoxification with formaldehyde creates heterogeneous molecules that leads to a purity of diphtheria toxoid of 60 – 70 %. Moreover, DTd can lose its natural structure and epitopes due to formaldehyde treatment (Metz et al. 2003).

An alternative to DTd was Cross Reactive Material 197 (CRM197). Here, the catalytic center of DT was genetic modified by a point mutation (G52E) to a non-toxic DT mutant with same confirmation (Uchida, Pappenheimer, and Harper 1973). Later, it was observed that the conformation of DT and CRM197 is not identical but similar (Bigio et al. 1987; Malito et al. 2012). This CRM197 is nowadays used as vehicle for therapeutic transport in cells or for children as alternative to DTd for vaccination (Shinefield 2010).

1.3.2 Current therapy

In 1890, it was first demonstrated by von Behring and Kitasato that susceptible animals could be immunized with *C. diphtheriae* and the serum of these immunized animals could protect other animals for diphtheria toxin (DT). In 1891, the first child was cured through preparation of a serum from an immunized animal. In 1901, von Behring received the first Nobel Prize in Physiology or Medicine for his development of serum therapy.

In 1923, it was discovered, that DT could be inactivated with formalin without destroying its immunogenicity. This DTd has since been used as vaccine against diphtheria toxin. The vaccine is normally given in combination with other vaccines (e.g. tetanus and/or

pertussis). This vaccination against diphtheria has reduced the mortality and morbidity of diphtheria dramatically, however diphtheria is still a significant health problem in children in countries with poor immunization coverage. Diphtheria is fatal in 5 – 10 % of cases, but children under the age of five have a higher mortality rate of up to 20 %. Treatment involves antibiotic treatment to kill the bacteria (erythromycin or penicillin for 14 days) and administering of diphtheria antitoxin (DAT) to neutralize the effects of the toxin ("Diphtheria | Clinical Features | CDC" 2016). This treatment with DAT, a purified serum from DT-immunized horses, has been the same treatment for more than 100 years now. As DAT is of animal origin, every product batch needs to be tested and screened for the presence of infectious agents. Also, DAT can cause serum sickness in humans. Serum sickness is a type of hypersensitivity reaction, due to proteins derived from the equine serum. The human immune system develops antibodies against foreign antigens from the animal anti-sera which leads to the formation of immune complexes which can precipitate in joints or small vessels, activating the complement cascade and initiating an inflammatory response (Kniker 1968; Jackson 2000). Today, DAT is in scarce supply and frequently unavailable to patients because of discontinued production in several countries (Both et al. 2014). There is an urgent need of an alternative to the equine DAT. Therefore, a new treatment with fully human, monoclonal antibodies is desirable.

1.4 Aim of the work

For therapy of diphtheria an equine serum is still used, like Emil von Behring developed it over 100 years ago. The aim of this work is the generation of recombinant, human anti-diphtheria toxin neutralizing antibodies to replace the equine serum.

The antibody generation will be done with *in vitro* phage display technology. With this technology fully human antibodies can be selected without the need for animal immunization. The developed antibodies will be characterized regarding their binding ability to diphtheria toxin and their neutralization potency. This characterization will be shown in the antibody formats scFv-Fc and IgG. Further, the domains will be mapped to demonstrate against which domain of DT the neutralizing antibodies are binding.

2 Materials and Methods

2.1 Material

2.1.1 Technical equipment and accessories

The equipment used in this study is listed in the following table 1.

Table 1: List of equipment and accessories

Equipment	Name	Supplier
Blot device	Trans-Blot Turbo Transfer	Bio-Rad (München, DE)
ELISA washer	Columbus Pro Columbus Plus Hydrospeed	Tecan (Crailsheim, DE) Tecan (Crailsheim, DE) Tecan (Crailsheim, DE)
ELISA reader	SUNRISE Epoch	Tecan (Crailsheim, DE) BioTek (Bad Friedrichshall, DE)
Electroporation device	Micro Pulser ™	BioRad (München, DE)
Gel documentation	Gel Jet Imager Chemi Doc MP Imaging System	Intas (Göttingen, DE) Bio-Rad (München, DE)
Gel electrophoresis chamber	PerfectBlue Mini S PerfectBlue Mini ExM Mini-Protean 3 Cell	Peqlab (Erlangen, DE) Peqlab (Erlangen, DE) Bio-Rad (München, DE)
Thermomixer	Thermomixer comfort Thermomixer compact Mixing Block MB-102	Eppendorf (Hamburg, DE) Eppendorf (Hamburg, DE) Bioer (Binjiang, CHN)
Incubator	HeraCell (with CO_2) Incubation-shaker Minitron (with CO_2) Incubation-shaker Multitron Certomat BS-1 Incubator BE400 VorTemp 56	Kendro (Langenselbold, DE) Lab Products Infors HT (Einsbach, DE) Infors HT (Einsbach, DE) Satorius (Göttingen, DE) Memmert (Schwabach, DE) Labnet (Austin, USA)
Power supply	EPS 301/601	Amersham Pharmacia (Freiburg, DE)
Thermocycler	PTC-200	MJ Research (Waltham, USA)
pH meter	CG810	Schott (Mainz, DE)
Spectrophotometer	Nano Drop ND1.000 Libra S11	Peqlab (Erlangen, DE) Biochrom (Holliston, USA)
Pipets	Research Pipetman Proline Plus	Eppendorf (Hamburg, DE) Gilson (Middelton, USA) BioHit (Satorius, Göttingen, DE)

Equipment	Name	Supplier
Sonicator	Bioruptor® Pico	Diagenode (Denville, USA)
Pipet helper	Acu-Jet	Brand (Wertheim, DE)
Protein purification	Profinia	Bio-Rad (München, DE)
Water purification system	Arium 611	Sartorius (Göttingen, DE)
Rocker	Titramax 101	Heidolph Instruments (Schwabach, DE)
	Platform Rocker STR6	Stuart Scientific (Staffordshire, UK)
Laminar flow bench	HeraSafe	Heraeus Instruments (Hanau, DE)
	LaminAir HLB 2472 MSC Advantage	Thermo Scientific (Waltham, USA)
Vacuum pump	Laboport	KNF Neuberger (Freiburg, DE)
Vortex	Vortex-Genie 1	Scientific Industries (New York, USA)
Scale	E 1200 S	Sartorius (Göttingen, DE)
	EMB 220-1	Kern (Balingen, DE)
	Analytic A 120 S	Sartorius (Göttingen, DE)
Centrifuge	Eppendorf 5810R	Eppendorf (Hamburg, DE)
	Eppendorf 5415D	Eppendorf (Hamburg, DE)
	Biofuge fresco	Heraeus (Hanau, DE)
	Multifuge 3 S-R	Heraeus (Hanau, DE)
Waterbath	Waterbath GFL	Laborbedarf (Braunschweig, DE)

2.1.2 Consumables

The consumables used in this study are listed in the following table 2.

Table 2: List of consumables used in this study

Consumables	Supplier
Air-o-Seal hydrophobic Gas permeable seal	4titude (Dorking, UK)
Blotting paper (550 g/m^2)	Sartorius (Göttingen, DE)
Chromatography paper 3 mm	Whatman (GE Healthcare, Freiburg, DE)
Disposable spatula (L-shape)	VWR (Darmstadt, DE)
DynabeadsTM M-280 Streptavidin	Thermo Fisher Scientific (Waltham, USA)
Filter sterile 0.45 µm	Sartorius Stedim Biotech (Göttingen, DE)
Filter sterile 0.2 µm	Whatman (GE Healthcare, Freiburg, DE)
Inoculation loops	Sarstedt (Nürmbrecht, DE)
PP Screw lid micro caps 2 mL	Sarstedt (Nürmbrecht, DE)

Consumables	Supplier
Microtiter-polypropylene plate 96 well, U-shape	Greiner Bio-One (Frickenhausen, DE)
Parafilm	American National Can (Chicago, USA)
Multiply-µStrip Pro 8-strip	Sarstedt (Nürmbrecht, DE)
Petri dish 10 cm Petri dish 15 cm	Greiner Bio-One (Frickenhausen, DE) Sarstedt (Nürmbrecht, DE)
Pipet tips 10 µL; 200 µL; 1000 µL; 5000 µL	Sarstedt (Nürmbrecht, DE) Biohit (Satorius, Göttingen, DE)
Pipet tips, filtered 10 µL; 200 µL; 1000 µL	Sarstedt (Nürmbrecht, DE), NerbePlus (Winsen, DE)
Polycarbonat Erlenmeyer Flask graduated	Corning (New York, USA)
Polypropylen 96 well plate U-shape (Costar)	Corning (New York, USA)
Polypropylene tubes (15 mL, 50 mL)	Corning (New York, USA)
Polypropylene plate 24 well	Sarstedt (Nürmbrecht)
Polystyrene lid	Greiner Bio-One (Frickenhausen, DE)
Polystyrene assay plate 96 Well high binding (Costar)	Corning (New York, USA)
Dialysis tube MWCO 14000	Carl Roth (Karlsruhe, DE)
PVDF membrane	Bio-Rad (München, DE)
Reaction tube 1.5 mL; 2 mL	Sarstedt (Nürmbrecht, DE)
Column for Affinity chromatography (Protein A), BioScale Mini UNOsphere SUPrA 1 mL	Bio-Rad (München, DE)
Column for Desalting, BioScale Mini Bio-Gel P-6 Desalting Cartridge 10 mL	Bio-Rad (München, DE)
Serological pipets 2 mL; 5 mL; 10 mL; 25 mL steril	Corning (New York, USA)
Syringe Inject 1 mL; 2 mL; 5 mL; 20 mL	B. Braun (Melsungen, DE)
Polystyrene TC plate 12 well/24 well	SPL Life Sciences (Pocheon, KOR)
TC plate 96 well V shape with lid	Greiner Bio-One (Frickenhausen, DE)
Disposable cuvettes 1.5 mL half-micro	Brand (Wertheim, DE)
Cellulose acetate filter 0.45 µm	Sartorius Stedim Biotech (Göttingen, DE)

2.1.3 Chemicals

All chemicals used in this study were purchased from Carl Roth (Karlsruhe, DE), Sigma-Aldrich (Taufkirchen, DE), Merck KGaA (Darmstadt, DE), AppliChem GmbH (Darmstadt, DE), Roche Diagnostics GmbH (Penzberg, DE) and SERVA Electrophoresis GmbH (Heidelberg, DE).

2.1.4 Solutions and buffers

All buffers and solutions used in this study were prepared with ultra pure water or as indicated (table 3).

Table 3: List of used solutions and buffers

Buffer/ Solution	Recipe
General	
Glycerine	80 % (v/v) Glycerine
PBS	137 mM NaCl; 1.76 mM KH_2PO_4 • 2 H_2O
PBS-T	0.05 % (v/v) Tween20 in PBS
DNA electrophoresis	
Agarose gel	1 % (w/v) Agarose in TAE
Ethidium bromide solution	10 µg/L Ethidium bromide
TAE	40 mM Tris; 20 mM Acetate; 2 mM EDTA
Coomassie staining	
Coomassie®- Destaining	10 % (v/v) Acetic acid
Coomassie®- Staining	10 % (v/v) Acetic acid; 0.05 % (w/v) Coomassie® Brilliant Blue R250
ELISA	
ELISA stop solution	0.5 M H_2SO_4
PBST ELISA-Washer	0.05 % (v/v) Tween20 in PBS
M-PBST (Blocking)	2 % (w/v) Milk powder in PBS; 0.05 % Tween20
TMB solution A	30 mM Potassium citrate; 1 % (w/v) Citric acid (pH 4.1)
TMB solution B	10 mM Tetramethylbenzidine; 10 % (v/v) Acetone; 90 % (v/v) Ethanol; 80 mM H_2O_2 (30 %)

Buffer/ Solution	Recipe
TMB solution	20 parts TMB-A; 1 part TMB-B
Chemical competent cells	
TFB1	10 mM $CaCl_2$; 30 mM Potassium acetate; 100 mM RbCl; 50 mM $MnCl_2$; 15 % (v/v) Glycerine (pH 5.8)
TFB2	10 mM MOPS; 10 mM Cl; 75 mM $CaCl_2$; 15 % (v/v) Glycerine (pH 5.8)
SDS-polyacrylamid gel electrophoresis	
APS-solution	10 % (w/v) Ammonium persulfate in H_2O
Laemmli buffer (5x)	500 g/L Glycerine; 100 g/L SDS; 250 mL β-Mercaptoethanol; 200 mL 1.5 M Tris-HCl (pH 6.8); 0.5 g/L Bromphenol Blue
Running gel buffer	1.5 M Tris-HCl (pH 8.8)
SDS solution	10 % (w/v) SDS
SDS-PAGE buffer	25 mM Tris; 192 mM Glycine; 0.1 % (w/v) SDS solution
Stacking gel buffer	1.0 M Tris-HCl (pH 6.8)
Silver staining	
Develop solution	3 g $NaCO_3$; 25 µL 37 % Formaldehyde; 1 mL Sodium thiosulfate to 50 mL dH_20
Fixation solution	50 mL Stop solution; 25 µL 37 % Formaldehyde
Sodium thiosulfate	10 mg $Na_2S_2O_3$ • 5 H_2O to 50 mL dH_20
Silver solution	0.5 mL 20 % $AgNO_3$; 37.5 µL 37 % Formaldehyde to 50 mL dH_20
Stop solution	50 % Methanol; 12 % Acetic acid
Western blot and immuno staining	
AP substrate buffer	100 mM Tris; 0.5 mM $MgCl_2$ (pH 9.5)
BCIP solution	1.5 % (w/v) BCIP in 100 % (v/v) Dimethylformamide
Blotting buffer	25 mM Tris; 192 mM Glycine (pH 8.3)
MPBS (Blocking)	2 % (w/v) milk powder in PBS-T
NBT solution	3 % (w/v) NBT in 70 % (v/v) Dimethylformamide
FACS	
FACS buffer	1x PBS; 1 mM EDTA

Buffer/ Solution	Recipe
Toxin Neutralisation Test	
MTT solution	5 mg/mL 3-(4,5-dimethylthiazol-2-yl)-2,5-diphenyltetrazolium bromide (MTT) in PBS
MTT Extraction solutiom	50 % DMF; 10 % SDS (pH 4.7)

2.1.5 Materials for cultivation and supplements

2.1.5.1 Prokaryotes

All media and solutions are prepared with ultra pure water and autoclaved or sterile filtrated before use for culture of *E. coli* (table 4). Supplements are added immediately prior to use.

Table 4: List of culture media and supplements (prokaryotes)

Medium	Recipe
Media	
SOC	2 % (w/v) Tryptone; 0.5 % (w/v) Yeast extract; 0.05 % (w/v) NaCl (pH 7.0); 20 mM Mg^{2+} solution (1 M $MgCl_2$, 1 M $MgSO_4$); 20 mM Glucose
LB	1 % (w/v) Tryptone; 0.5 % (w/v) Yeast extract; 1 % (w/v) NaCl
2xYT	1.6 % (w/v) Tryptone; 1 % (w/v) Yeast extract; 0.5 % (w/v) NaCl (pH 7.0)
2xYT-GA	2xYT medium; 100 mM D-Glucose; 100 µg/mL ampicillin
2xYT-GA-Agar	2xYT medium; 1.5 % (w/v) Agar; 100 mM D-Glucose; 100 µg/mL ampicillin
2x YT-T	2xYT medium; 20 µg/mL tetracycline
2x YT-AK	2xYT medium; 100 µg/mL ampicillin; 50 µg/mL kanamycin
Supplements	
Ampicillin solution	100 mg/mL Ampicillin stock solution
Glucose solution	2 M Glucose stock solution
IPTG solution	1 M Isopropyl-β-D-thiogalactopyranosid stock solution
Kanamycin solution	50 mg/mL Kanamycin stock solution
Tetracycline solution	10 mg/mL Tetracycline stock solution
TN1	Trypton N1 (Casein Pepton)

2.1.5.2 Eukaryotes

All media, solutions and supplements used for cultivation of mammalian cells are listed in table 5.

Table 5: List of culture media and supplements (eukaryotes)

Product	Supplier	Catalog number
Media		
MEM Earle's medium	Biochrom	F0325
Free Style™ F17 Expression medium	gibco® (Life Technologies, Darmstadt)	A13835-01
HK-TF	Xell AG	861-0001
HK-FS	Xell AG	871-0001
Supplements		
Trypsin/EDTA	Biochrom	L2153
Glucose	Carl Roth	9155.1
Penicillin/streptomycin	Biochrom	A2212
L-Glutamine	Biochrom	K0283
Fetal bovine serum (FBS)	Biochrom	S0615
DMSO	Carl Roth	A994.2
HEPES	Carl Roth	6763
Pluronic-F68	PAN™ BIOTECH	P08-02100

2.1.6 Bacterial strains, bacteriophage and cell lines

The bacterial strains and cell lines used in this study are listed in table 6.

Table 6: List of bacterial strains and cell lines

Strain/Cell lines	Genotype	References
Bacterial strain		
E. coli XL1-Blue MRF`	_(mcrA)183 _(mcrCB-hsdSMR-mrr)173 endA1 supE44 thi-1 recA1 gyrA96 relA1 lac [F_ proAB lacIqZ_M15 Tn10 (Tetr)]	Stratagene (LA Jolla, USA)
E. coli TG1	K-12 supE thi-1 _(lac-proAB) _(mcrB-hsdSM)5, (rK-mK-) F' [traD36 proAB+ lacIq lacZ_M15]	GE Healthcare (Freiburg, DE)

Strain/Cell lines	Genotype	References
BLR(DE3)	F^- ompT $hsdS_B(r_B^- m_B^-)$ gal lac ile dcm Δ(srl-recA)306::Tn10 (tet^R) (DE3)	Merck (Darmstadt, DE)
E. coli ER2738	[F'proA+B+ lacIq Δ(lacZ)M15 zzf::Tn10 (tetr)] fhuA2 glnVΔ(lac-proAB) thi-1Δ(hsdS-mcrB)5	Lucigen (Middleton, USA)
Bacterio phage		
Helperphage M13K07		(Vieira and Messing 1987)
Helperphage Hyperphage		(Rondot et al. 2001)
Eukaryotic cell lines		
Expi293F™ Cells	Derived from HEK293-6E cells, optimized for growth in higher densities	Thermo Fisher Scientific Inc. (Waltham, USA)
Vero (WHO)	Provided by NIBSC	(Osada et al. 2014)

2.1.7 Expression vectors

The plasmids used in this study are listed in table 7.

Table 7: List of plasmids

Plasmid	Description	Source
pCSE2.6-hIgG1-Fc-Xp	Secretion vector for the expression of scFv-Fc-fusions in EXPI293F cells	(Beer et al. 2018; Russo et al. 2018) AG Dübel
pCSE2.7-hIgG1-Fc-Xp	Secretion vector for the expression of scFv-Fc-fusions in EXPI293F cells	AG Dübel
pHAL30	Phagemid, Phage-Display, Expression of scFvs in *E. coli*	(Kügler et al. 2015) AG Dübel
pHAL51	Phagemid, Phage-Display, Expression of scFvs in *E. coli*	AG Dübel
pHAL52	Phagemid, Phage-Display, Expression of scFvs in *E. coli*	AG Dübel
pET21a(+)	Secretion vector for expression of proteins in BLR(DE3) cells	AG Dübel
pCSE1c	Secretion vector for the expression of IgG heavy chain in EXPI293F cells	AG Dübel
pCSL3l	Secretion vector for the expression of IgG lambda light chain in EXPI293F cells	AG Dübel

Plasmid	Description	Source
pCSL3k	Secretion vector for the expression of IgG kappa light chain in EXPI293F cells	AG Dübel

2.1.8 Enzymes

All enzymes used in this study are listed in table 8.

Table 8: List of enzymes

Enzymes	Supplier
Restriction endonuclease	
BstNI, *HindIII*-HF, *NcoI*-HF, *NheI*-HF, *NotI*-HF, *MfeI*-HF, *MluI*-HF, *BsiWI*-HF, *AgeI*-HF, *DraIII*, *BssHII*-HF, *AscI*-HF	New England Biolabs (Frankfurt a. M., DE)
T4 DNA Ligase	New England Biolabs (Frankfurt a. M., DE)
GoTag® DNA polymerase	Promega (Mannheim, DE)
Q5 DNA polymerase	New England Biolabs (Frankfurt a. M., DE)
Phusion DNA polymerase	Promega (Mannheim, DE)
Calf Intestinal alkaline phosphatase	New England Biolabs (Frankfurt a. M., DE)
Trypsin	Sigma-Aldrich (Taufkirchen, DE)

2.1.9 Antigens and antibodies

The antibodies and antigens used in this study are listed in table 9 and 10.

Table 9: List of antigens

Antigen	Description/ Supplier
A-fragment (= C-domain)	Produced in BLR(DE3) with His-Tag
B-fragment	Produced in BLR(DE3) with His-Tag
T-domain	Produced in BLR(DE3) with His-Tag
R-domain	Produced in BLR(DE3) with His-Tag
Diphtheria Toxin (#150)	List Biological Laboratories (Campbell, USA)
CRM197 (#149)	List Biological Laboratories (Campbell, USA)
Diphtheria Antitoxin Human IgG (product no 10/262)	NIBSC (London, UK)

Table 10: List of antibodies

Antibody	Catalog No	Supplier/ Origin
Mouse α c-Myc		Clone 9E10, AG Dübel
goat α mouse IgG HRP (Fc)	A0168	Sigma-Aldrich (Hamburg, DE)
goat α mouse IgG AP (Fc γ)	115-055-071	Dianova (Hamburg, DE)
goat α hIgG AP (Fc γ)	109-055-098	Dianova (Hamburg, DE)
goat α hIgG HRP (Fc γ)	A0170	Sigma-Aldrich (Hamburg, DE)
mouse α pIII	PSKAN3	MoBiTec (Göttingen, DE)
mouse α CD138 (FITC)	ab27390	abcam (Cambridge, UK)
mouse α CD19 (PE)	ab93562	abcam (Cambridge, UK)
goat α human IgG Fc (APC)	109-135-098	Dianova (Hamburg, DE)
goat α-M13 (pVIII)	BM5516F	Acris (Herford, DE)
scFv-Fragment (AG Dübel)		
DM321-F11		α Lysozym, AG Dübel

2.1.10 Commercial kits

The used kits are listed in table 11.

Table 11: List of commercial kit systems

Kit	Description	Hersteller
NucleoBond®PC500 Xtra Midi	Preparation of plasmid DNA	Macherey-Nagel (Düren, DE)
NucleoSpin® Plasmid easy pure	Preparation of plasmid DNA	Macherey-Nagel (Düren, DE)
NucleoSpin® Gel and PCR clean-up	Clean up of DNA-fragments	Macherey-Nagel (Düren, DE)

2.1.11 Software and databases

All software and databases used are listed in table 12.

Table 12: Software and databases

Software	Reference	Purpose
MultAlgin	(Corpet 1988)	Sequence alignment
VBase2	(Retter 2004)	Analysis of antibody sequences
NCBI	http://www.ncbi.uhm.nih.gov	Literature, Protein- and Gene-

Software	Reference	Purpose
		sequences
LibreOffice	https://de.libreoffice.org	Text- and data processing
Geneious	https://www.geneious.com	Generation and analysis of vector maps
GraphPad Prism 6	http://www.graphpad.com/scientific-software/prism/	Graphical data

2.1.12 DNA- and protein standards

For size determination of DNA agarose gels, GeneRuler™ 1kb Plus DNA Ladder (Fermentas, St. Leon-Rot, DE) was used. For size determination of proteins in a SDS-PAGE followed by Coomassie or silver staining, Precision Plus Protein™ Standards unstained (Bio-Rad, München, DE) was used. For Western blot analysis with immuno staining, Precision Plus Protein™ All Blue Prestained Protein Standards (Bio-Rad, München, DE) was used.

2.2 Microbiological methods

2.2.1 Sterilization

Most of the used media and solutions were sterilized by pressurized steam for 20 minutes at 121 °C. Heat or pressure sensitive substances were sterile filtrated with a 0.2 µm or 0.45 µm filter.

2.2.2 Cultivation of *E. coli* and cell density measurement

E. coli was cultivated in 2x YT medium supplemented with 0.1 M glucose at 37 °C and 250 rpm. Depending on the cultivation aim, different substances and antibiotics were added. For single clones, *E. coli* was plated on a 2x YT agar and incubated at 37 °C overnight and afterwards inoculated in liquid culture. Density of cells were determined by measuring the optical density at 600 nm.

2.2.3 Storage

E. coli cells on 2x YT-Agar plates were stored up to 2 weeks at 4 °C. For long-term storage of bacteria, glycerol cultures were used. Therefor, *E. coli* was cultured overnight in 2x YT-GA medium. On the next day, freshly cultured *E. coli* cells were mixed with 80 % (w/v) glycerol to final concentration of 20 % (w/v) glycerol. Suspensions were stored at -80 °C.

2.2.4 Transformation of *E. coli* by heatshock

Chemically competent *E. coli* cells were transformed by heat shock. DNA was mixed with 25 µL of *E. coli* cells and was placed on ice for 20 min. After heating the cells for 60 sec to 42 °C, the cells were cooled down on ice for 2 min. To regenerate the transformed cells, they were incubated in 250 µL of SOC medium at 37 °C with shaking for 30 min. The cells were plated on a 2x YT agar plate with appropriate antibiotics. Plates were incubated overnight at 37 °C.

2.2.5 Transformation of *E. coli* by electroporation

Electroporation was used for the transformation of electro-competent *E. coli* cells for antibody phage display library construction. Before transforming cells, a buffer exchange of the DNA was performed 3 times with 470 µL H_2O using Amicon Ultra Centrifugal Filters (30K) (Merck Millipore). Frozen electro-competent *E. coli* cells were thawed on ice and mixed with DNA. The cell/DNA mixture was transferred to pre-chilled (-20 °C) electroporation cuvettes and transformation was performed at 1.7 kV (*E.coli* XL1 Blue MRF') or 1.8 kV (*E. coli* ER2738) (MicroPulser™, BioRad). Immediately after the electroporation pulse, 1 mL of 37 °C pre-warmed SOC was added. After 60 min of incubation at 600 rpm and 37 °C, cells were plated on 2x YT agar containing appropriate supplements.

2.2.6 Production of soluble scFvs in microtiter plates

Soluble antibody fragments (scFvs) were produced in microtiter plates. Briefly, 140 µL 2x YT-GA medium were inoculated with 10 µL overnight culture. Incubation was performed at 37 °C and 850 rpm using a microtiter plate shaker. When OD_{600nm} reached a value of 0.5, the microtiter plate was centrifuged (10 min at 3220 xg) and the supernatant was discarded. To induce the expression of the antibody genes, the pellets were resuspended in 150 µL 2x YT-A with 50 µM IPTG and were incubated for 20 h at 30 °C and 850 rpm. Cells were separated from the antibody containing supernatant by centrifugation for 10 min at 3220 xg.

2.2.7 Production and infection of antibody phage

Antibody phage were produced in microtiter plates. Briefly, 140 µL 2x YT-GA medium were inoculated with 10 µL overnight culture. Incubation was performed at 37 °C and 850 rpm using a microtiter plate shaker. After incubation of 2 h, the culture were infected with $5 \cdot 10^{11}$ hyperphage particles by incubation at 37 °C for 30 min followed by a second incubation for 30 min at 37 °C and 850 rpm. The microtiter plate was centrifuged (10 min at 3220 xg), the supernatant was discarded, the pellets were resuspended in 150 µL 2x YT-

AK and the plate was incubated for 20 h at 30 °C and 850 rpm. Cells were separated from the antibody containing supernatant by centrifugation for 10 min at 3220 xg.

2.2.8 Determination of phage titer

Phage titers were determined for preparation of antibody phage libraries to monitor panning output. Phage titers were determined by infection of *E. coli* cells. In PBS a ten-fold serial dilutions of the phage were prepared. For infection, 50 µL of an *E. coli* XL1 Blue MRF' culture at exponential growth (OD_{600} = 0.5 in 2xYT-T) was briefly mixed with 10 µL of a phage dilution and incubated at 37 °C for 30 min. After the infection, 3x 10 µL of each dilution were spotted on 2x YT-GA agar plates. The plates were incubated overnight at 37 °C and on the next day, colonies were counted and the cfu/mL determined. To exclude phage contamination of the used PBS, a control with 50 µL *E. coli* culture and PBS was treated equally to the infection with phage. The used PBS and *E. coli* culture alone was spotted on 2x YT-GA agar plates to exclude bacterial contamination of the PBS or ampicillin resistance of the *E. coli* culture. Another 50 µL of the *E. coli* culture were infected with 10 µL of a phage solution with known titer as a positive control e.g. the library HAL7.

2.2.9 Selection of antibodies with antibody phage-display

Panning allows the selection of displayed antibodies based on specific binding to a protein.

2.2.9.1 Panning in microtiter plate

For the panning procedure the antigen was immobilized on a 96 well plate. Therefor, 1 µg diphtheria toxin was diluted in PBS and coated to a well at 4 °C overnight. Afterwards, the well was blocked with 350 µL blocking solution for 1 h at RT and then washed 3 times with PBST. Before adding the libraries in the coated well, the libraries ($5 \cdot 10^{10}$ cfu) were preincubated with blocking solution on a blocked well for 1 h at RT. The libraries were transferred to the coated wells, incubated for 2 h at RT and washed 10 times. Bound phage were eluted with trypsin (10 µg/mL) at 37 °C and 5 µL of eluate were used for titration.
The remaining 145 µL were transferred to a 96 deepwell plate and incubated with 145 µL

E. coli TG1 (OD_{600} = 0.5) first 30 min at 37 °C, then, 30 min at 37 °C and 650 rpm to infect the phage particles. 1 mL 2x YT-GA was added and incubated for 1 h at 37 °C at 650 rpm, then, add ($1 \cdot 10^{10}$ cfu) M13KO7 helperphage. Again the infected bacteria were incubated 30 min at 37 °C and 30 min at 37 °C and 650 rpm before a centrifugation for 10 min at 3220 xg was done. The supernatant was discarded and the pellet resuspended in fresh 2x YT-AK. The phage antibodies were amplified overnight at 30 °C and 650 rpm.
For the selection of antibodies, three panning rounds were needed. In each round, the washing procedures had to be intensified (20x in 2. panning round and 30x in 3. panning round). After the third panning round, the titerplate was used to select monoclonal antibody clones.

2.2.9.2 Panning in solution

For the panning procedure the antigen was biotinylated. 100 ng of the biotinylated antigen was preincubated in 1.5 mL low Protein binding tube with 2 % BSA-PBS on an overhead shaker. After 2 h, magnetic streptavidin beads were given to the tube and incubated for further 30 min. The tube were placed 5 min on a magnetic rack and the supernatant was discarded. The streptavidin beads were washed 10 times with 0.8 mL PBST. Bound phage were eluted with trypsin (10 µg/mL) at 37 °C and 5 µL were used for titration.
The remaining 145 µL were transferred to a 96 deepwell plate and incubated with 145 µL *E. coli* TG1 (OD_{600} = 0.5) first 30 min at 37 °C, then, 30 min at 37 °C and 650 rpm to infect the phage particles. 1 mL 2xYT-GA was added and incubated for 1 h at 37 °C at 650 rpm, then, add ($1 \cdot 10^{10}$ cfu) M13KO7 helperphage. Again the infected bacteria were incubated 30 min at 37 °C and 30 min at 37 °C and 650 rpm before a centrifugation for 10 min at 3220 xg was done. The supernatant was discarded and the pellet resuspended in fresh 2x YT-AK. The phage antibodies were amplified at 30 °C overnight and 650 rpm.
For the selection of antibodies, three panning rounds were performed. In each round, the washing procedures had to be intensified (20x in 2. panning round and 30x in 3. panning round). After panning round three, the phage were again incubated with TG1 to produce antibody phage for performing a phage ELISA.

2.3 Molecular methods

2.3.1 Agarose gel electrophoresis

Gel electrophoresis separates DNA fragments due to their size and conformation. Therefor, an agarose gel consisting of 1 % (w/v) agarose in TAE buffer was prepared. Ethidium bromide was added to the gel in a final amount of 1 µg. The DNA samples were mixed with 6 x DNA loading dye (Fermentas) and GeneRuler^{TM} 1kb Plus DNA Ladder Mix (Fermentas) was used as a size standard. A voltage of 100 – 120 V and a current of 400 mA was applied for 25 – 35 min. Due to the intercalating ethidium bromide, the DNA could be detected under UV light after electrophoresis.

2.3.2 Extraction of DNA from agarose gel

For extraction of DNA fragments after separation in gel electrophoresis, the fragment was cut out with a scalpel. Afterwards, the gel fragment was purified with the NucleoSpin® Gel and PCR clean-up-Kit (Macherey & Nagel).

2.3.3 Plasmid DNA preparation

Plasmid DNA was prepared from *E. coli* using a kit (Macherey & Nagel, Germany) depending on the culture volume. For 5 mL *E. coli* culture the NucleoSpin® Plasmid EasyPure kit was used with 30 – 50 µL elution buffer or ddH_2O for elution.
For higher culture volume (50 – 100 mL) the NucleoBond® Xtra Midi-Kit was used with 200 – 500 µL elution buffer or ddH_2O for elution.

2.3.4 Determination of DNA concentration and purity

Concentration and purity of DNA were determined by measuring the absorbance at 260 nm and 280 nm. For a pure DNA solution, an A_{260nm} of 1 corresponds to a concentration of dsDNA of 50 µg/mL. For a ratio of A_{260nm}/A_{280nm} = 1.8 – 2.0, the DNA can be considered to be pure.

2.3.5 Restriction digestion and dephosphorylation of DNA

For enzymatic DNA digestion restriction endonucleases purchased from New England Biolabs (NEB, USA) were used. Reaction buffers and incubation temperatures were chosen according to the manufacturer's instructions. Digestion was done for 1 – 4 h at 37 °C or for up to 16 h at 16 °C and was followed by heat inactivation of the restriction enzymes (20 min, 65 °C or 80 °C).

To avoid re-ligation of the digested vector DNA, the 5'-phosphate groups of the linearized plasmid were removed prior to ligation. For dephosphorylation 1 µL CIP (calf intestine phosphatase) was added for 30 – 60 min at 37 °C. Afterwards, purification was done with NucleoSpin® Gel and PCR Clean up-Kit (Macherey & Nagel) according to the manufacturer's instructions.

2.3.6 Ligation of DNA-fragments

DNA ligation was performed using T4 DNA ligase (NEB) at room temperature for 1 – 4 h or at 16 °C overnight. A molar ratio of vector to insert of 1:3 was chosen:

$$Insert\,(ng) = 3 \cdot \frac{Vector\,(ng) \cdot size\ Insert\,(bp)}{size\ Vector\,(bp)}$$

If the vectors pCSE2.7-hIgG1-Fc-Xp or pHAL51 were used an additional *AscI* restriction step was performed after ligation. Therefor, 1 µL *AscI*-HF was added to the ligation and incubated for 30 min at 37 °C.

After ligation, the mixture was heat inactivated at 60 °C for 10 min and was used for transformation of competent *E. coli* cells.

2.3.7 Sequencing of DNA

All plasmids derived by cloning via PCR were sequenced by SeqLab (Göttingen, DE). Therefor, 1.2 µg purified plasmid was premixt with 2.5 µL sequencing primer (10 mM). The analysis of all sequencing results was done using the programs MultAlign and VBASE2.

2.3.8 Generation of bacterial and mammalian expression vectors

Two bacterial (pHAL51 and pHAL52) and one mammalian (pCSE2.7-hIgG1-Fc-Xp) expression vector were constructed that have addition restriction sites in the cloning site.
The vectors pHAL51 and pHAL52 derived from the vector pHAL30. Both vectors have an *AscI* restriction site in the VL stuffer and pHAL52 has an additional *SalI* restriction site in the VH stuffer.
The vector pCSE2.7-hIgG1-Fc-Xp derived from pCSE2.6-hIgG1-Fc-Xp and has an *AscI* restriction site between the *NcoI* and *NotI* restriction site.
The new stuffer were ligated into the *NcoI* and *NotI* restricted vectors. The used stuffers are shown in table 13.

Table 13: Sequences of new generated expression vector

Vector	Stuffer 5' — 3'
pHAL51	CTAACTAAGGCGCGCCTCTGA
pHAL52	CTAGTCGACTAACTT
pCSE2.7-hIgG1-Fc-Xp	CTAACTAAGGCGCGCCTCTGA

2.3.9 Amplification of DNA-fragments by PCR

For amplification of DNA polymerase chain reaction (PCR) was used. All oligonucleotides used in this study are listed in supplemental table 31.

2.3.9.1 PCR to amplify DNA-fragments with restriction sites

For cloning into IgG vectors new restriction sites were added to the ends of the inserts by PCR. Therefor, oligonucleotide primers were designed. The mixture for PCR and the protocol is given in table 14 and 15.

Table 14: Mixture for PCR

Amount	Components
10 µL	5x Phusion HF Buffer
1 µL	10 mM dNTPs
2.5 µL	10 mM Primer I
2.5 µL	10 mM Primer II
0.5 µL	Phusion Polymerase
5-10 ng	DNA
to 50 µL	ddH_2O

Table 15: Protocol PCR

Temperature	Time	
98 °C	30 sec	
98 °C	20 sec	30x
56 °C	30 sec	
72 °C	30 sec (3-4 kb/min)	
72 °C	8 min	
16 °C	∞	

2.3.9.2 Colony-PCR

For colony PCR a bacteria colony was used as template for DNA amplification. This PCR was used to screen single colonies after cloning, for detection of inserts and insert rates. The mixture for PCR and the protocol is given in table 16 and 17.

Table 16: Mixture for colony-PCR

Amount	Components
2 µL	5x GoTaq Buffer
0.8 µL	25 mM $MgCl_2$
0.2 µL	10 mM dNTPs
0.5 µL	10 mM Primer I
0.5 µL	10 mM Primer II
0.05 µL	GoTaq
to 10 µL	ddH_2O

Table 17: Protocol colony-PCR

Temperature	Time	
95 °C	2 min	
94 °C	15 sec	25 x
56 °C	20 sec	
72 °C	1:20 - 2:30 min (1 kb/min)	
72 °C	3 min	
16 °C	∞	

2.3.10 Generation of an immune antibody gene library

For the generation of a human immune library against diphtheria toxin blood of three persons who have been regularly boost-vaccinated was collected 7 days after they received a boost vaccination of diphtheria toxin and tetanus. The peripheral blood mononuclear cells (PBMC) were extracted from the blood via Ficoll® and RNA isolated with Trizol and a Trizol RNA purification kit. For the B-cell sorted libray, B-cells were stained with mouse α-CD138 (FITC conjugated) antibody and sorted via FACS. Also the RNA of the sorted B cells were extracted. The RNA was converted into cDNA. The cDNA was amplified with specific primers for the VH chain, primers for κ light chain and primer for λ light chain. These PCR products were again amplified with primers adding a restriction site for further cloning into the *E. coli* expression vector pHAL51. First the light chain was cloned with the restriction sites *MluI* and *NotI*, second the VH chain was cloned with the restriction sites *HindIII* and *NcoI*. The efficiency of cloning was tested with a colony PCR and the rate of complete scFv were determined. The libraries were further packaged with hyperphage or glycerine (20 % (v/v)) was added and stored at – 80 °C.

2.4 Protein biochemical methods

2.4.1 Purification of antibodies with protein A

In EXPI293F cell produced scFv-Fc and IgG were purified from supernatant with protein A. All buffers and the distilled water were filtered (0.45 µm) and degassed. The cell culture medium containing the antibodies was centrifuged at 750 xg for 10 min at 4 °C and was filtered as well.

2.4.1.1 Protein A purification in 24 well plate

For affinity chromatography in 24 well vacuum filtration plate (10 mL Uniplate PP, 10 mL Unifilter, 10 µm melt blown PP) with a MabSelect™ SuRe Protein A affinity matrix (GE 7701-5110; GE 7700-9917; GE 17-5438-01; Whatman, Munich, Germany) was used. The wells were equilibrated with buffer and afterwards loaded with filtered, antibody-containing supernatant. The supernatant passed the wells by gravity flow. The wells were washed with binding buffer and the bound antibodies were eluted with elution buffer (pH 3) in three steps. First, 750 µL of protein A elution buffer was added to the matrix and incubated for 5 minutes with vacuum applied. The second and third elution were performed with 500 µL elution buffer. Afterwards, the buffer was exchange to PBS either by dialysis or by the use of Zeba™ Desalt Spin column and the purified antibodies were stored for short time at 4 °C or for long time storage aliquoted and stored at -20 °C.

2.4.1.2 Profinia™- purification system

For affinity chromatography in Profinia™- purification system (BioRad) a 1 mL Protein A BioScale Mini UNOsphere SUPrA column (BioRad) and a 10 mL BioScale Mini Bio-Gel P-6 Desalting cartridge (BioRad) were used. The columns were equilibrated with buffer and afterwards loaded with filtered, antibody-containing supernatant with a flow rate of 0.5 mL/min. The column was washed with binding buffer and the bound antibodies were eluted with elution buffer and desalted. The collected antibodies were buffered in PBS and stored for short time at 4 °C or for long time storage aliquoted and stored at -20 °C.

2.4.2 Purification of proteins with IMAC

Recombinant proteins containing a HIS-tag were purified using immobilized metal ion affinity chromatography (IMAC). The bacteria culture was centrifuged at 10,000 xg for 15 min at 4 °C. Then, the pellet was resuspended in binding buffer and sonicated 3 times for 2 min with pulsed cycles. Afterwards, the suspension was centrifuged at 16,000 xg for 10 min at 4 °C and the supernatant was loaded to a support column containing 1 mL of Sepharose (activated with 0.1 M $NiSO_4$). The column was washed with washing buffer until a $OD_{280} \approx 0$ of the flow-through was reached. Then, the bound antibodies were eluted with elution buffer. The buffer was exchange to PBS by dialysis and the purified proteins were stored for short time at 4 °C or aliquoted and stored at -20 °C for long time.

2.4.3 Determination of protein concentration

Concentration of protein was determined by measuring the absorbance at 280 nm via UV/ VIS spectrometry using Nanodrop ND1000. The molecular weight and molar extinction coefficient (according to Geneious 4.8.5) were considered in the calculation of the protein concentration.

2.4.4 Antigen-enzyme-linked immunosorbent assay (ELISA)

In an ELISA (enzyme-linked immunosorbent assay) antigen-antibody specific interactions are detected via an enzymatic color reaction.

Nunc MaxiSorp microtiter plates were coated with 100 ng target protein or 100 ng BSA in 100 µL coating buffer per well at 4 °C overnight. The plate was washed three times with PBS-T using an ELISA washer and blocked with 350 µL milk-PBS-T per well for 1 h at RT.

2.4.4.1 Indirect antigen-ELISA

For the indirect ELISA, 50 µL soluble antibody and 50 µL blocking solution per well is incubated for 1 h at RT. The plate was washed three times with PBS-T using an ELISA washer and 100 µL primary antibody mouse α-c-Myc (1:50 in blocking solution) were

added per well for 1 h at RT. Afterwards the plates were washed again. Goat α-mouse IgG (Fc-specific) antibody conjugated with horse radish peroxidase (HRP, 1:50,000) was used as secondary detection antibody and was incubated for 1 h at RT. Unbound antibodies were removed by additional washing steps. Bound antibodies were visualized with TMB substrate (20 parts TMB solution A and 1 part TMB solution B were mixed). After stopping the reaction by adding 100 µL stopping solution, absorbance at 450 nm with a 620 nm reference was measured in an ELISA reader.

2.4.4.2 Titration-ELISA

The titration ELISA was performed like the indirect antigen ELISA. For the titration ELISA a serial dilution was made in blocking solution starting with 1 µg antibody. Afterwards, the dilution were prepared in $(\sqrt{10})^{-1}$ - steps. 100 µL of each dilution was added per well and incubated for 1 h at RT. The plate was washed 3 times with PBS-T. Goat α-human IgG (Fc-specific) antibody conjugated with horse radish peroxidase (HRP, 1:70,000) was used as secondary detection antibody and was incubated for 1 h at RT. Unbound antibodies were removed by additional washing steps. Bound antibodies were visualized with TMB substrate (20 parts TMB solution A and 1 part TMB solution B were mixed). After stopping the reaction by adding 100 µL stopping solution, absorbance at 450 nm with a 620 nm reference was measured in an ELISA reader.

2.4.4.3 Phage ELISA

For the phage ELISA 50 µL phage antibodies and 50 µL blocking solution per well were incubated in the first well followed by a serial 1:2 dilution up to 1:2000 for 1 h at RT. The plate was washed three times with PBS-T using an ELISA washer and 100 µL primary antibody goat α-M13 (pVIII) conjugated with horse radish peroxidase (HRP, 1:40,000 in blocking solution) were added per well for 1 h at RT. Unbound antibodies were removed by additional washing steps. Bound antibodies were visualized with TMB substrate (20 parts TMB solution A and 1 part TMB solution B were mixed). After stopping the reaction by adding 100 µL stopping solution, absorbance at 450 nm with a 620 nm reference was measured in an ELISA reader.

2.4.5 SDS-polyacrylamid-gelelectrophorese (SDS-PAGE)

Sodium dodecyl sulfate polyacrylamide gel electrophoresis (SDS-PAGE) was used to separate proteins according to their electrophoretic mobility. The running and stacking gel (table 18) were cast between 2 glass plates separated by a 0.75 mm spacer. The running gel was prepared and overlaid with ddH_2O. After gel polymerization, the ddH_2O was removed, the stacking gel was cast and a comb was inserted.

Table 18: Recipe for running and stacking gel for a SDS-PAGE

Components	**running gel (12 %)**	**stacking gel (4 %)**
ddH_2O	1.3 mL	1 mL
30 % Acrylamid (Rotiphorese)	1.6 mL	0.26 mL
1.5 M Tris (pH 8.8)	1.0 mL	-
1 M Tris (pH 6.8)	-	0.2 mL
10 % SDS	40 µL	15 µL
10 % APS	40 µL	15 µL
TEMED	2 µL	2 µL

The protein samples were mixed with 5x Laemmli's sample buffer and were boiled for 10 min at 95 °C. Afterwards, a protein standard and samples were loaded onto the gel. Electrophoresis was performed at 200 V and 400 mA per gel for 45 min followed by either staining (Coomassie or silver) or Western blot analysis.

2.4.6 Coomassie staining of SDS gels

Proteins on SDS gels were stained with Coomassie staining solution that dyes non-covalently the amino and carboxyl groups of proteins. To destain the gels, destaining solution was applied until only the protein bands were left clearly visible. For documentation, the gels were scanned with a computer scanner.

2.4.7 Silver staining

SDS gels can be stained by silver ions that are taken up by negatively charged side chains of proteins. This interaction can then be visualized through color change by reduction of the silver ions to silver leaving a black stain. Proteins on SDS gels were fixated with 50 mL fixation solution for 1 h. After 3 times washing with 50 % ethanol for 20 min, the gel was incubated in sodium thiosulfate for 1 min. Three times washing for 20 s with H_2O followed by 1 – 5 min staining with develop solution. Again, washing with water 2 times for 2 min and subsequently stopping the reaction with stop solution. For documentation the gels were scanned with a computer scanner.

2.4.8 Western Blot and immuno staining

A semi-dry Western blot was performed to transfer proteins from SDS gels onto polyvinylidene fluoride (PVDF) membranes. Blotting papers were pre-soaked in blotting buffer and stacked together with the ethanol-activated PVDF membrane and the SDS gel. Transfer of the proteins was performed at 20 V for 30 min.

After Western blotting, the membrane was blocked with M-PBST for 60 min at room temperature to limit unspecific antibody binding and then washed with PBST. Detection of proteins was performed indirectly via specific primary antibody followed by AP-conjugated secondary antibody. Antibodies were diluted in M-PBST and incubated for 1 h at room temperature. After washing with PBST and substrate buffer, bound antibodies were visualized in NBT/BCIP (NBT and BCIP solution 1:100 in substrate buffer). Finally, the membrane was washed with water and dried. For documentation the blots were scanned.

2.4.9 Epitope mapping

For epitope mapping a PepSpot membrane from JPT Peptide Technologies GmbH (Berlin, DE) was used. The amino acid sequence was cut in 15 amino acid long pieces with an overlap of 12 amino acids and covalently bound to a cellulose-β-alanine-membrane. Methanol activation of the membrane was followed by three washing steps and 2 h blocking in 2 % M-TBST. The scFv-Fc for the analysis was diluted to 1 µg/mL with

M-TBST and incubated for 3 h at RT. After three washing steps with TBST the membrane was incubated with the secondary antibody goat α-human Fc HRP conjugated (dilution 1:70,000 in M-TBST). After three times washing with TBST the membrane was incubated with SuperSignal West Pico Chemiluminescent Substrate and the chemiluminescence was analyzed in a Gel Doc XR+ System (Bio-Rad).

2.4.10 Size exclusion chromatography (SEC)

The aggregation behavior of IgG antibodies was analyzed with size exclusion chromatography (SEC). A Superdex^{TM} 200 Increase 10/300 GL column was used with the Äkta purifier system. An amount of 150 µg IgG were analyzed with a flow rate of 0.5 mL/ min. The absorption at 280 nm was measured and the molecular weight of the IgG antibody determined by using a standard curve.

2.5 Cell biological methods

2.5.1 Cultivation of EXPI293F cells

The suspension cell line EXPI293F (EXPI) was cultured in serum-free F17 medium supplemented with 7.5 mM L-glutamine and 0.1 % Pluronic-F68. They were incubated at 37 °C, 5 % CO_2 and 110 rpm.

2.5.2 Transient transfection of EXPI293F cells

Two days before transient transfection EXPI293F cells were seeded with $0.5 \cdot 10^6$ cells/mL. The cells had a concentration of $1.5 \cdot 10^6$ cells/mL with a vitality over 90 %. The used amounts of cells, DNA and transfection reagent PEImax (40 kDa, 1 mg/mL, Polysciences, Warrington, USA) are shown in table 19. PEImax and DNA were mixed well and incubated for 30 min before adding it to the EXPI293F cells. The antibodies were produced over 7 days. After 2 days of transfection cells were fed with HK-TF (5 parts) and HK-FS (1 part) to double the volume.

Table 19: Transfection mix according to scale

	Cultivation Flask	EXPI293F volume	End volume after feeding	Amount DNA (µg)	Amount PEImax (µL)
small scale	25 mL Sarstedt Flask	5 mL	10 mL	5	25
large scale	125 mL Erlenmeyer flask	25 mL	50 mL	25	125
micro scale	96 deepwell plate	0.4 mL	0.8 mL	0.4	2

2.5.3 Cultivation of Vero cells

The adherent cell line Vero(WHO) was cultured in EMEM medium, supplemented with 5 % FCS, 0.015 M HEPES, 2 mM L-glutamin, 0.1 % Glucose and 100 µg/mL penicillin/streptomycin. Cells were incubated at 37 °C, 5 % CO_2 and humidity of 96 %. To passage them, cells were washed with PBS and incubated with trypsin/EDTA until they detached from the tissue flask. The cells were seeded into fresh flasks containing appropriate volume of pre-heated medium at 37 °C.

2.5.4 Freezing and thawing of cells

For long-term storage, the cells were harvested as described above, centrifuged, resuspended in freezing medium (10 % DMSO and 90 % EMEM with all supplements) and transferred to cryo tubes. To allow a slow and gradual freezing, tubes were stored at -80 °C in a cell cryo container (Mr. Frosty™, Thermo Fisher Scientific) for one day. Afterwards, the tubes were transferred to liquid nitrogen.

For thawing, frozen cells were incubated in a 37 °C water bath and right upon thawing added to 10 mL cold EMEM medium. Cells in DMSO containing medium were centrifuged for 10 min at 250 xg and 4 °C. The medium was discarded and cells were resuspended in fresh, 37 °C warm medium and seeded in an appropriate cell culture flask.

2.5.5 Counting cells

To distinguish between living and dead cells, cells in suspension were mixed with trypan blue, a dye that only stains dead cells. Living and dead cells were counted in a hemocytometer (Countess II FL, life technologies, Waltham, USA). The cell density (cells/ mL), the total number of cells and the percentage of living cells (vitality) were calculated by the cell counter.

2.5.6 Diphtheria toxin titration to determine 4x MCD

To determine the minimal cytopathic dose diphtheria toxin was titrated in a 96 cell culture plate. Therefore, wells in row A and H and in column 12 are not used (blanks). 50 µL EMEM medium was added to all wells except column 1. 100 µL of the toxin working stock solution was added to the appropriate wells in column 1. A doubling dilution (50 µL) was performed across the plate down to column 10. Then, 50 µL EMEM medium was added to all wells to bring volume to 100 µL. 50 µL of the appropriate Vero cell suspension ($4 \cdot 10^5$ cells/mL) was added to all wells except the blanks. The plate was equilibrated for 1 h in a CO_2 incubator, sealed and further incubated for 6 days at 37 °C.

After 6 days, the seal was removed and the MTT assay performed. 5 mg MTT/mL in PBS

was prepared and sterile filtrated through a 0.2 µm filter. 10 µL MTT solution was added to each well and incubated at 37 °C, 5 % CO_2 for 4 h. All supernatant was removed and 100 µL extraction buffer was added to each well. After 1 day of incubation at 37 °C, the plate was measured at an absorption of 570 nm.

The geometric mean OD of the untreated Vero cells were calculated and then the 50 % of the geometric mean was determined. The first concentration of the wells of a geometric mean OD lower than the 50 % untreated Vero cells were determined. This concentration is the minimal cytopathic dose (MCD) and was multiplied with factor four to get the 4x MCD. This 4x MCD was used as a constant amount of toxin for the toxin neutralization assay with Vero cells.

2.5.7 Toxin neutralization assay with Vero cells

The Vero cell assay is an *in vitro* toxin neutralization test (TNT) which measures the ability of antibodies to protect Vero cells from a cytotoxic dose of diphtheria toxin. The TNT Vero cell assay was performed according to in-house protocols from NIBSC (London, UK). The first WHO International Standard (IS) for human diphtheria antitoxin was included as a reference antitoxin and, if available, an equine therapeutic DAT product was included for comparison.

The candidate antibodies were titrated with pre-dilution starting undiluted or at 1:2 or 1:500 in Vero cell medium. Occasionally, a pre-dilution starting at 1:100,000 was necessary.

A 96 well cell culture plate was used to dilute the antibodies. 100 µL of antitoxin reference, comparator or antibody were added to wells A1-H1. 50 µL EMEM was added to all remaining wells except control without DT in column 11 which get 100 µL. Then, perform doubling dilutions across plate up to column 10 and add 50 µL of toxin preparation 4x minimal cytopathic dose (4x MCD) to all wells – except control without DT. To occur toxin neutralization, the plate was covered with a lid and left for 1 h at RT. 50 µL of the appropriate Vero cell suspension ($4 \cdot 10^5$ cells/mL) was added to all wells. The plate was equilibrated for 1 h in a CO_2 incubator, sealed and further incubated for 6 days at 37 °C.

After 6 days, the seal was removed and the MTT assay performed. 5 mg MTT/mL in PBS

was prepared and sterile filtrated through a 0.2 µm filter. 10 µL MTT solution was added to each well and incubated at 37 °C, 5 % CO_2 for 4 hour. All supernatant was removed and 100 µL extraction solution was added to all wells. After 1 day of incubation at 37 °C, the plate was measured at an absorption of 570 nm.

The geometric mean OD of the untreated Vero cells were calculated and then 50 % of the geometric mean determined. The last concentration above the 50 % untreated Vero cells were determined. This concentration is the minimal effective dose 50 % (MED50%) of an antibody.

2.5.8 Extraction of PBMC

EDTA-treated blood was mixed to equal parts with FACS buffer and slowly added over a layer of Ficoll Parque, centrifuged at 400 xg for 30 min at RT with no breaks applied to stop. The PBMCs are in the lymphocyte layer between the plasma and the Ficoll Parque. This layer was carefully removed with a pipette and transferred in FACS buffer. PBMCs were washed three times with FACS buffer by centrifugation for 10 min at 300 xg. Amount of PBMC after the last resuspension step in FACS buffer was determined.

2.5.9 Flow cytometry of PBMC

A total of $1 \cdot 10^7$ cells were transferred into 1.5 mL tubes. Cells were stained with α-CD138 (FITC) or α-IgG Fc (APC). Therefor, cells were centrifuged at 300 xg, 10 min at 4 °C and the pellet was resuspended in 100 µL of primary antibody dilution and incubated for 1 h on ice in the dark. Afterwards, cells were washed twice with FACS buffer, resuspended in 1000 µL FACS buffer and analyzed by flow cytometry using a Sony SH-800 (San Jose, USA) with two lasers (488 nm and 638 nm) and appropriate detectors for detection of FITC and APC. For each sample 10^4 events were counted and resulting data was analyzed using Sony analysis software.

3 Results

3.1 Antibody gene extraction for an immune library

Three persons were regularly boost-vaccinated with dDT, a diphtheria and tetanus combination. After seven days, EDTA-treated blood samples were collected and PBMCs extracted with Ficoll. An average concentration of $4.74 \bullet 10^7$ PBMC/mL were counted. Two immune libraries were constructed. For the first library the total PBMCs were used, the RNA was isolated and an average concentration of 209 ng/mL was measured followed by cDNA synthesis. This first immune library was called VJN. For the second library the fresh prepared PBMCs were stained with a florescence conjugated $CD138^+$ antibody to stain the antibody-producing B cells. In the next step the positively stained cells were selected via FACS (figure 4).

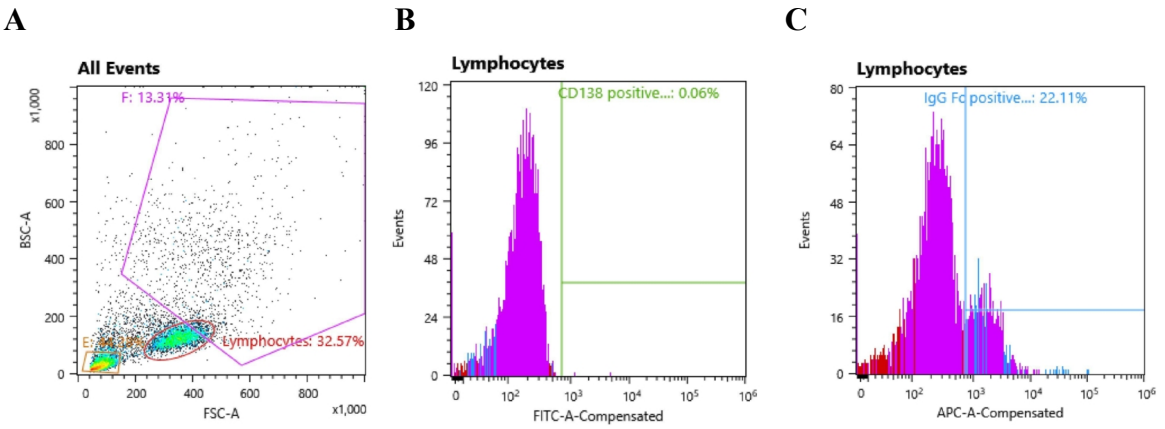

Figure 4: FACS analysis of PBMC for selection of $CD138^+$ cells. Shown is the pre-analysis with 10,000 cells before the sorting started. Cell Sorting with $CD138^+$ (FITC) and IgG Fc (APC).

The erythrocytes and debris (orange), lymphocytes (red) and monocytes (purple) were gated in a forward-sideward scatter plot in the FACS software (figure 4A). Lymphocytes were present with 32.5 % in the PBMC mixture. Monocytes were present with 13.3 %. A goat α-CD138 antibody conjugated with FITC was used to stain plasma cells in the PBMC mixture. Lymphocytes were further selected via FACS for $CD138^+$ cells (figure 4B). As a

control Fc presenting cells in the PBMCs were stained with an α-IgG Fc and in the lymphocyte fraction 22.11 % Fc positives cells were detected (figure 4C). Afterwards, the sorting was started and over 88,000,000 PBMCs were analyzed and 2,501 $CD138^+$ cells were sorted (= 0.003 %). These selected cells were further used for library construction. The RNA was extracted and a concentration of 7.7 ng/µL was measured. Afterwards a reverse transcription was performed to obtain cDNA. This second immune library was called the CD138+ library.

3.2 Library construction

The cDNA from total PBMC and $CD138^+$ sorted cells were used to amplify the VH and VL gene sequences. The VH and VL were cloned into the phage display vector pHAL51. The cDNAs derived from the blood of the persons were kept separated for the total PBMC library and also lambda and kappa light chains were kept separated. The cloning was performed in two steps: firstly, the VL cloning with the restriction sites *MluI* and *NotI* and secondly, the VH cloning with the restriction sites *NcoI* and *HindIII* were performed. The diversity over all sub-libraries were between 1,31 – 3,45 • 10^8 individual clones per mL with an insert rate of 73 – 95 % (table 20).

Table 20: Overview of all constructed immune libraries with titer (cfu/mL) and insert rate (%).

Library type	Sub-Library name	Titer (cfu/mL)	Insert rate (%)
Immune Library	V λ Library	3.45 • 10^8	90.9
Immune Library	V κ Library	2.39 • 10^8	95.4
Immune Library	J λ Library	2.18 • 10^8	86.4
Immune Library	J κ Library	1.75 • 10^8	72.7
Immune Library	N λ Library	2.00 • 10^8	81.8
Immune Library	N κ Library	1.31 • 10^8	81.8
Immune Library sorted	CD138+ λ Library	4.00 • 10^8	86.9
Immune Library sorted	CD138+ κ Library	3.70 • 10^8	78.2

Subsequently, the libraries were packaged with hyperphage to present the scFv antibody coupled to the pIII on the phage. For the packaging, the sub-libraries of the total PBMC

library were mixed to receive the VJN library as a pool. The lambda and kappa libraries were still kept separate. This resulted in phage titers of 7.4 • 10^{12} cfu/mL for VJN lambda, 7.2 • 10^{12} cfu/mL for VJN kappa, 2.6 • 10^{12} cfu/mL for CD138+ lambda and 6.0 • 10^{12} cfu/mL for CD138+ kappa. The packaging was further analyzed in a pIII stained western blot (figure 5).

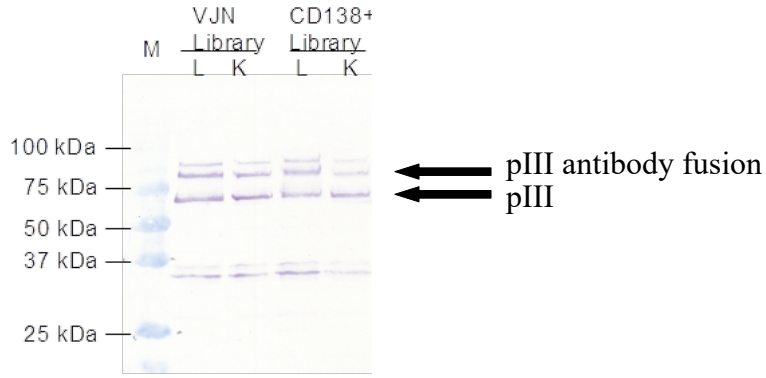

Figure 5: Immunoblot of hyperphage packaged immune libraries. 5 • 10^{8} cfu used. Detection with α-pIII antibody. L=lambda, K = kappa light chain.

All libraries showed the native pIII (60 kDa) and the pIII-antibody-fusion (90 kDa).

3.3 Selection of monoclonal antibodies

For antibody selection three different libraries were used: the naive HAL9/HAL10 libraries and the two constructed immune libraries VJN and CD138+. Two different strategies were chosen for selecting antibodies: on the one hand, the antigen is immobilized on a plate and on the other hand, the antigen is biotinylated and free in solution. The unnicked diphtheria toxin produced in *Corynebacterium diphtheriae* (List Biological Laboratories, Inc.) was chosen as antigen in all strategies. With these 2 methods 660 antibodies were selected in total.

3.3.1 Panning on plates

171 scFv antibodies were isolated from the three libraries (one naive and two immune libraries) using the strategy of immobilization on plate (table 21).

Table 21: Number of scFv developed from a panning with immobilized antigen

Library type	Library name	No. of DT binder	scFv after *BstNI* digestion	No. of lambda scFv	No. of kappa scFv	Unique scFv after sequencing	Unique VH chains
Naive	HAL9/ HAL10	39	29	29	0	29	24
Immune	VJN	67	52	42	10	51	34
Immune	CD138+	65	56	44	12	50	10
Sum:		171	137	115	24	130	68

These antibodies were further analyzed regarding their genetic information. First, a *BstNI* digestion was done to identify identical clones by identical patterns during electrophoresis (data not shown). A number of 137 different clones were identified after *BstNI* digestion. Second, the 137 antibodies were sequenced to confirm the result. 130 of these scFv were identified as unique after sequencing (supplemental table 32).

For all further characterizations the selected scFv antibodies against diphtheria toxin were converted in a IgG-similar scFv-Fc format. Therefor, the gene sequence of the scFv antibodies were cloned into the pCSE2.7-hIgG1-Fc expression vector. The transient transfection and later the production were performed in 96 deepwell plates in EXPI293F cells over 7 days. The produced antibodies were secreted in the growth medium and the supernatant was used for performing the neutralization assay. A serial dilution of the supernatant was incubated with a constant amount of diphtheria toxin (4x MCD) and after 6 days of incubation with Vero cells, the cytopathic effect was measured with an MTT assay. The produced antibodies were analyzed regarding their neutralization efficacy in neutralization assay (figure 6 and supplemental figure 25 and 26).

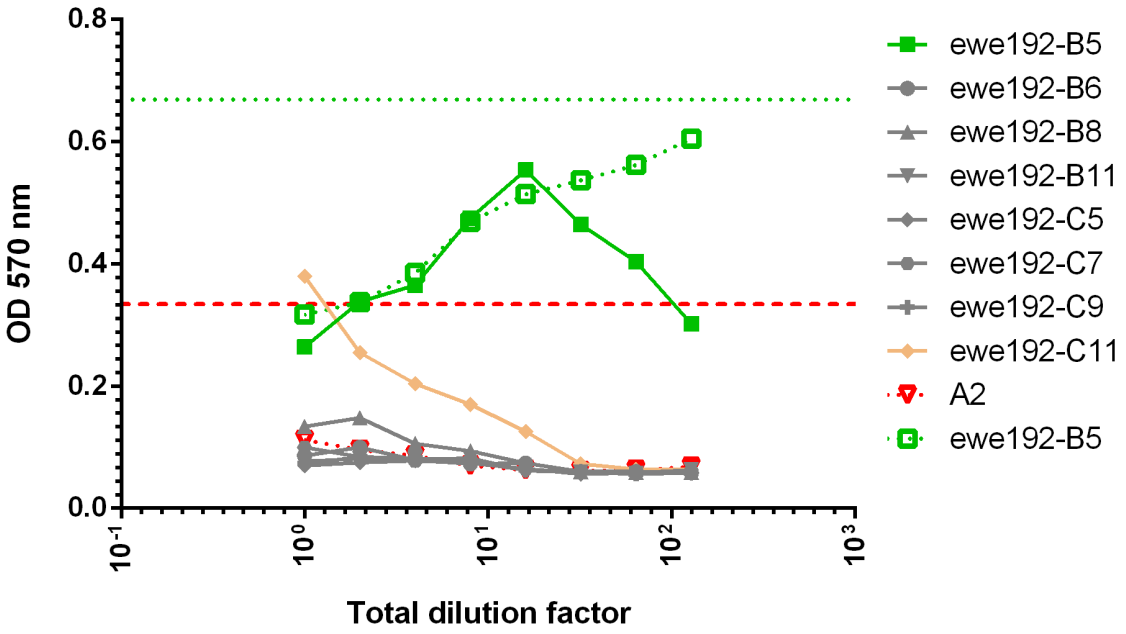

Figure 6: Neutralization assay of scFv-Fc in supernatant for screening. Untreated Vero cells are shown as green dotted line. The threshold for neutralization is shown as red dotted line (50% of untreated Vero cells). The antibody A2 (red, open symbol and dotted line) is considered as negative control, ewe192-B5 (green, open symbol and dotted line) as positive control (derived from a pre test). scFv-Fc antibodies shown in colored and gray symbols were further analyzed. Mitochondrial activity was measured with an MTT assay after 6 days at OD_{570nm}.

Cells reaching a neutralization effect above 50 % (red dotted line) were regarded as neutralizers. In the exemplary figure 6, the colored antibodies ewe192-B5 (green square) and ewe192-C11 (nude diamond) were considered neutralizers. All other gray colored antibodies were not further analyzed. The antibody ewe192-B5 (green open square, dotted line) was identified as a good neutralizer in a pre-test and was used further purified as positive control in all neutralization assays. In this assay, 22 scFv-Fc antibodies showed a neutralization in the assay. These 22 scFv-Fc antibodies were further analyzed. The V genes for the 22 selected antibodies are shown in table 22.

Table 22: V genes of 22 scFv clones selected for further analysis

Name of Antibody clone	VH			VL	
	V	D	J	V	J
ewe191-A7	IGHV3-33*01	IGHD6-13*01	IGHJ4*02	IGLV1-47*01	IGLJ3*01
ewe191-A9	IGHV3-21*01	IGHD6-6*01inv	IGHJ3*02	IGLV1-44*01	IGLJ3*01
ewe191-C1	IGHV1-3*01	IGHD3-10*01	IGHJ6*02	IGKV3-15*01	IGKJ4*01
ewe191-C10	IGHV3-21*01	IGHD2-21*02	IGHJ4*02	IGLV3-21*02	IGLJ3*01
ewe191-C11	IGHV3-33*01	IGHD6-13*01	IGHJ4*02	IGLV1-47*01	IGLJ3*01
ewe191-C12	IGHV5-51*01	IGHD3-10*02	IGHJ5*02	IGLV1-44*01	IGLJ3*01
ewe191-D1	IGHV3-21*01	IGHD2-21*02	IGHJ4*02	IGLV1-47*02	IGLJ3*01
ewe191-E12	IGHV5-51*01	IGHD3-16*01	IGHJ5*02	IGLV1-44*01	IGLJ1*01
ewe191-H8	IGHV3-23*04	IGHD3-10*01	IGHJ4*02	IGLV1-44*01	IGLJ3*02
ewe191-H10	IGHV3-21*01	IGHD2-21*02	IGHJ4*02	IGLV3-21*02	IGLJ3*02
ewe192-A6	IGHV4-39*01	IGHD6-6*01	IGHJ6*02	IGKV3-15*01	IGKJ5*01
ewe192-B5	IGHV4-34*01	IGHD4-17*01	IGHJ2*01	IGKV1D-39*01	IGKJ4*01
ewe192-C11	IGHV3-21*01	IGHD5-24*01	IGHJ3*02	IGLV8-61*01	IGLJ3*01
ewe192-D7	IGHV3-21*01	IGHD5-24*01	IGHJ3*02	IGLV2-23*03	IGLJ3*02
ewe192-D8	IGHV4-39*01	IGHD6-6*01	IGHJ6*02	IGLV3-21*02	IGLJ3*02
ewe192-E4	IGHV4-39*01	IGHD6-6*01	IGHJ6*02	IGKV3-20*01	IGKJ4*01
ewe192-F6	IGHV4-39*01	IGHD6-6*01	IGHJ6*02	IGKV3-20*01	IGKJ1*01
ewe192-F11	IGHV4-39*01	IGHD6-6*01	IGHJ6*02	IGLV1-40*01	IGLJ3*01
ewe192-G12	IGHV4-39*01	IGHD6-6*01	IGHJ6*02	IGKV3-15*01	IGKJ3*01
ewe192-H7	IGHV3-21*01	IGHD6-6*01inv	IGHJ3*02	IGLV2-23*03	IGLJ3*02
ewe192-H8	IGHV4-39*01	IGHD6-6*01	IGHJ6*02	IGKV3D-15*01	IGKJ5*01
ewe192-H11	IGHV3-21*01	IGHD6-6*01inv	IGHJ3*02	IGLV2-11*01	IGLJ3*02

One antibody contained a stop codon in the sixth position of the VH chain (ewe192-B5). For this antibody, the germline was analyzed which confirmed that IGHV4-34*01 has the amino acid glutamine (Q) at position 6. After PIPE cloning the stop codon was changed to the amino acid Q. Further, this antibody will be called ewe192-B5(P).

3.3.2 Panning in solution

For the strategy of panning in solution biotinylated antigen was used and pulled down with magnetic streptavidin beads. Here, only the immune libraries were used for antibody selection, because the naive library did not result in neutralizing antibodies in the former plate panning. To monitor the enrichment of diphtheria toxin binding phage by panning in solution, a phage ELISA was performed with phage particles of all three panning rounds (figure 7).

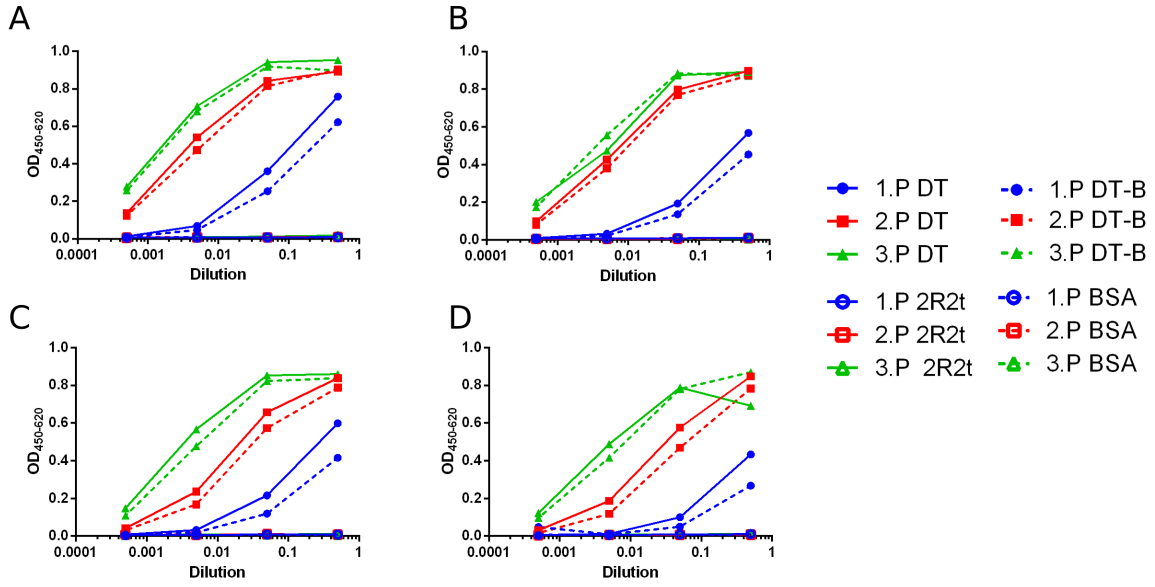

Figure 7: Titration phage ELISA with packaged antibody-phage from panning round 1 (1.P; blue), panning round 2 (2.P; red) and panning round 3 (3. P; green). The two immune libraries (VJN & CD138+) were analyzed, separated by lambda and kappa. A) VJN lambda, B) VJN kappa, C) CD138+ lambda and D) CD138+ kappa. Binding was tested on diphtheria toxin (DT; filled symbol, solid line), the biotinylated diphtheria toxin (DT-B; filled symbol, dotted line), 2R2t (non related protein; open symbol, solid line) and BSA (negative control; open symbol, dotted line). Detected with goat α pVIII HRP conjugated antibody, visualized with TMB substrate and measured at 450 nm with a 620 nm reference.

An enrichment of binders to diphtheria toxin and biotinylated diphtheria toxin was shown over 3 panning rounds. Best binding capability was achieved after 3 panning rounds (green lines). Biotinylated DT was the antigen used for the panning in solution. All immune libraries bound the DT (filled symbol, solid line) as well as the biotinylated DT (filled symbol, dotted line). No cross reactivity to 2R2t (open symbol, solid line) or BSA (open

symbol, dotted line) was observed.

The antibody pool was directly cloned in scFv-Fc format (pCSE2.7-hIgG1-Fc-xp). 384 (4x 96) scFv-Fc monoclonal antibodies were selected. All of these antibodies were further produced in EXPI293F cells in 96 deepwell plates. The produced antibodies were secreted in the growth medium and the supernatant was used for performing the neutralization assay. A serial dilution of the supernatant was incubated with a constant amount of diphtheria toxin (4x MCD) and after 6 days of incubation with Vero cells, the cytopathic effect was measured with an MTT assay. These produced antibodies were analyzed regarding their neutralization efficacy in neutralization assay (figure 8 and supplemental figure 27, 28, 29 and 30).

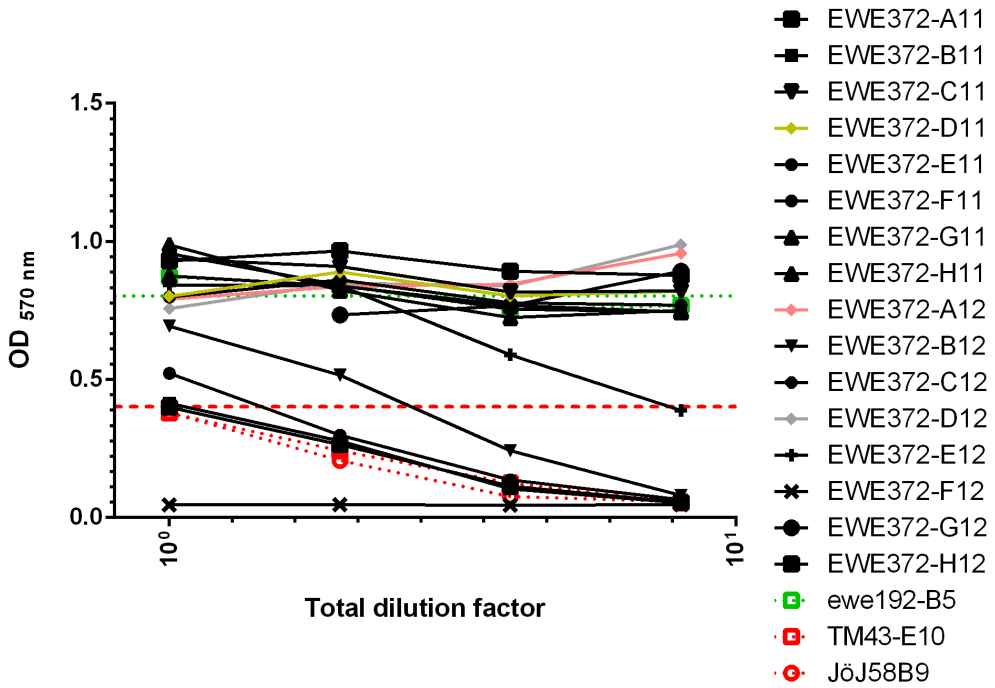

Figure 8: Neutralization assay of scFv-Fc in supernatant for screening. Untreated Vero cells are given as horizontal green dotted line. The threshold for neutralization is given as horizontal red dotted line (50 % of untreated Vero cells). The antibodies TM43-E10 and JöJ58B9 (red, open symbols and dotted line) are considered as negative control, ewe192-B5 (green, open symbol and dotted line) as positive control. scFv-Fc antibodies shown in color and gray were further analyzed. Samples with black symbol were not further considered. Mitochondrial activity was measured with an MTT assay after 6 days at OD_{570nm}.

Cells reaching a neutralization effect above the 50 % line (red dotted line) were regarded as neutralizers. In the exemplary figure 8, the colored antibodies ewe372-A12 (pink diamond), ewe372-D11 (dark yellow diamond) and ewe372-D12 (gray diamond) were further analyzed. The antibody ewe192-B5 was used as positive control in the neutralization assays (green open square, dotted line) and as negative control the antibodies TM43-E10 (red open square, dotted line) and JöJ58B9 (red open circle, dotted line) were used. In total, 268 scFv-Fc showed neutralization and of these, 36 scFv-Fc antibodies were further analyzed. The V genes of these 36 scFv-Fc antibodies are shown in table 23.

Table 23: V gene analysis of 36 scFv-Fc clones selected for further analysis.

Name of clone	VH			VL	
	V	D	J	V	J
ewe371-A2	IGHV3-33*01	IGHD2-2*01inv	IGHJ3*02	IGLV2-14*04	IGLJ3*01
ewe371-A6	IGHV5-51*01	IGHD3-10*02	IGHJ5*02	IGLV3-21*01	IGLJ3*01
ewe371-B12	IGHV3-33*01	IGHD6-13*01	IGHJ4*03	IGLV1-47*01	IGLJ3*01
ewe371-D10	IGHV5-51*01	IGHD3-10*02	IGHJ5*02	IGLV1-44*01	IGLJ3*02
ewe371-D4	IGHV5-51*01	IGHD3-10*02	IGHJ5*02	IGLV3-19*01	IGLJ3*01
ewe371-D7	IGHV5-51*01	IGHD3-10*02	IGHJ5*02	IGLV1-44*01	IGLJ3*01
ewe371-E4	IGHV3-23*01	IGHD3-10*01	IGHJ4*02	IGLV2-14*04	IGLJ1*01
ewe371-E7	IGHV5-51*01	IGHD2-2*01	IGHJ5*02	IGLV2-8*01	IGLJ3*01
ewe371-G2	IGHV5-51*01	IGHD3-10*02	IGHJ5*02	IGLV1-44*01	IGLJ1*01
ewe371-G4	IGHV4-34*01	IGHD5-12*01	IGHJ6*02	IGLV1-44*01	IGLJ3*02
ewe371-G8	IGHV1-3*01	IGHD2-2*01	IGHJ6*02	IGLV1-44*01	IGLJ3*02
ewe371-H1	IGHV3-23*04	IGHD3-10*01	IGHJ4*02	IGLV1-44*01	IGLJ3*01
ewe371-H9	IGHV5-51*01	IGHD3-10*02	IGHJ5*02	IGLV1-44*01	IGLJ3*02
ewe372-A12	IGHV1-3*01	IGHD6-19*01	IGHJ3*01	IGKV1-27*01	IGKJ4*01
ewe372-A8	IGHV1-69*04	IGHD6-13*01	IGHJ3*02	IGKV1D-39*01	IGKJ3*01
ewe372-C10	IGHV4-34*01	IGHD2-2*02	IGHJ2*01	IGKV1D-39*01	IGKJ4*01
ewe372-C4	IGHV1-69*04	IGHD1-1*01	IGHJ4*02	IGKV1D-39*01	IGKJ4*01
ewe372-C5	IGHV1-69*04	IGHD2-2*02	IGHJ4*02	IGKV1D-39*01	IGKJ4*01
ewe372-C8	IGHV1-69*04	IGHD2-2*02	IGHJ4*02	IGKV1D-39*01	IGKJ4*01
ewe372-D11	IGHV1-18*01	IGHD3-10*01	IGHJ6*02	IGKV3-20*01	IGKJ4*01
ewe372-D12	IGHV1-69*04	IGHD2-2*02inv	IGHJ4*02	IGKV1D-39*01	IGKJ4*01

Name of clone	VH			VL	
	V	D	J	V	J
ewe372-D3	IGHV4-34*02	IGHD2-15*01	IGHJ4*02	IGKV3-15*01	IGKJ1*01
ewe372-D7	IGHV1-69*04	IGHD2-21*02	IGHJ4*02	IGKV1D-39*01	IGKJ4*01
ewe372-D9	IGHV1-46*03	IGHD1-20*01	IGHJ4*02	IGKV1D-33*01	IGKJ5*01
ewe372-F3	IGHV1-46*03	IGHD1-20*01	IGHJ4*02	IGKV1-12*02	IGKJ4*01
ewe372-F6	IGHV3-23*04	IGHD4-17*01inv	IGHJ6*02	IGKV1-5*03	IGKJ5*01
ewe372-G2	IGHV1-69*06	IGHD2-15*01	IGHJ4*02	IGKV1D-39*01	IGKJ4*01
ewe372-H1	IGHV4-34*02	IGHD4-17*01	IGHJ2*01	IGKV1D-39*01	IGKJ4*01
ewe374-C9	IGHV4-34*01	IGHD5-12*01	IGHJ6*02	IGLV1-44*01	IGLJ3*01
ewe374-E6	IGHV4-34*01	IGHD5-18*01	IGHJ6*02	IGLV3-19*01	IGLJ1*01
ewe374-F7	IGHV3-21*01	IGHD6-6*01inv	IGHJ3*02	IGLV2-23*03	IGLJ3*02
ewe375-B8	IGHV5-51*01	IGHD1-7*01	IGHJ5*02	IGKV3-20*01	IGKJ3*01
ewe375-G7	IGHV1-69*04	IGHD1-26*01	IGHJ4*02	IGKV1D-39*01	IGKJ3*01
ewe375-D2	IGHV4-39*01	IGHD6-6*01	IGHJ6*02	IGKV3-20*01	IGKJ5*01
ewe375-D4	IGHV4-34*02	IGHD4-17*01	IGHJ2*01	IGKV1D-39*01	IGKJ4*01
ewe375-H4	IGHV5-51*01	IGHD1-7*01	IGHJ5*02	IGKV3-20*01	IGKJ3*01

Three antibodies (ewe372-C10, ewe372-D3 and ewe372-H1) contained a stop codon in the sixth position of the VH chain. For these three antibodies, the germline was analyzed and confirmed that IGHV4-34 has the amino acid glutamine (Q) at position six. An introduced point mutation changed the stop codon to the amino acid Q. Additionally, it was checked the amino acid position 7 of the VH chain. At this position the already developed antibody ewe192-B5(P) had the amino acid serine (S) but germline analysis confirmed the amino acid tryptophan (W) occurred at this position. Hence, two versions were developed of each of the three antibodies and named after their seventh amino acid position ewe372-C10-S/ ewe372-C10-W, ewe372-D3-S/ ewe372-D3-W and ewe372-H1-S/ ewe372-H1-W. After these modifications, 39 scFv-Fc antibodies were further analyzed.

3.4 Characterization of monoclonal antibodies in scFv-Fc format

The 22 antibodies from panning on plates and 39 antibodies from panning in solution that showed good neutralization potency were characterized regarding their binding to diphtheria toxin and neutralization potency in a cell based *in vitro* assay. Finally, a domain mapping was performed to determine which domain was recognized by each scFv-Fc antibody.

3.4.1 Binding of monoclonal antibodies in scFv-Fc format

The half maximal effective concentration (EC50) was determined for all scFv-Fc antibodies by performing a titration ELISA on immobilized diphtheria toxin and the non-toxic DT-mutant CRM197 (figure 9). EC50 for diphtheria toxin widely ranged from 0.0086 µg/mL to 11.9 µg/mL. The non-toxic mutant CRM197 showed binding in the range of 0.0108 µg/mL to 18.38 µg/mL. For better visualization, antibodies with the lowest EC50 are marked in yellow, antibodies with the highest EC50 are marked in gray (table 24).
Out of 61 scFv-Fc antibodies, 16 showed a more than 3-fold increased binding to diphtheria toxin than to the similarly folded non-toxic DT-mutant CRM197. None of the antibodies showed unspecific binding to BSA. All antibodies were further tested for their neutralization potency.

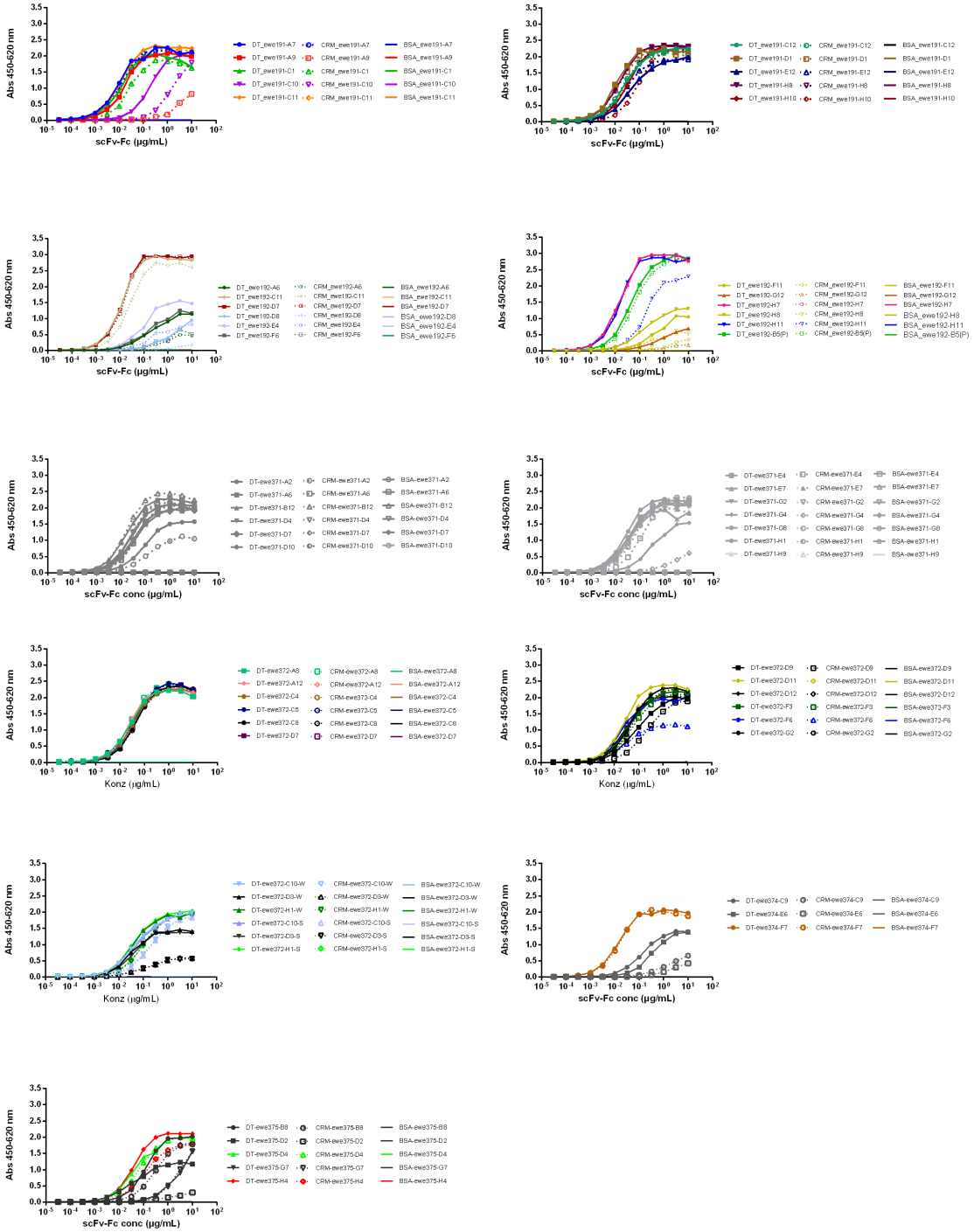

Figure 9: Titration ELISA of scFv-Fc antibodies for binding to diphtheria toxin (filled symbol, solid line) and CRM197 (non-toxic mutant; open symbol, dotted line) with BSA as negative control (line). Detected with goat α human Fc antibody HRP conjugated, visualized with TMB substrate and measured at 450 nm with 620 nm reference. Data was statistically evaluated with a non-linear fit (sigmoidal four parameters logistic, X-axis is log).

Table 24: EC50 (in µg/mL) of monoclonal scFv-Fc. EC50 was determined with a statistics software using a non-linear fit (sigmoidal four parameter logistic, X-axis is log).

#	Name antibody clone	DT EC50 (µg/mL)	CRM197 EC50 (µg/mL)	#	Name antibody clone	DT EC50 (µg/mL)	CRM197 EC50 (µg/mL)
1	ewe191-A7	0.0086	0.0108	31	ewe371-G2	0.02945	0.04119
2	ewe191-A9	0.0154	2.8240	32	ewe371-G4	0.2942	4.738
3	ewe191-C1	0.0101	0.0218	33	ewe371-G8	0.03405	0.04117
4	ewe191-C10	0.1748	1.5410	34	ewe371-H1	0.02254	0.06175
5	ewe191-C11	0.0105	0.0122	35	ewe371-H9	0.03138	0.04574
6	ewe191-C12	0.0254	0.0200	36	ewe372-A12	0.02153	0.03627
7	ewe191-D1	0.0100	0.0125	37	ewe372-A8	0.02257	0.02301
8	ewe191-E12	0.0459	0.0246	38	ewe372-C10-S	0.05643	0.2061
9	ewe191-H10	0.0335	0.0839	39	ewe372-C10-W	0.04717	0.1936
10	ewe191-H8	0.0143	0.0251	40	ewe372-C4	0.03015	0.03387
11	ewe192-A6	0.2031	0.6579	41	ewe372-C5	0.03221	0.03299
12	ewe192-B5(P)	0.0441	0.0587	42	ewe372-C8	0.03915	0.04011
13	ewe192-C11	0.0113	0.0227	43	ewe372-D11	0.02329	0.03616
14	ewe192-D7	0.0119	0.0133	44	ewe372-D12	0.04246	0.04771
15	ewe192-D8	3.9280	3.3680	45	ewe372-D3-S	0.05643	0.2061
16	ewe192-E4	0.0920	0.2222	46	ewe372-D3-W	0.04717	0.1936
17	ewe192-F11	0.49	2.0760	47	ewe372-D7	0.03223	0.0365
18	ewe192-F6	0.1558	0.5040	48	ewe372-D9	0.08502	0.2127
19	ewe192-G12	0.89	1.4080	49	ewe372-F3	0.03983	0.05432
20	ewe192-H11	0.0143	0.1678	50	ewe372-F6	0.01995	0.0313
21	ewe192-H7	0.0138	0.0144	51	ewe372-G2	0.02719	0.03091
22	ewe192-H8	0.1589	0.3111	52	ewe372-H1-S	0.0382	0.1002
23	ewe371-A2	0.08299	0.1176	53	ewe372-H1-W	0.0364	0.09968
24	ewe371-A6	0.03316	0.04078	54	ewe374-C9	0.1311	2.049
25	ewe371-B12	0.01456	0.0141	55	ewe374-E6	0.3193	2.255
26	ewe371-D10	0.02058	0.02136	56	ewe374-F7	0.01272	0.01367
27	ewe371-D4	0.02356	0.02439	57	ewe375-B8	0.1135	0.2739
28	ewe371-D7	0.02815	0.03871	58	ewe375-D2	0.03781	18.38
29	ewe371-E4	0.03578	0.1132	59	ewe375-D4	0.04593	0.06574
30	ewe371-E7	0.02544	0.03123	60	ewe375-G7	11.9	3.429
				61	ewe375-H4	0.03662	0.1174

3.4.2 Neutralization in scFv-Fc format

After the validation of binding to diphtheria toxin, the neutralization was analyzed in a cell based *in vitro* assay (figure 10 and 11).

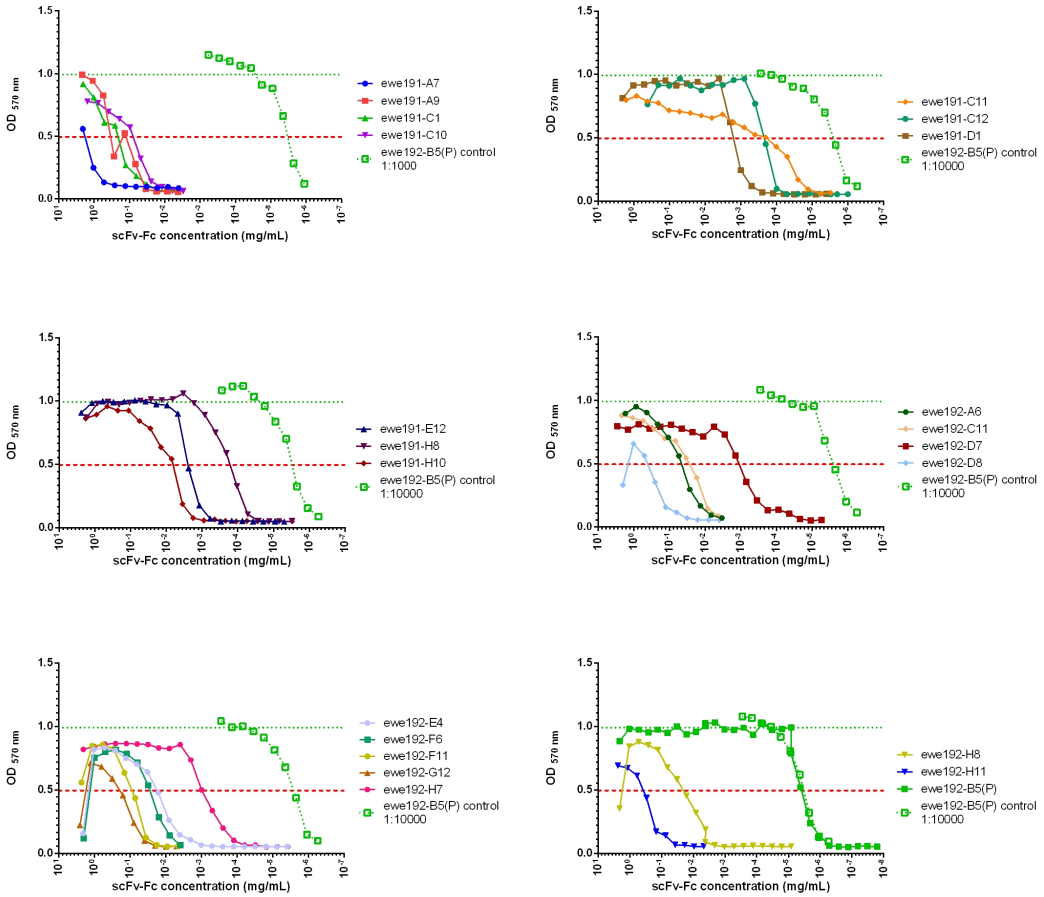

Figure 10: Cell based neutralization assay of scFv-Fc antibodies. Untreated Vero cells are given as green dotted line. The threshold for neutralization is given as red dotted line (50 % of untreated Vero cells). The antibody ewe192-B5(P) (green, open symbol and dotted line) is considered as positive control. All antibodies shown were further analyzed. Mitochondrial activity was measured with an MTT assay after 6 days at OD_{570nm}.

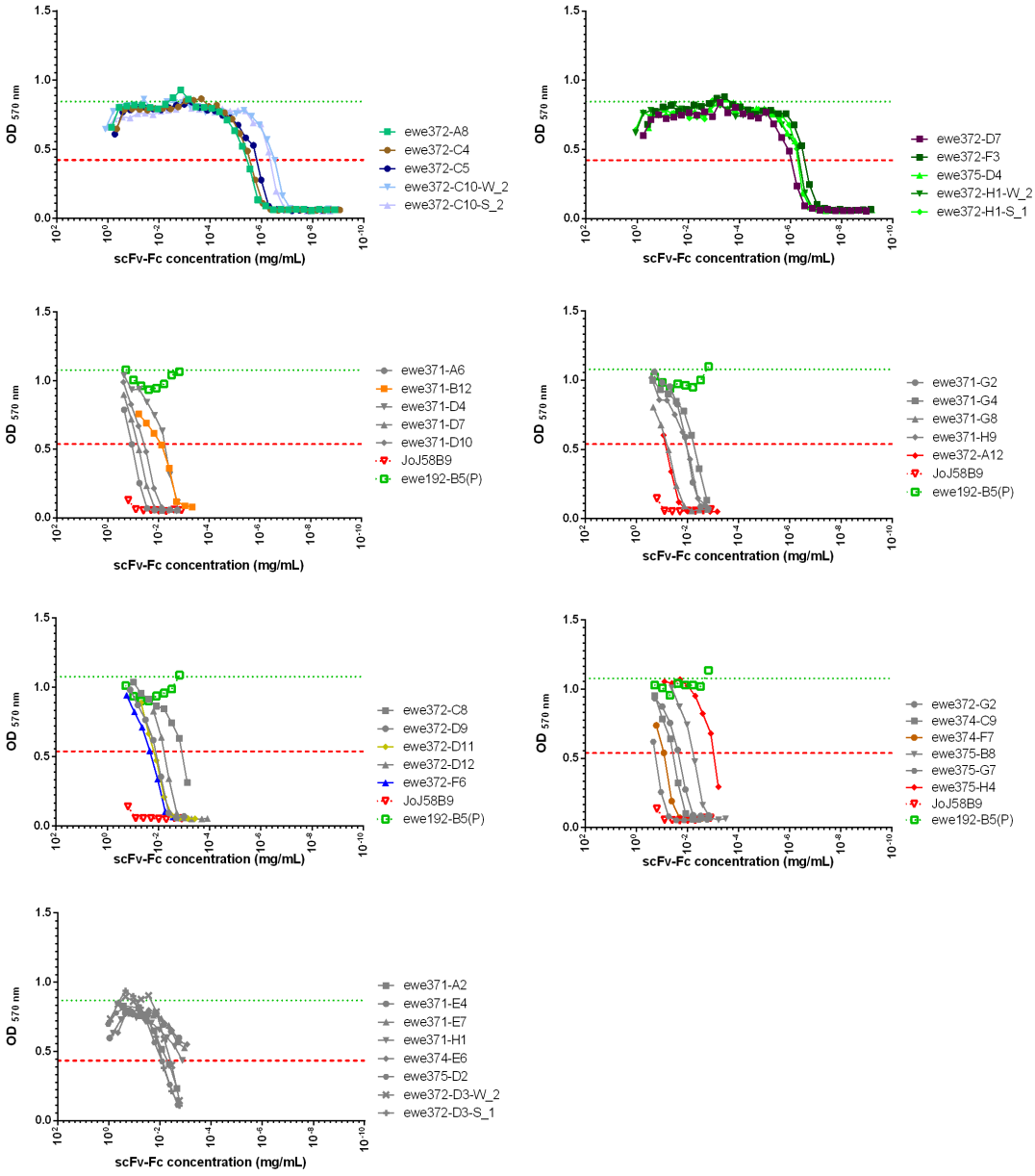

Figure 11: Cell based neutralization assay of scFv-Fc antibodies. Untreated Vero cells are given as green dotted line. The threshold for neutralization is given as red dotted line (50 % of untreated Vero cells). The antibody JöJ58B9 (red, open symbols and dotted line) is considered as negative control, the antibody ewe192-B5(P) (green, open symbol and dotted line) as positive control. Antibodies represented in colored symbols were further analyzed, antibodies represented in gray symbols were disregarded in further analysis. Mitochondrial activity was measured with an MTT assay after 6 days at OD_{570nm}.

Table 25: Minimal effective dose 50 % (MED50%) in nM for scFv-Fc antibodies.

#	Name antibody clone	MED 50% (nM)	#	Name antibody clone	MED 50% (nM)
1	ewe191-A7	18854.3	31	ewe371-G2	1.107
2	ewe191-A9	1266.1	32	ewe371-G4	0.622
3	ewe191-C1	2360.9	33	ewe371-G8	9.841
4	ewe191-C10	1821.7	34	ewe371-H1	24.007
5	ewe191-C11	7.6	35	ewe371-H9	1.419
6	ewe191-C12	7.3	36	ewe372-A12	8.032
7	ewe191-D1	36.9	37	ewe372-A8	0.05126
8	ewe191-E12	43.2	38	ewe372-C10-S	0.00483
9	ewe191-H10	65.4	39	ewe372-C10-W	0.00551
10	ewe191-H8	3.9	40	ewe372-C4	0.03261
11	ewe192-A6	500.8	41	ewe372-C5	0.01906
12	ewe192-B5(P)	0.075	42	ewe372-C8	0.140
13	ewe192-C11	313.8	43	ewe372-D11	2.231
14	ewe192-D7	26.4	44	ewe372-D12	0.723
15	ewe192-D8	4667.8	45	ewe372-D3-S	128.760
16	ewe192-E4	301.3	46	ewe372-D3-W	63.490
17	ewe192-F11	1312.7	47	ewe372-D7	0.01039
18	ewe192-F6	287.9	48	ewe372-D9	1.470
19	ewe192-G12	2911.9	49	ewe372-F3	0.00339
20	ewe192-H11	5506.8	50	ewe372-F6	2.011
21	ewe192-H7	18.8	51	ewe372-G2	2.236
22	ewe192-H8	303.6	52	ewe372-H1-S	0.00515
23	ewe371-A2	77.27	53	ewe372-H1-W	0.00508
24	ewe371-A6	20.32	54	ewe374-C9	4.238
25	ewe371-B12	1.407	55	ewe374-E6	7.6778
26	ewe371-D10	5.496	56	ewe374-F7	7.641
27	ewe371-D4	0.642	57	ewe375-B8	0.946
28	ewe371-D7	10.621	58	ewe375-D2	151.617
29	ewe371-E4	16.373	59	ewe375-D4	0.00619
30	ewe371-E7	10.134	60	ewe375-G7	20.02
			61	ewe375-H4	0.114

The neutralization of the purified scFv-Fc was between 18.8 µM and 3.3 pM at a constant amount of DT (4x MCD). For better visualization, antibodies with the lowest MED50% are marked in yellow, antibodies with the highest MED50% are marked in gray (table 25).
It was shown, that all purified scFv-Fc antibodies have neutralizing potency against DT. Most of the scFv-Fc had a neutralization efficacy in the nanomolar range.

3.4.3 Domain mapping

The diphtheria toxin is an AB-toxin. It consists of 2 fragments (A-fragment and B-fragment). The A-fragment is the catalytic part (= C-domain) and the B-fragment is divided into 2 domains, the receptor binding domain (R-domain) and the translocation domain (T-domain). Each fragment and domain was genetically His-tagged and expressed and purified from *E. coli*. The purity and integrity of all recombinant protein was controlled by SDS-PAGE followed by Coomassie blue staining (supplemental figure 31).

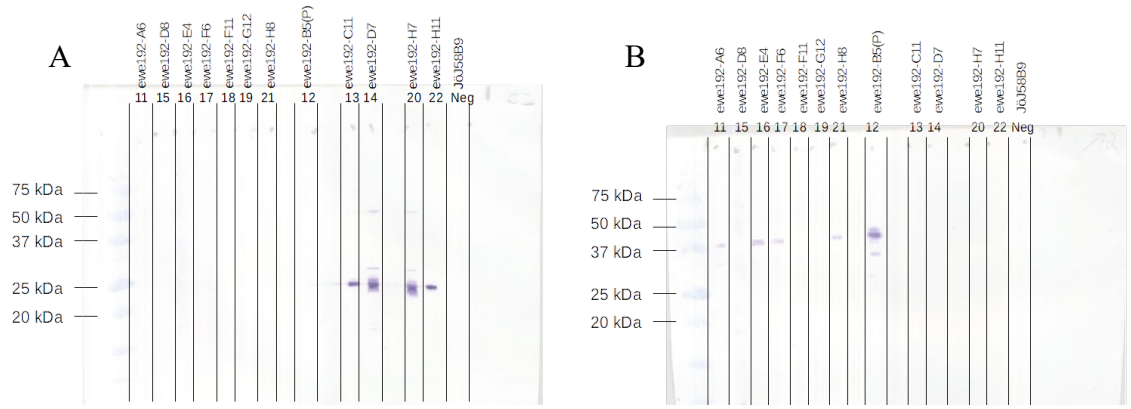

Figure 12: Western Blot and immuno stain after SDS-PAGE for domain mapping of scFv-Fc antibodies derived from panning with immobilized antigen. All scFv-Fc antibodies were tested on both fragments of diphtheria toxin: A) A-fragment (21 kDa) and B) B-fragment (37 kDa). Detected with goat α-human Fc antibody AP conjugated, visualized with NBT/BCIP. Antibodies showed different binding patterns, i.e. either to the A or the B fragment of DT. JöJ58B9 served as negative control.

The recombinant proteins were separated by SDS-PAGE followed by immuno staining to determine which domain of diphtheria toxin was recognized by each scFv-Fc (figure 12, supplemental figure 32, 33 and 34).

Each scFv-Fc antibody bound specifically to one of the two fragments. Here, the antibodies ewe192-C11, ewe192-D7, ewe192-H7 and ewe192-H11 bound specifically to the A-fragment. The antibodies ewe192-A6, ewe192-E4, ewe192-F6, ewe192-H8 and ewe192-B5(P) bound specifically to the B-fragment. In case of B-fragment recognition, the antibodies were further tested on the R- and T-domain. The antibody ewe192-B5(P) bound to the R-domain, the other antibodies bound only the B-fragment (supplemental figure 34). The antibodies ewe192-D8, ewe192-F11 and ewe192-G12 did not bind in Western blot at all. Table 26 summarizes all scFv-Fc antibodies and which domain of the diphtheria toxin they recognize.

Table 26: Analyzed scFv-Fc antibodies and their respective binding domain. nd = not determined

#	Name antibody clone	Domain	#	Name antibody clone	Domain
1	ewe191-A7	C-domain	31	ewe371-G2	R-domain
2	ewe191-A9	C-domain	32	ewe371-G4	nd
3	ewe191-C1	C-domain	33	ewe371-G8	R-domain
4	ewe191-C10	nd	34	ewe371-H1	nd
5	ewe191-C11	C-domain	35	ewe371-H9	R-domain
6	ewe191-C12	R-domain	36	ewe372-A12	C-domain
7	ewe191-D1	C-domain	37	ewe372-A8	R-domain
8	ewe191-E12	R-domain	38	ewe372-C10-S	R-domain
9	ewe191-H10	C-domain	39	ewe372-C10-W	R-domain
10	ewe191-H8	C-domain	40	ewe372-C4	R-domain
11	ewe192-A6	B-fragment	41	ewe372-C5	R-domain
12	ewe192-B5(P)	R-domain	42	ewe372-C8	R-domain
13	ewe192-C11	C-domain	43	ewe372-D11	C-domain
14	ewe192-D7	C-domain	44	ewe372-D12	R-domain
15	ewe192-D8	nd	45	ewe372-D3-S	nd
16	ewe192-E4	B-fragment	46	ewe372-D3-W	nd
17	ewe192-F11	nd	47	ewe372-D7	R-domain
18	ewe192-F6	B-fragment	48	ewe372-D9	B-fragment
19	ewe192-G12	nd	49	ewe372-F3	R-domain
20	ewe192-H11	C-domain	50	ewe372-F6	T-domain
21	ewe192-H7	C-domain	51	ewe372-G2	R-domain

#	Name antibody clone	Domain	#	Name antibody clone	Domain
22	ewe192-H8	B-fragment	52	ewe372-H1-S	R-domain
23	ewe371-A2	nd	53	ewe372-H1-W	R-domain
24	ewe371-A6	B-fragment	54	ewe374-C9	nd
25	ewe371-B12	C-domain	55	ewe374-E6	nd
26	ewe371-D10	R-domain	56	ewe374-F7	C-domain
27	ewe371-D4	R-domain	57	ewe375-B8	nd
28	ewe371-D7	B-fragment	58	ewe375-D2	nd
29	ewe371-E4	nd	59	ewe375-D4	R-domain
30	ewe371-E7	nd	60	ewe375-G7	B-fragment
			61	ewe375-H4	C-domain

It was shown, that eight scFv-Fc antibodies bound specifically the B-fragment and 16 bound the C-domain (= A-fragment). 21 scFv-Fc antibodies bound specifically the R-domain and one bound the T-domain. The domain of the other 15 scFv-Fc could not be determined.

3.4.4 Epitope mapping of ewe192-B5

The scFv-Fc antibody ewe192-B5(P) was the first neutralizer developed with a neutralization potency over 100 IU/mg. This antibody recognizes the R-domain of diphtheria toxin. For determination of the epitope of this antibody a PepSpot membrane with the sequence of the R-domain of diphtheria toxin was used (figure 13).

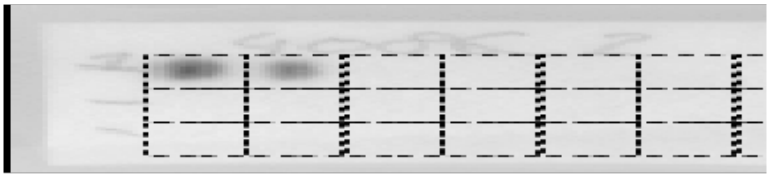

Figure 13: Epitope mapping for ewe192-B5(P) on a PepSpot membrane of fragmented R-domain with 15 amino acid (aa) spots and overlap of 12 aa. Detection of ewe192-B5(P) with goat α-human HRP conjugated secondary antibody.

The first 2 spots on the membrane were stained by the ewe192-B5(P) scFv-Fc antibody. This corresponds to the amino acids AYSPGHKTQPFLHDG (first spot) and PGHKTQPFLHDGYAV (second spot). The overlapping sequence is underlined AYSPGHKTQPFLHDGYAV and gives the potential epitope. Figure 14 shows the epitope (purple) in the structure of the full diphtheria toxin (shown in pdb-file 1DDT).

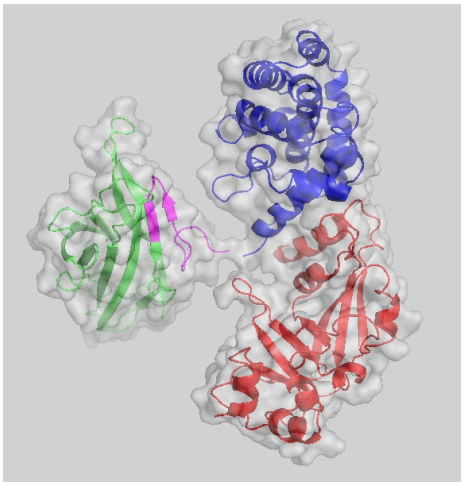

Figure 14: Protein structure of diphtheria toxin (in pdb-file 1DDT). With the 3 domains C-domain (red), T-domain (blue) and R-domain (green). The epitope detected with PepSpot membrane is marked purple.

3.5 Characterization of monoclonal antibodies in IgG

The best neutralizing scFv-Fc antibodies were converted into IgG format. Therefor, additional restriction sites were added on the VH and VL 5' and 3' end to fit into the IgG vectors pCSE1c for VH or one of the two VL vectors pCSL3l or pCSL3k. The 38 antibodies were produced for 7 days in EXPI293F cells, afterwards purified with protein A and buffered in PBS. Three of the IgG antibodies were not producible in IgG format (ewe372-C10-S, ewe372-F3 and ewe374-F7).

3.5.1 Binding on diphtheria toxin and CRM197 in IgG

After converting antibodies in the IgG format, the ability of the IgG antibodies to bind diphtheria toxin and CRM197 was tested (figure 15).

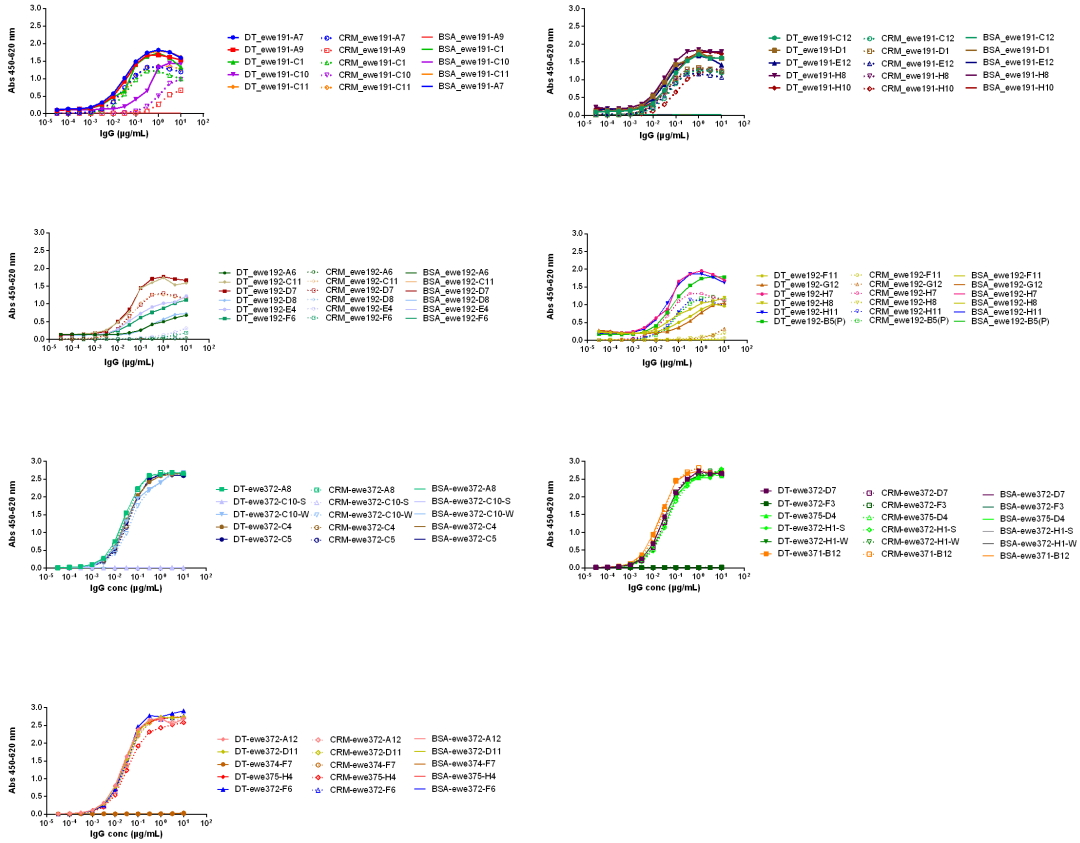

Figure 15: Titration ELISA of scFv-Fc antibodies for binding to diphtheria toxin (filled symbol, solid line) and CRM197 (non-toxic mutant; open symbol, dotted line) with BSA as negative control (line). Detected with goat α-human Fc HRP conjugated antibody, visualized with TMB substrate and measured at 450 nm with 620 nm reference. Data was statistically evaluated with a non-linear fit (sigmoidal four parameters logistic, X-axis is log).

Table 27: EC50 (in µg/mL) of monoclonal IgG.

#	Name antibody clone	DT EC50 (µg/mL)	CRM197 EC50 (µg/mL)
1	ewe191-A7	0.0244	0.0245
2	ewe191-A9	0.0264	1.4110
3	ewe191-C1	0.0381	0.0311
4	ewe191-C10	0.3541	1.0200
5	ewe191-C11	0.0253	0.0312
6	ewe191-C12	0.0466	0.0468
7	ewe191-D1	0.0266	0.0310

#	Name antibody clone	DT EC50 (µg/mL)	CRM197 EC50 (µg/mL)
8	ewe191-E12	0.0297	0.0329
9	ewe191-H8	0.0285	0.0332
10	ewe191-H10	0.0578	0.0931
11	ewe192-A6	0.4095	40.0800
12	ewe192-B5(P)	0.0535	0.0679
13	ewe192-C11	0.0337	0.0312
14	ewe192-D7	0.0333	0.0291
15	ewe192-D8	0.3612	2.4640
16	ewe192-E4	0.0681	30.9200
17	ewe192-F6	0.1380	7.5480
18	ewe192-F11	0.2021	31.6400
19	ewe192-G12	0.5226	34.1600
20	ewe192-H7	0.0349	0.0245
21	ewe192-H8	0.0938	3.5430
22	ewe192-H11	0.0263	0.0453
23	ewe371-B12	0.0182	0.0214
24	ewe372-A12	0.0210	0.0291
25	ewe372-A8	0.0239	0.0279
26	ewe372-C10-W	0.0356	0.0548
27	ewe372-C4	0.0323	0.0381
28	ewe372-C5	0.0344	0.0398
29	ewe372-D11	0.0243	0.0311
30	ewe372-D7	0.0286	0.0329
31	ewe372-F6	0.0264	0.0284
32	ewe372-H1-S	0.0282	0.0467
33	ewe372-H1-W	0.0283	0.0416
34	ewe375-D4	0.0274	0.0362
35	ewe375-H4	0.0220	0.0343

All IgG antibodies bound the diphtheria toxin. Not all antibodies showed a proper binding to the non-toxic mutant CRM197. EC50 for diphtheria toxin ranged from 0.0182 µg/mL to 0.523 µg/mL. The non-toxic mutant CRM197 showed binding in the range of 0.0214 µg/mL to 40.08 µg/mL. For better visualization, antibodies with the lowest EC50

are marked in yellow, antibodies with the highest EC50 are marked in gray (table 27).
Out of 35 scFv-Fc antibodies, 15 showed a more than 3-fold increased binding to diphtheria toxin than to the similarly folded non-toxic DT-mutant CRM197. None of the antibodies showed unspecific binding to BSA. All antibodies were further tested for their neutralization potency.

3.5.2 Neutralization in IgG format

All the IgG were tested for their ability to neutralize the diphtheria toxin in a cell-based neutralization assay (figure 16).
Nearly all produced IgG antibodies kept their neutralization abilities while changing the format from scFv-Fc to IgG. One IgG lost its neutralization behavior, ewe191-C10. The minimal effective dose 50 % of all purified IgG antibodies was between 1.4 µM and 3.0 pM at a constant amount of DT (4x MCD). For better visualization, antibodies with the lowest MED50% are marked in yellow, antibodies with the highest MED50% are marked in gray (table 28).

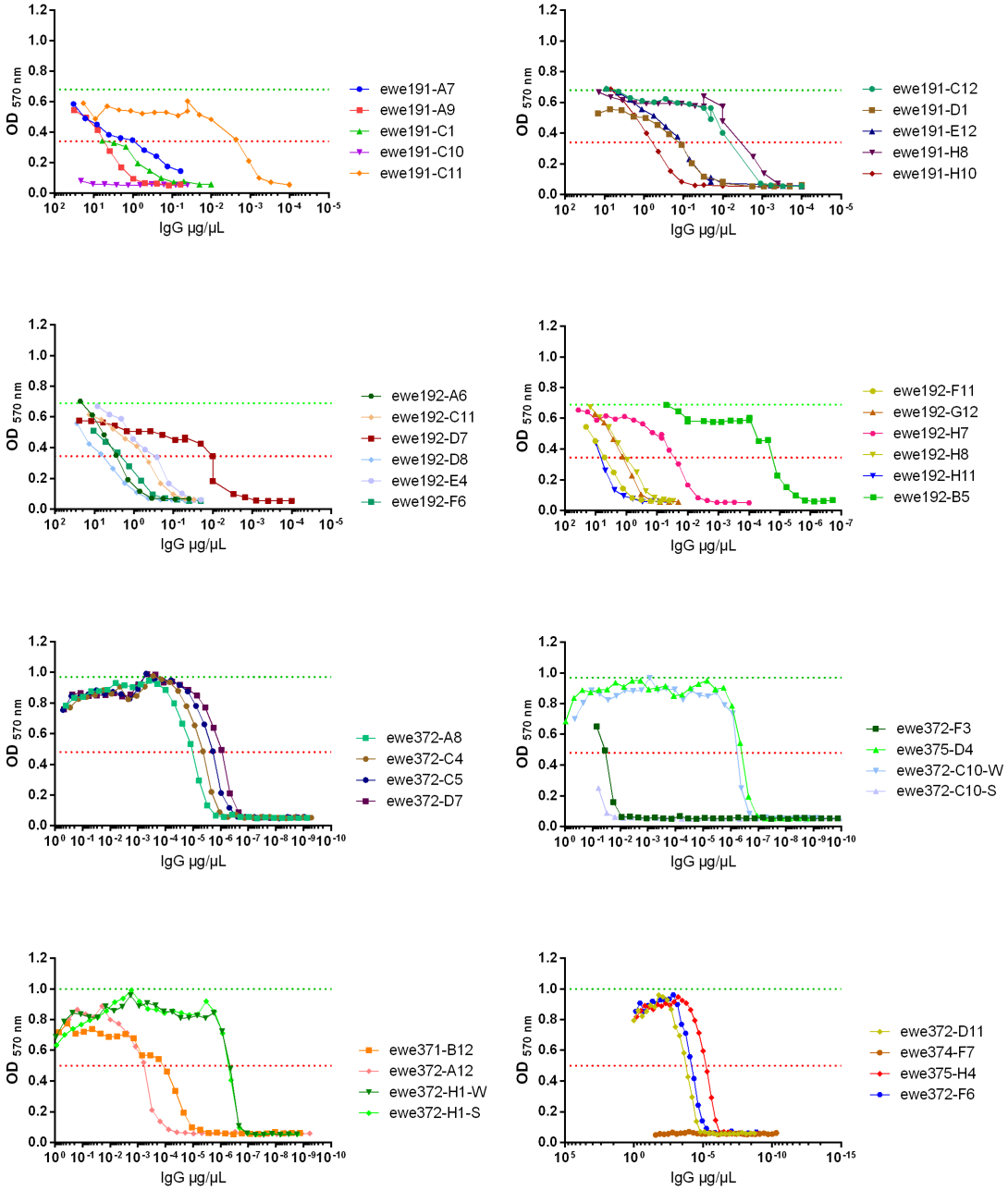

Figure 16: Cell-based neutralization assay of IgG antibodies. Untreated Vero cells are given as green dotted line. The threshold for neutralization is given as red dotted line (50 % of untreated Vero cells). Mitochondrial activity was measured with an MTT assay after 6 days at OD_{570nm}.

Table 28: Minimal effective dose 50 % (MED50) for IgG antibodies.

#	Name antibody clone	Minimal effective dose 50% (nM)
1	ewe191-A7	140.3
2	ewe191-A9	1098.5
3	ewe191-C1	818.5
4	ewe191-C10	-
5	ewe191-C11	0.6
6	ewe191-C12	2.4
7	ewe191-D1	31.2
8	ewe191-E12	19.2
9	ewe191-H8	1.0
10	ewe191-H10	119.1
11	ewe192-A6	780.7
12	ewe192-B5(P)	0.007
13	ewe192-C11	116.7
14	ewe192-D7	3.4
15	ewe192-D8	949.3
16	ewe192-E4	35.7
17	ewe192-F6	357.6
18	ewe192-F11	1415.9
19	ewe192-G12	180.8
20	ewe192-H7	10.9
21	ewe192-H8	254.0
22	ewe192-H11	1351.3
23	ewe371-B12	1.2028
24	ewe372-A12	4.1944
25	ewe372-A8	0.0826
26	ewe372-C10-W	0.0057
27	ewe372-C4	0.0297
28	ewe372-C5	0.0133
29	ewe372-D11	1.6808
30	ewe372-D7	0.0062
31	ewe372-F6	0.6098
32	ewe372-H1-S	0.0057

#	Name antibody clone	Minimal effective dose 50% (nM)
33	ewe372-H1-W	0.0030
34	ewe375-D4	0.0031
35	ewe375-H4	0.0669

The MED50 % was converted in International Unit (IU) per mg by using the WHO International Standard for DT. The results are summarized in figure 17.

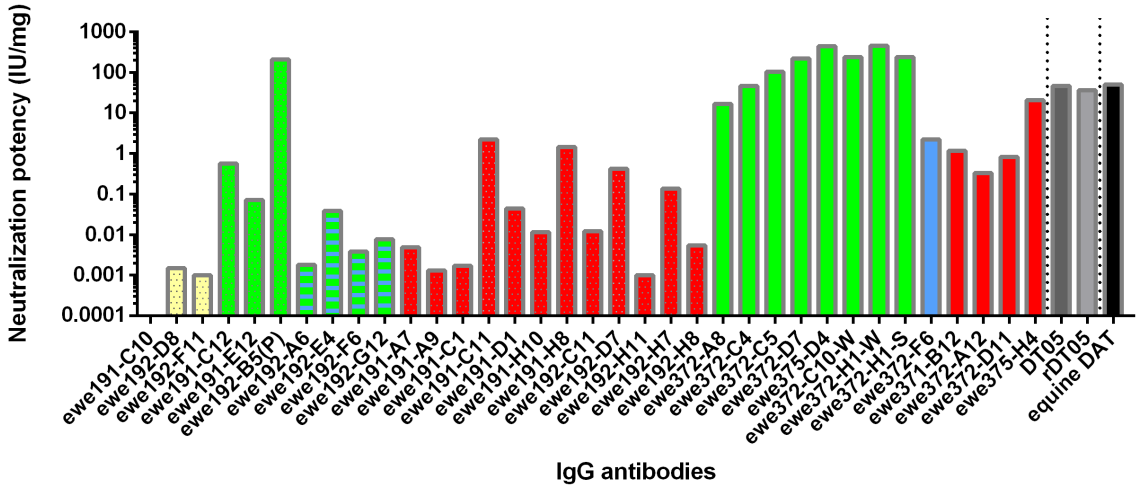

Figure 17: Neutralization potency (IU/mg) of a Vero cell based neutralization assay. All measured IgGs are given in the colors of their corresponding binding domain (red = C-domain, green = R-domain, blue = T-domain, green/blue-striped = B-fragment, yellow = unknown domain). All striped or dotted bars belongs to the IgG derived from panning on microtiter plates, all full colored bars are IgGs derived from panning in solution. The gray colored antibodies are the best neutralizing antibodies from NIBSC, DT05 = rat hybridoma and rDT05 = recombinat IgG from DT05. Black colored is the equine Diphtheria Anti Toxin (DAT) serum.

The monoclonal antibodies showed neutralization between 0 – 455 IU/mg. Rat hybridoma antibodies from NIBSC showed neutralization around 50 IU/mg with the hybridoma antibody (gray) and the recombinant version of DT05 (rDT05; light gray). Equine Diphtheria Anti Toxin (DAT) is the currently common used therapeutic against diphtheria. This polyclonal equine serum showed a neutralization of approximately 50 IU/mg (black). The best neutralizing mAbs showed binding against the receptor binding domain. Binders

derived from panning in solution (full colored bars) showed on average a better neutralization potency than antibodies derived from panning on microtiter plates (dotted or striped bars). The best neutralizing antibody against the receptor binding domain is ewe375-D4, the best neutralizer against the catalytic domain is ewe375-H4 and the neutralizer against the T-domain is ewe372-F6. The next step was to test the combinations of antibodies against different domains.

3.5.3 Synergistic effect (combination of antibodies)

Combinations of the antibodies determined with the best neutralization were used to mimic a polyclonal serum and to detect potential synergistic effects. A cell-based neutralization assay was performed combining antibodies. Three different approaches were performed. First, all antibodies from either panning with immobilized antigen or panning in solution were combined. Second, all antibodies recognizing the C-domain were combined. And third, all antibodies recognizing the R-domain were combined (figure 18). For the antibodies derived from the panning in solution, combinations with antibodies against the T-domain were also performed.

It was shown, when combining antibodies, the neutralization performance adjusts to the best neutralizing antibody in the mixture. For the panning with immobilized antigen (figure 18 A) the antibody ewe192-B5(P) was the best neutralizing antibody and determined the effect in the mixture. For antibodies from the panning in solution (figure 18 B) the antibody ewe375-D4 was the best neutralizing antibody. Combining all antibodies together did not show a synergistic effect.

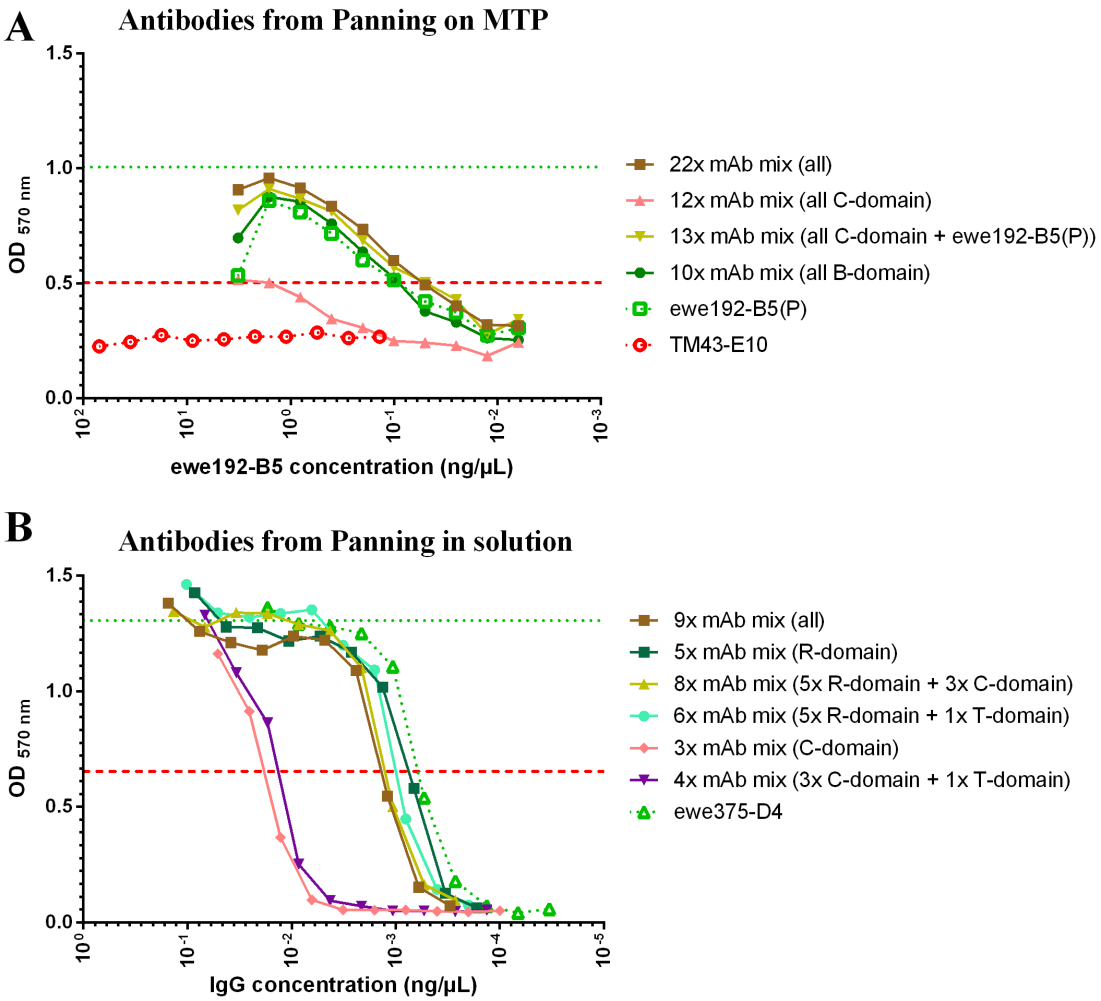

Figure 18: Cell-based neutralization assay of IgG antibody combinations. Untreated Vero cells are given as green dotted line. The threshold for neutralization is given as red dotted line (50 % of untreated Vero cells). Combinations of antibodies are given in the following colors with filled symbols and solid lines: All monoclonal antibodies (mAb) combined in brown, all mAbs against C-domain in pink, mAbs against R-domain combined with mAbs against C-domain in yellow, mAbs against R-domain in green, mAbs against R-domain combined with mAb against T-domain in turquoise and mAbs against C-domain combined with mAb against T-domain in purple. Negative control was an unrelated antibody (TM43-E10; red circle with dotted line), positive control was the best neutralizing mAb alone A) ewe192-B5(P) B) ewe375-D4; green open symbol with dotted line). Mitochondrial activity was measured with the MTT assay after 6 days at OD570nm.

For the antibodies derived from panning in solution, a more detailed analysis of combination was done. The best five neutralizing IgG antibodies were further tested in each possible combination with the best neutralizers against the C-domain and the one neutralizer against the T-domain (supplemental figure 35). An example of the best R-domain neutralizer (ewe375-D4), combined with the best T- and C-domain neutralizers (ewe372-F6 and ewe375-H4, respectively) is shown in figure 19.

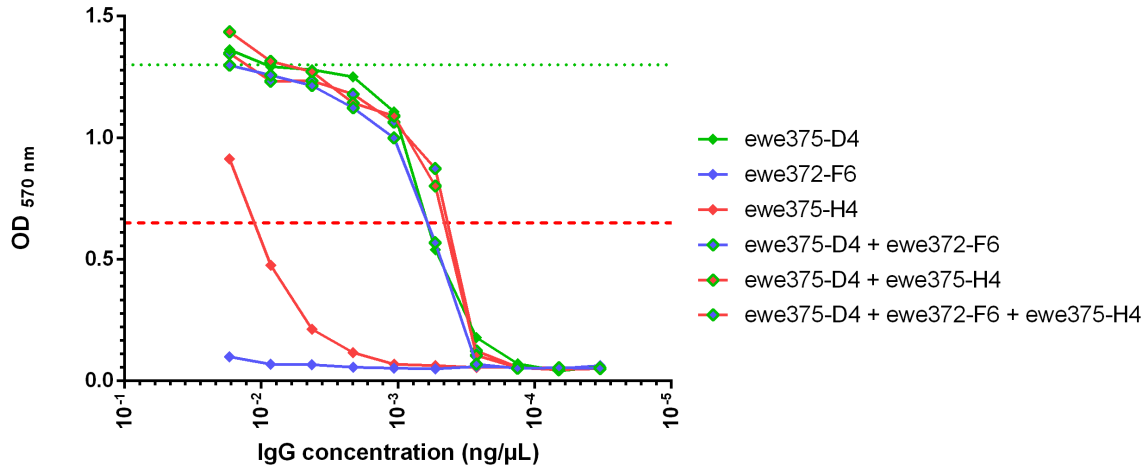

Figure 19: Cell-based neutralization assay of IgG antibody combinations. Untreated Vero cells are given as green dotted line. The threshold for neutralization is given as red dotted line (50 % of untreated Vero cells). Single antibodies are given in a single color (filled symbol, solid line), combinations of antibodies are given in the colors they domain is binding against (red = C-domain, green = R-domain and blue = T-domain; filling of symbol and color of line variant). Mitochondrial activity was measured with an MTT assay after 6 days at OD_{570nm}.

It was shown that the neutralization potency of the best neutralizer in the mixture determined the neutralization potency of all combinations. This was in all studied cases the R-domain binder, here ewe175-D4. No additive or synergistic effect was observed while analyzing combinations of monoclonal antibodies *in vitro*.

3.5.4 Antibody specificity test by immunoblot

All antibodies were tested for specificity. For that, a EXPI293F cell lysate was prepared and separated on a SDS-PAGE followed by Western blot and immuno staining performed with all IgG antibodies (figure 20, supplemental figure 36).

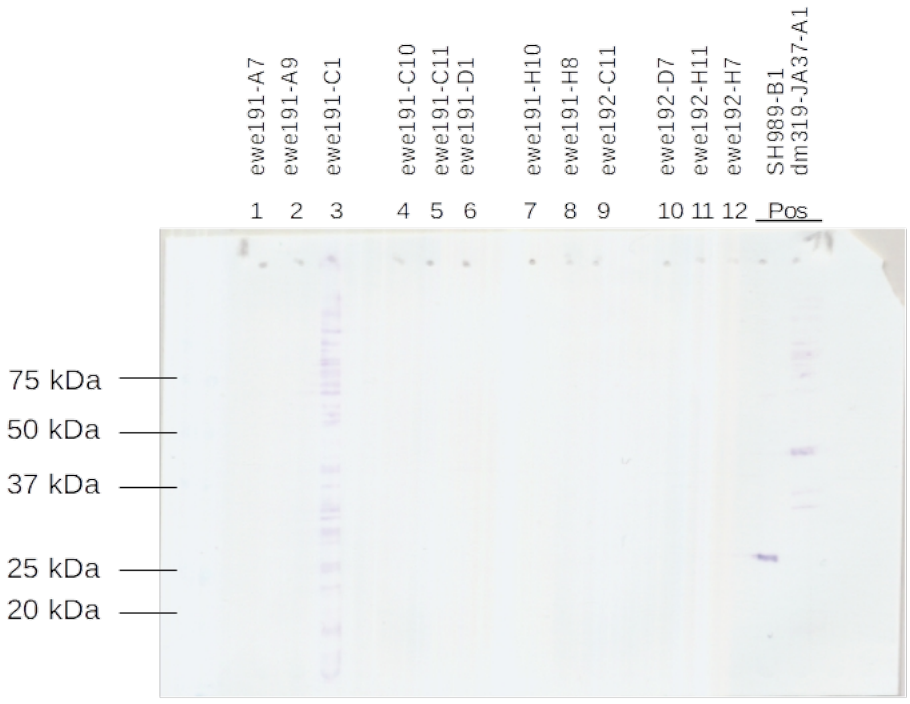

Figure 20: Specificity immuno blot. EXPI293F cell lysate blotted and stained with DT neutralizing IgG antibodies. Detection with goat α-human Fc secondary antibody conjugated with AP and colored with AP substrate + NBT/ BCIP.

The specificity test showed that ewe191-C1 reacted unspecifically with the EXPI293F cell lysate. All other samples showed no reaction and therefore, no unspecific reaction with the cell lysate.

3.5.5 Aggregation determination by SEC

An analytic size exclusion chromatography (SEC) was used to determine different aggregation behavior of the best R-domain neutralizing IgG antibodies (figure 21).

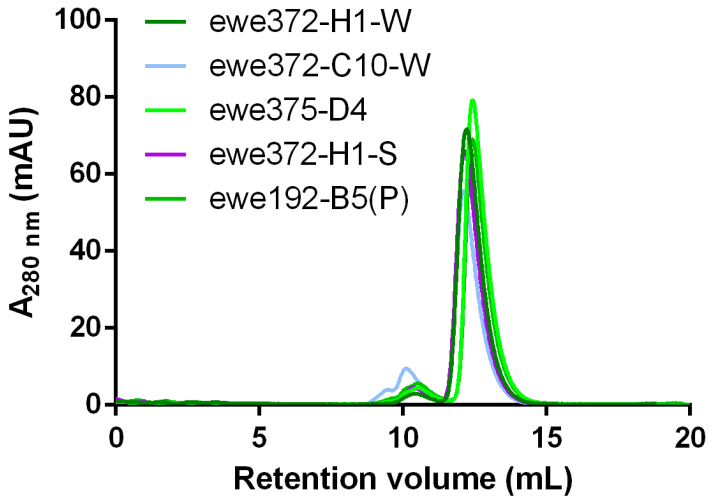

Figure 21: Size exclusion chromatography of the best five R-domain neutralizing IgG antibodies. Superdex200 increase 10/300 GL column was used with a flow rate of 0.5 mL/min. An amount of 150 µg IgG was separated in 50 mM sodium phosphate buffer (pH 7.0). Shown is the absorption at 280 nm (mAU) in correlation to the retention volume (mL).

The five analyzed IgG antibodies showed a peak for the monomer IgG (86 – 98.5 % area) between 12.1 – 12.4 min (149 – 170 kDa) and a second peak for the dimers IgG (1.4 – 13.7 % area) between 10.1 – 10.5 min (328 – 394 kDa). The IgG antibody ewe372-C10-W showed additionally a shoulder in front of the dimer peak. None of the IgG antibodies showed an additional peak indicating aggregation.

4 Discussion

Diphtheria is a disease caused by toxigenic strains of *Corynebacterium* spp. that produce diphtheria toxin (DT). The disease can be controlled by immunization and is therefore rare in countries with sufficient immunization coverage. However, diphtheria is a significant health problem in countries with poor immunization coverage or disrupted immunization programs (Both et al. 2014).

In 2017, the WHO reported 8819 diphtheria cases worldwide, 35 of those in Europe. That was the highest number since 2004 ("WHO World Health Organization: Immunization, Vaccines And Biologicals. Vaccine Preventable Diseases Vaccines Monitoring System 2018 Global Summary Reference Time Series: DIPHTHERIA" 2018). Current outbreaks of diphtheria are in Venezuela, Yemen and Bangladesh. In Venezuela, 2,170 suspected cases were reported since 2016, of these 1,249 were confirmed. A total of 287 deaths were reported. The cumulative case fatality rate among confirmed cases is 23 % ("Venezuela Diphtheria Case Tally Hits 800 in 2018" 2018). In Yemen, 1,584 suspected cases were reported since 2016. A total of 85 deaths were reported. The cumulative case fatality rate is 5.4 %. Children (<5 years of age) represent 20 % of suspected diphtheria cases and 38 % of associated deaths ("Yemen Diphtheria and Cholera Update" 2018). In Bangladesh, 3,954 suspected cases were reported between November and December 2017. A total of 31 deaths were reported ("Cox's Bazar: 475,000 Rohingya Children Being Vaccinated as Diphtheria Tally Rises" 2018).

In Europe, there were 2 fatal cases of infected children, 2016 in Belgium and 2015 in Spain. These children died because the life-saving diphtheria anti-toxin (DAT) was not available in Europe. Already in 2014 it was reported that several EU countries posted information that they have problems in re-stocking their current DAT supplies (Both et al. 2014). In 2017 a market survey showed that the Western world is running out of the only medicine against the toxin itself. The main producers for DAT are located in India and Russia ("Diphtheria Antitoxin (DAT) Serum" 2017). Beside the scarce supply of DAT, there are other obvious disadvantages. First, it is an animal product and can cause serum sickness, an immune response to proteins in the antiserum. Second, batch-dependent variation between DAT production from different animals occur. Third, the stability and

shelf-life of serum, especially in the regions where it is needed the most is a severe problem. And fourth, the production in horses is not complying with the animal welfare rules.

4.1 Antibody development

In this study, two different types of libraries were used. The naive libraries HAL9 and HAL10 (Kügler et al. 2015) and two different immune libraries (VJN and CD138+ library) were generated from the blood of diphtheria toxin boost-vaccinated volunteers.

Naive antibody gene libraries are IgM based and contain a huge variation of V-gene families and because of random combinations of VH- and VL-genes the diversity of antibodies is increased. Theoretically, an antibody against almost every antigen can be selected with this library type (Schwimmer et al. 2013). The naive human antibody gene library HAL9 and HAL10 used in this study have a diversity of $1.5 \bullet 10^{10}$ individual antibody clones for HAL9 and $5 \bullet 10^{9}$ for HAL10 (Kügler et al. 2015).

It was expected that antibodies from the naive library against diphtheria toxin could be selected because the library should theoretically contain antibodies against every possible antigen. Twenty nine unique antibodies were found binding diphtheria toxin but non of these antibodies showed the ability to neutralize diphtheria toxins in a cell-based *in vitro* assay. The reason could be the epitope or the affinity of the selected antibodies. These antibodies may not bind to neutralizing epitopes. If the affinity is too low, an *in vitro* affinity maturation could improve the naive library derived antibodies in neutralization ability. Because of the huge number of antibodies derived from the panning with immune libraries this approach was not pursued any further.

Compared to naive libraries, immune libraries have the advantage of higher-affinity antibodies, because these are already affinity matured *in vivo* (Wild et al. 2003). After vaccination, B cells are stimulated to produce pathogen-specific antibodies. During the first vaccination in childhood, the plasma cells produce low affinity antibodies (mainly IgM). After first contact with the antigen several rounds of hypermutation occurs followed by selection of B cells in the germinal center for improved antigen binding. These improved B cells can differentiate to memory B cells and persist in spleen or nodes. During

a boost vaccination these persisting memory B cells can readily proliferate and differentiate into plasma cells secreting a large amount of high-affinity antibodies (Siegrist, Claire-Anne 2013). The plasma cells can be identified by their specific surface marker CD138 which is not expressed by T or B cells (Lin et al. 2004).

The VJN library used all peripheral blood mononuclear cells (PBMC), the CD138+ library used the genetic information of antibodies directly coming from matured B lymphocytes, i.e. the antibody producing plasma cells. In this study, CD138 was used to select plasma cells from the whole PBMCs. Normally, plasma cells are rarely found in the circulating blood (2/ µL blood which corresponds to approximately 0.02 %) (Caraux et al. 2010). That was confirmed during selection process with only 2,501 CD138 positive cells out of 88,000,000 total cells (0.003 %). Here, additionally the instability of the surface marker could have decreased the number of $CD138^+$ total cell count. It is known that CD138 can degrade in cold temperatures or when sample processing is delayed (Lin et al. 2004). With the selected $CD138^+$ cells a library with a diversity of $4.0 \cdot 10^8$ cfu/mL for the lambda light chain library and $3.7 \cdot 10^8$ cfu/mL for the kappa light chain library was built. The total PBMC libraries (VJN) had a diversity between $1.3 – 3.45 \cdot 10^8$ cfu/mL. Even though the diversity of the immune libraries were lower compared to the naive libraries, they contain more antibodies against the antigen used for immunization (Moon et al. 2011).

It was shown that immune libraries had much more benefit on the outcome of neutralizing antibodies in both panning strategies. This was according to the expectations since IgG antibodies from boost-vaccinated volunteers were already affinity matured *in vivo* to neutralizing antibodies. In this study, 290 unique, neutralizing antibodies derived from immune libraries were selected. When targeting an antigen that was already used for immunization, it is preferred to use an immune library because the antibodies are naturally pre-selected and matured against the antigen.

Table 29: Summary of all selected antibodies separated by library type, light chain type, panning strategy, screening strategy and further characterization.

Library type	Light chain type	Panning strategy	Screening strategy	selected Ab	Produced & purified as scFv-Fc	Binding in ELISA as scFv-Fc	Neutralizing as scFv-Fc	Produced & purified as IgG	Binding in ELISA as IgG	Neutralizing as IgG
Naive (HAL 9/ HAL 10)	Lambda+Kappa (mix)	MTP	scFv binding	39/92	29/39	29/29	0/29	-	-	-
Immune	Lambda+Kappa (mix)	MTP	scFv binding	67/92	51/67	35/51	10/35	9/10	9/9	9/9
Immune (CD138+ selected)	Lambda+Kappa (mix)	MTP	scFv binding	65/92	50/65	38/50	12/38	12/12	12/12	12/12
Immune	Lambda	in solution	scFv-Fc neutralization	71/96	13/71	13/13	13/13	1/13	1/1	1/1
Immune	Kappa	in solution	scFv-Fc neutralization	66/96	18/66	18/18	18/18	10/18	10/10	10/10
Immune (CD138+ selected)	Lambda	in solution	scFv-Fc neutralization	54/96	3/54	3/3	3/3	0/3	-	-
Immune (CD138+ selected)	Kappa	in solution	scFv-Fc neutralization	77/96	5/77	5/5	5/5	2/5	2/2	2/2

Moreover, two different panning strategies (figure 22) were used additional to the two library types: first, panning on microtiter plate (MTP) with immobilized antigen in a well and using naive and immune libraries, and second, panning in solution with biotinylated antigen, using only immune libraries (table 29).

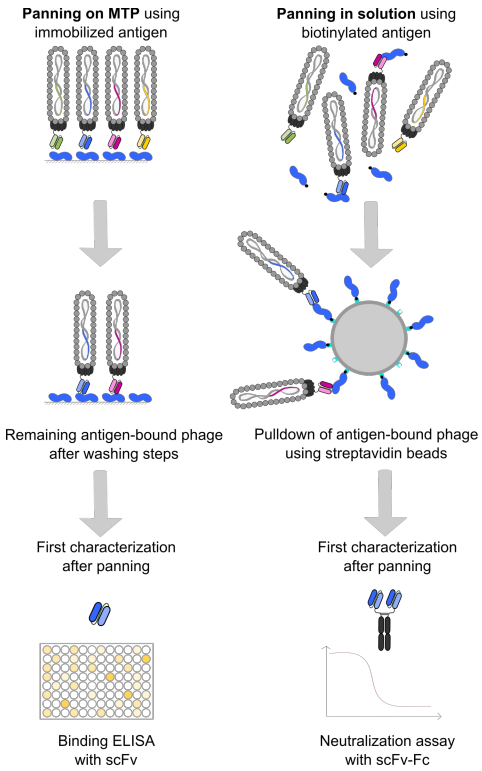

Figure 22: Graphical comparison of the two panning strategies: Panning on microtiter plate (MTP) and Panning in solution.

Using panning on MTP, only 22 out of 184 antibodies derived from immune libraries (12 %) showed neutralization after a selection strategy based on binding to diphtheria toxin. In comparison, with the panning in solution strategy 268 out of 384 (70 %) neutralizing antibodies were selected.

During immobilization of the antigen on an MTP unspecific absorption to the well surface led to undirected binding of the antigen in different orientations and partial denaturation on the surface. Proteins bind in polystyrene surfaces because of their hydrophobic interaction (Pyun et al. 1997). That leads to an unnatural folding of antigens to the surface and therefrom binders against discontinuous epitopes are enriched (Schütte et al. 2009; Mansur

et al. 2005). A disadvantage of the panning on MTP could be that due to the bound and partially denatured antigen, not every epitope is potentially accessible. Probably, some epitopes were covered by overlapping parts of the protein next to it or denaturation damaged epitopes.

To circumvent this disadvantages of immobilized proteins, biotinylated proteins were used with the panning in solution strategy. Therefore, the antigens were not bound on a surface thus kept in their natural folding. The antibodies were selected via pull down with magnetic beads coupled to streptavidin. But also this strategy has its disadvantages. The biotinylation is a non-directional reaction, that may lead to potential epitopes. With the used biotinylation protocol up to three biotins were added to one diphtheria toxin. Comparing the phage ELISA experiment on biotinylated and not-biotinylated diphtheria toxin it was shown that biotinylation had no effect on the binding ability of the antibodies coming from the panning in solution strategy.

But the panning strategy itself was not the only difference between the selection strategies, the screening strategy changed with the panning strategy. When using panning on MTP, the monoclonal scFv antibodies were screened for their ability to bind to diphtheria toxin in a binding ELISA. The antibodies coming from panning in solution were directly sub-cloned into scFv-Fc format and screened for their capability to neutralize diphtheria toxin in a cell-based *in vitro* assay. The latter strategy could lead to better results, because the production of scFv fragments in *E. coli* is omitted. *E. coli* can solely fold proteins correctly in the periplasm due to the oxidizing environment that permits disulfide bond formation. But the periplasm only account for approximately 8 – 16 % of the cell volume (Gaciarz et al. 2016). The periplasm can easily overload or miss-folded antibodies can accumulate and cause cell death that could result in a bias due to production quality and quantity. In order to avoid that a production in mammalian cells was performed. The benefit of the production immediately in mammalian cells was that the monoclonal antibodies were directly screened for their ability to neutralize diphtheria toxin in a cell-based *in vitro* assay.

This study showed that the combination of using an immune library, panning in solution and production as scFv-Fc in mammalian cells with functional screening benefited the discovery of DT neutralizing antibodies. It was, however, not analyzed whether the

combination of all strategies or one single component was most relevant for the outcome. The only possible conclusion that can be made at this point is that the screening strategy has to be specifically designed for the purpose of the desired antibodies. Here, the focus is clearly on neutralization so the selection assay of choice was a functional assay testing directly for neutralization *in vitro*.

4.2 Antibody format switching from scFv-Fc to IgG

After selecting neutralizing antibodies via panning, the characterization was further done in IgG format. It was analyzed whether the previously characterized properties binding and neutralization were effected after switching the antibody format from scFv-Fc to IgG.

For most of the generated antibodies from panning with immobilized antigen on MTP affinity decreased after switching from scFv-Fc to IgG (14 out of 22) (table 30). This reduced affinity was already described for another antibody (Thie et al. 2011). In scFv-Fc format, the variable domains have a linker in between. This linker leads to an increased flexibility of the variable domains compared to the IgG or Fab. The flexibility may result in a changed angle between VH and VL that influence the binding ability (Krebs et al. 2001; Thie et al. 2011).

This effect of decreased binding was mainly observed when binders were selected in the MTP panning strategy, because here the selection criteria was the ability to bind DT. The antibodies generated by panning in solution did not show this effect, but these antibodies were already selected as scFv-Fc regarding their ability to neutralize diphtheria toxin. The affinity remained the same or even increased for the panning in solution strategy while binding to DT played a minor role (table 30).

Regarding the neutralization potency after format switching, nearly every antibody had an increased ability to neutralize DT in a cell based *in vitro* assay (table 30). IgG increased their potency compared to scFv-Fc up to 100-fold (ewe191-A7). Just one antibody lost the ability to neutralize diphtheria toxin *in vitro* (ewe191-C10). Switching the scFv format back to the original Fab format increased the neutralization efficacy. On average the potency increased 7-fold. This effect was even higher in the antibodies derived from panning on MTP. Here, the potency increase on average 10-fold.

Table 30: Comparison of half effective concentration (EC50 in µg/mL) against diphtheria toxin and minimum effective dose 50 % (MED50% in nM) against diphtheria toxin in the antibody formats scFv-Fc and IgG. Antibodies developed with panning on microtiter plates are highlighted in gray, those from panning in solution have a white background.

#	Name antibody clone	DT EC50 (µg/mL) scFv-Fc	DT EC50 (µg/mL) IgG	MED50% (nM) scFv-Fc	MED50% (nM) IgG
1	ewe191-A7	0.0086	0.0244	18,854.3	140.3
2	ewe191-A9	0.0154	0.0264	1266.1	1098.5
3	ewe191-C1	0.0101	0.0381	2360.9	818.5
4	ewe191-C10	0.1748	0.3541	1821.7	-
5	ewe191-C11	0.0105	0.0253	7.6	0.6
6	ewe191-C12	0.0254	0.0466	7.3	2.4
7	ewe191-D1	0.0100	0.0266	36.9	31.2
8	ewe191-E12	0.0459	0.0297	43.2	19.2
9	ewe191-H10	0.0335	0.0285	65.4	119.1
10	ewe191-H8	0.0143	0.0578	3.9	1.0
11	ewe192-A6	0.2031	0.4095	500.8	780.7
12	ewe192-B5(P)	0.0441	0.0535	0.075	0.007
13	ewe192-C11	0.0113	0.0337	313.8	116.7
14	ewe192-D7	0.0119	0.0333	26.4	3.4
15	ewe192-D8	3.9280	0.3612	4667.8	949.3
16	ewe192-E4	0.0920	0.0681	301.3	35.7
17	ewe192-F11	0.49	0.2021	1312.7	1415.9
18	ewe192-F6	0.1558	0.1380	287.9	357.6
19	ewe192-G12	0.89	0.5226	2911.9	180.8
20	ewe192-H11	0.0143	0.0263	5506.8	1351.3
21	ewe192-H7	0.0138	0.0349	18.8	10.9
22	ewe192-H8	0.1589	0.0938	303.6	254.0
23	ewe371-B12	0.01456	0.0182	1.407	1.2028
24	ewe372-A12	0.02153	0.0210	8.032	4.1944
25	ewe372-A8	0.02257	0.0239	0.05126	0.0826
26	ewe372-C10-W	0.04717	0.0356	0.00551	0.0057
27	ewe372-C4	0.03015	0.0323	0.03261	0.0297
28	ewe372-C5	0.03221	0.0344	0.01906	0.0133
29	ewe372-D11	0.02329	0.0243	2.231	1.6808
30	ewe372-D7	0.03223	0.0286	0.01039	0.0062

#	Name antibody clone	DT EC50 (µg/mL) scFv-Fc	DT EC50 (µg/mL) IgG	MED50% (nM) scFv-Fc	MED50% (nM) IgG
31	ewe372-F6	0.01995	0.0264	2.011	0.6098
32	ewe372-H1-S	0.0382	0.0282	0.00515	0.0057
33	ewe372-H1-W	0.0364	0.0283	0.00508	0.0030
34	ewe375-D4	0.04593	0.0274	0.00619	0.0031
35	ewe375-H4	0.03662	0.0220	0.114	0.0669

4.3 Domain Mapping

The three domains of DT have different functions (Choe et al. 1992). Therefore, it is important to know which domain are bound. The selected neutralizing antibodies are binding to all three DT domains. However, in this study just one neutralizing antibody could be identified that targets the T-domain. Most of the antibodies bind to the C- (16 mAbs) or R-domain (21 mAbs) (figure 23).

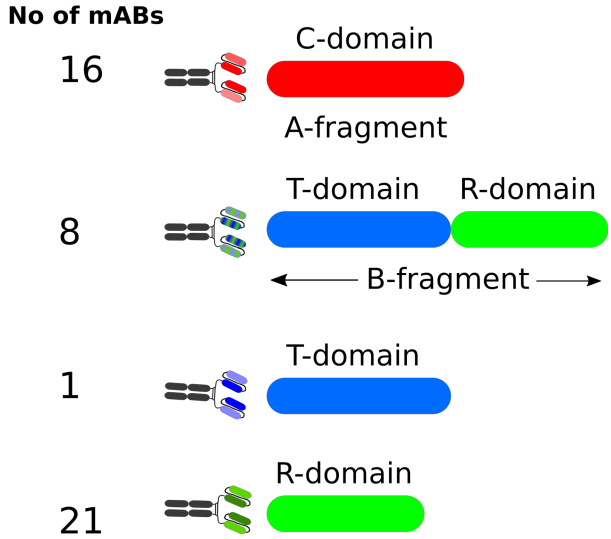

Figure 23: Overview of analyzed monoclonal antibodies (mABs) and their respective binding domain

The best neutralizing antibodies have a neutralization potency of 3 – 30 pM, including the neutralizing antibody ewe375-D4 (3 pM) and ewe192-B5(P) (7 pM). All of these antibodies bind to the receptor binding domain and might physically block the toxin from

binding to the receptor, the heparin-binding epidermal growth factor-like growth factor (HB-EGF). Three other studies showed already that antibodies against the receptor binding domain lead to effective neutralization (Sevigny et al. 2013; Kakita et al. 2006; Danelli et al. 1991). The epitope for the R-domain binding antibody ewe192-B5(P) was mapped. It was shown, that the epitope is at the N-terminus of the R-domain and therefore not directly blocking the binding site (brown, figure 24). The antibody might inhibit the conformational change of the T-domain, because it binds to the N-terminal part of R-domain probably proceeding to the C-terminal part of the T-domain (the used peptide spot membrane included only the R-domain).

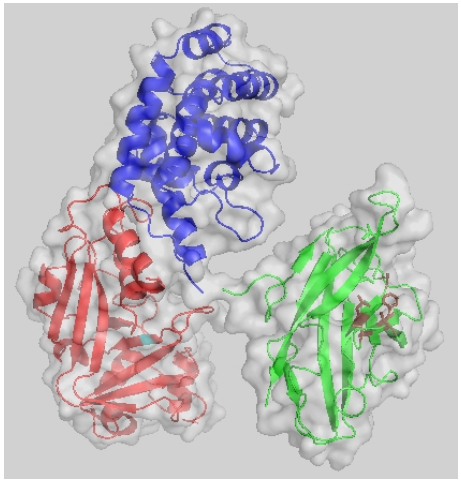

Figure 24: DT with active site in C domain (cyan) and Receptor binding site (brown)

The antibody against the T-domain might prevent the DT from changing the conformation to form the pore for endosomal escape. Here, steric hindrance may lead to neutralization while binding the T-domain.

Binding the C-domain might have two different mechanism of neutralization. The first mode of action of neutralizing antibodies might be the blocking of the catalytic site. While blocking the NAD-binding pocket the elongation factor 2 can not be ribosylated and thus cells have a functional protein synthesis. Up to now it is not known in which way the C-domain binding antibodies are neutralizing. But to cover more than just blocking the receptor binding or to prevent the catalytic function, antibodies against different domains were combined to mimic a polyclonal serum.

4.4 No synergistic effect with antibody combinations *in vitro*

We hypothesized that a combination of neutralizing antibodies against different domains of DT lead to an additive or synergistic effect. Some publications already reported that mixing of protective monoclonal antibodies targeting different epitopes of a toxin can synergize protective efficacy and thus an increase protection against toxicity, examples are given for AB-toxins (Cheng et al. 2009; Ngundi et al. 2012; Brossier et al. 2004) and enterotoxins (Demarest et al. 2010; Varshney et al. 2011).

In this study, cell-based neutralization assays were performed and no synergistic effects were observed. Neutralization of the mixture was always as good as the best neutralizing antibody by itself. In contrast to this *in vitro* study, previous studies were mainly conducted *in vivo*. Positive effects that may be caused by the immune system of the *in vivo* model may be able to tip the scale in favor of a specific antibody or antibody mix. However, in an *in vitro* assay characterization of antibodies is easier and can be done with a huger panel of antibodies.

In an *in vitro* assay, only the variable part of an antibody can influence the mode of action because the Fc-part of the antibody can only be activated together with the immune system. It was already observed, that Fcγ receptor (FcγR) mediated mechanisms are important for toxin protection. For example, the Fc-mediated uptake of anthrax, a toxin secreted by *B. anthracis* that is eponymic to the disease, by effector cells like macrophages contributes substantially to the neutralizing activity of anti-anthrax toxin mAbs (Abboud et al. 2010; Chow et al. 2013). During my study, the cell-based *in vitro* assay reached its limits. Nonetheless, the assay was well suited to pre-select the best 35 candidates out of nearly 300 human, DT-neutralizing, monoclonal antibodies generated in the study.

4.5 Conclusion and Outlook

In this study, the antibody phage display technology was used to generate a broad panel of fully human monoclonal antibodies that neutralize diphtheria toxin. These antibodies have four striking advantages over commonly used antisera. First, these new developed antibodies are fully human. Second, they are a defined product with known sequences. Third, they are a stable product, that can be lyophilized and stored over long periods of time (data not shown). And finally, the antibodies can be produced in cell culture avoiding the need for animals.

In this study, 660 monoclonal antibodies were selected. They were analyzed for binding and neutralization in scFv-Fc and IgG format and 290 scFv-Fc antibodies have neutralizing potency. All of these new developed antibodies derived from an immune library generated with the blood of DT boost-vaccinated persons. Three best neutralizing lead candidates were selected, one against each of the three domains of DT. The IgG targeting the receptor binding domain is ewe372-D4 and has a neutralization potency of 446 IU/mg. ewe375-H4 has a neutralization potency of 20.4 IU/mg and binds the catalytic domain and ewe372-F6 binds the translocation domain with a neutralization potency of 2.25 IU/mg. These IgG antibodies together with the well characterized, R-domain binding ewe192-B5(P) antibody (124 IU/mg) will be further analyzed.

In the next step, the antibodies ewe192-B5(P), ewe375-D4, ewe372-F6 and ewe375-H4 and antibody mixtures will be tested in a non-lethal *in vivo* guinea pig model. This skin irritation model should show how the antibodies will react in an *in vivo* system.

In addition, the epitopes of all good neutralizing antibodies should be mapped. This can provide more information about the epitopes and possible explanations for the way of neutralization.

5 References

Abbas, Abul K., Andrew H. Lichtman, Shiv Pillai, and David L. Baker. 2015. *Cellular and Molecular Immunology*. 8. ed., internat. ed. Philadelphia, Pa: Elsevier, Saunders.

Abboud, Nareen, Siu-Kei Chow, Carolyn Saylor, Alena Janda, Jeffery V. Ravetch, Matthew D. Scharff, and Arturo Casadevall. 2010. "A Requirement for FcγR in Antibody-Mediated Bacterial Toxin Neutralization." *The Journal of Experimental Medicine* 207 (11): 2395–2405. https://doi.org/10.1084/jem.20100995.

Barbas, C. F., A. S. Kang, R. A. Lerner, and S. J. Benkovic. 1991. "Assembly of Combinatorial Antibody Libraries on Phage Surfaces: The Gene III Site." *Proceedings of the National Academy of Sciences of the United States of America* 88 (18): 7978–82.

Beer, Lara-Antonia, Helma Tatge, Carmen Schneider, Maximilian Ruschig, Michael Hust, Jessica Barton, Stefan Thiemann, Viola Fühner, Giulio Russo, and Ralf Gerhard. 2018. "The Binary Toxin CDT of Clostridium Difficile as a Tool for Intracellular Delivery of Bacterial Glucosyltransferase Domains." *Toxins* 10 (6): 225. https://doi.org/10.3390/toxins10060225.

Behring, Emil, and Shibasaburō Kitasato. 1890. "Über Die Zustanderkommen Der Diphtherie-Immunitat Und Der Tetanus-Immunitat Bei Thieren," no. 16: 1113–14.

Bernard, Kathryn A., and Guido Funke. 2015. "Corynebacterium." In *Bergey's Manual of Systematics of Archaea and Bacteria*, edited by William B Whitman, Fred Rainey, Peter Kämpfer, Martha Trujillo, Jonsik Chun, Paul DeVos, Brian Hedlund, and Svetlana Dedysh, 1–70. Chichester, UK: John Wiley & Sons, Ltd. http://doi.wiley.com/10.1002/9781118960608.gbm00026.

Bigio, Massimo, Roberta Rossi, Daniele Nucci, Guido Antoni, Rino Rappuoli, and Giulio Ratti. 1987. "Conformational Changes in Diphtheria Toxoids." *FEBS Letters* 218 (2): 271–76. https://doi.org/10.1016/0014-5793(87)81060-8.

Both, L, J White, S Mandal, and A Efstratiou. 2014. "Access to Diphtheria Antitoxin for Therapy and Diagnostics." *Eurosurveillance* 19 (24): 20830. https://doi.org/10.2807/1560-7917.ES2014.19.24.20830.

Breitling, F., and S. Dübel. 1997. *Rekombinante Antikörper*. Heidelberg: Spektrum Akademischer Verlag.

Breitling, Frank, Stefan Dübel, Thomas Seehaus, Iris Klewinghaus, and Melvyn Little. 1991. "A Surface Expression Vector for Antibody Screening." *Gene* 104 (2): 147–53. https://doi.org/10.1016/0378-1119(91)90244-6.

Brossier, F., M. Levy, A. Landier, P. Lafaye, and M. Mock. 2004. "Functional Analysis of Bacillus Anthracis Protective Antigen by Using Neutralizing Monoclonal Antibodies." *Infection and Immunity* 72 (11): 6313–17. https://doi.org/10.1128/IAI.72.11.6313-6317.2004.

Caraux, A., B. Klein, B. Paiva, C. Bret, A. Schmitz, G. M. Fuhler, N. A. Bos, et al. 2010. "Circulating Human B and Plasma Cells. Age-Associated Changes in Counts and Detailed Characterization of Circulating Normal CD138- and CD138+ Plasma Cells." *Haematologica* 95 (6): 1016–20. https://doi.org/10.3324/haematol.2009.018689.

Cheng, L. W., L. H. Stanker, T. D. Henderson, J. Lou, and J. D. Marks. 2009. "Antibody Protection against Botulinum Neurotoxin Intoxication in Mice." *Infection and Immunity* 77 (10): 4305–13. https://doi.org/10.1128/IAI.00405-09.

Choe, Seunghyon, Melanie J. Bennett, Gary Fujii, Paul M. G. Curmi, Katherine A. Kantardjieff, R. John Collier, and David Eisenberg. 1992. "The Crystal Structure of

Diphtheria Toxin." *Nature* 357 (6375): 216–22. https://doi.org/10.1038/357216a0.

Chow, Siu-Kei, Cameron Smith, Thomas MacCarthy, Mary Ann Pohl, Aviv Bergman, and Arturo Casadevall. 2013. "Disease-Enhancing Antibodies Improve the Efficacy of Bacterial Toxin-Neutralizing Antibodies." *Cell Host & Microbe* 13 (4): 417–28. https://doi.org/10.1016/j.chom.2013.03.001.

Collier, R. J., and H. A. Cole. 1969. "Diphtheria Toxin Subunit Active in Vitro." *Science (New York, N.Y.)* 164 (3884): 1179–81.

Collier, R. J., and Judith Kandel. 1971. "Structure and Activity of Diphtheria Toxin I. THIOL-DEPENDENT DISSOCIATION OF A FRACTION OF TOXIN INTO ENZYMICALLY ACTIVE AND INACTIVE FRAGMENTS." *Journal of Biological Chemistry* 246 (5): 1496–1503.

Cook, Graham P., and Ian M. Tomlinson. 1995. "The Human Immunoglobulin VH Repertoire." *Immunology Today* 16 (5): 237–42. https://doi.org/10.1016/0167-5699(95)80166-9.

Corpet, F. 1988. "Multiple Sequence Alignment with Hierarchical Clustering." *Nucleic Acids Research* 16 (22): 10881–90. https://doi.org/10.1093/nar/16.22.10881.

"Cox's Bazar: 475,000 Rohingya Children Being Vaccinated as Diphtheria Tally Rises." 2018. *Outbreak News Today* (blog). January 14, 2018. http://outbreaknewstoday.com/coxs-bazar-475000-rohingya-children-vaccinated-diphtheria-tally-rises-99745/.

Danelli, Maria das Graças M., Lúcia M. Teixeira, Luiz Carlos D. Formiga, and J. Mauro Peralta. 1991. "Protective Monoclonal Antibodies to Diphtheria Toxin." *Memórias Do Instituto Oswaldo Cruz* 86 (2): 265–67. https://doi.org/10.1590/S0074-02761991000200017.

Demarest, Stephen J., Mangala Hariharan, Marikka Elia, Jared Salbato, Ping Jin, Colin Bird, Jay M. Short, et al. 2010. "Neutralization of Clostridium Difficile Toxin A Using Antibody Combinations." *MAbs* 2 (2): 190–98. https://doi.org/10.4161/mabs.2.2.11220.

"Diphtheria | Clinical Features | CDC." 2016. January 20, 2016. https://www.cdc.gov/diphtheria/clinicians.html.

"Diphtheria Antitoxin (DAT) Serum." 2017. UNICEF. 2017. https://www.unicef.org/supply/index_94943.html.

Dorland, R. B., J. L. Middlebrook, and S. H. Leppla. 1979. "Receptor-Mediated Internalization and Degradation of Diphtheria Toxin by Monkey Kidney Cells." *The Journal of Biological Chemistry* 254 (22): 11337–42.

Draper, R. K. 1980. "The Entry of Diphtheria Toxin into the Mammalian Cell Cytoplasm: Evidence for Lysosomal Involvement." *The Journal of Cell Biology* 87 (3): 849–54. https://doi.org/10.1083/jcb.87.3.849.

Drazin, Rae, Judith Kandel, and R. J. Collier. 1971. "Structure and Activity of Diphtheria Toxin II. ATTACK BY TRYPSIN AT A SPECIFIC SITE WITHIN THE INTACT TOXIN MOLECULE." *Journal of Biological Chemistry* 246 (5): 1504–10.

Edelman, G. M., and J. A. Gally. 1964. "A MODEL FOR THE 7S ANTIBODY MOLECULE." *Proceedings of the National Academy of Sciences of the United States of America* 51 (May): 846–53.

Emmons, C., and L. G. Hunsicker. 1987. "Muromonab-CD3 (Orthoclone OKT3): The First Monoclonal Antibody Approved for Therapeutic Use." *Iowa Medicine: Journal of the Iowa Medical Society* 77 (2): 78–82.

Frenzel, André, Jonas Kügler, Sonja Wilke, Thomas Schirrmann, and Michael Hust. 2014. "Construction of Human Antibody Gene Libraries and Selection of Antibodies by Phage Display." *Methods in Molecular Biology (Clifton, N.J.)* 1060: 215–43.

https://doi.org/10.1007/978-1-62703-586-6_12.

Frenzel, André, Thomas Schirrmann, and Michael Hust. 2016. “Phage Display-Derived Human Antibodies in Clinical Development and Therapy.” *MAbs* 8 (7): 1177–94. https://doi.org/10.1080/19420862.2016.1212149.

Frippiat, Jean-Pol, Samuel C. Williams, Lan M. Tomlinson, Graham P. Cook, Dorra Cherif, Denis Le Paslier, John E. Collins, lan Dunham, Greg Winter, and Marie-Paule Lefranc. 1995. “Organization of the Human Immunoglobulin Lambda Light-Chain Locus on Chromosome 22q11.2.” *Human Molecular Genetics* 4 (6): 983–91. https://doi.org/10.1093/hmg/4.6.983.

Gaciarz, Anna, Johanna Veijola, Yuko Uchida, Mirva J. Saaranen, Chunguang Wang, Sohvi Hörkkö, and Lloyd W. Ruddock. 2016. “Systematic Screening of Soluble Expression of Antibody Fragments in the Cytoplasm of E. Coli.” *Microbial Cell Factories* 15 (1). https://doi.org/10.1186/s12934-016-0419-5.

Gao, Changshou, Shenlan Mao, Henrik J. Ditzel, Lauge Farnaes, Peter Wirsching, Richard A. Lerner, and Kim D. Janda. 2002. “A Cell-Penetrating Peptide from a Novel PVII-PIX Phage-Displayed Random Peptide Library.” *Bioorganic & Medicinal Chemistry* 10 (12): 4057–65.

Gill, D. M., and A. M. Pappenheimer. 1971. “Structure-Activity Relationships in Diphtheria Toxin.” *The Journal of Biological Chemistry* 246 (5): 1492–95.

Greenfield, Lawrence, Michael J Bjorn, Glenn Horn, Darlene Fong, GREGORY A BUCKtt, R John Collier, and Donald A Kaplan. 1983. “Nucleotide Sequence of the Structural Gene for Diphtheria Toxin Carried by Corynebacteriophage 18.” *Proc. Natl. Acad. Sci. USA*, 5.

Hoet, René Michael, Edward H. Cohen, Rachel Baribault Kent, Kristin Rookey, Sonia Schoonbroodt, Shannon Hogan, Louise Rem, et al. 2005. “Generation of High-Affinity Human Antibodies by Combining Donor-Derived and Synthetic Complementarity-Determining-Region Diversity.” *Nature Biotechnology* 23 (3): 344–48. https://doi.org/10.1038/nbt1067.

Hu, V. W., and R. K. Holmes. 1984. “Evidence for Direct Insertion of Fragments A and B of Diphtheria Toxin into Model Membranes.” *The Journal of Biological Chemistry* 259 (19): 12226–33.

Hust, Michael, and Stefan Dübel. 2010. “Human Antibody Gene Libraries.” In *Antibody Engineering*, edited by Roland Kontermann and Stefan Dübel, 65–84. Berlin, Heidelberg: Springer Berlin Heidelberg. https://doi.org/10.1007/978-3-642-01144-3_5.

Hust, Michael, Edgar Maiss, Hans-Jörg Jacobsen, and Thomas Reinard. 2002. “The Production of a Genus-Specific Recombinant Antibody (ScFv) Using a Recombinant Potyvirus Protease.” *Journal of Virological Methods* 106 (2): 225–33.

Hust, Michael, Torsten Meyer, Bernd Voedisch, Torsten Rülker, Holger Thie, Aymen El-Ghezal, Martina Inga Kirsch, et al. 2011. “A Human ScFv Antibody Generation Pipeline for Proteome Research.” *Journal of Biotechnology* 152 (4): 159–70. https://doi.org/10.1016/j.jbiotec.2010.09.945.

Jackson, Robert. 2000. “Serum Sickness.” *Journal of Cutaneous Medicine and Surgery* 4 (4): 223–25. https://doi.org/10.1177/120347540000400411.

Jäger, Volker, Konrad Büssow, Andreas Wagner, Susanne Weber, Michael Hust, André Frenzel, and Thomas Schirrmann. 2013. “High Level Transient Production of Recombinant Antibodies and Antibody Fusion Proteins in HEK293 Cells.” *BMC Biotechnology* 13 (1): 52. https://doi.org/10.1186/1472-6750-13-52.

Kaczorek, M, F Delpeyroux, N Chenciner, R. Streeck, Murphy, P Boquet, and P Tiollais. 1983.

"Nucleotide Sequence and Expression of the Diphtheria Tox228 Gene in Escherichia Coli." *Science* 221 (4613): 855–58. https://doi.org/10.1126/science.6348945.

Kagan, B. L., A. Finkelstein, and M. Colombini. 1981. "Diphtheria Toxin Fragment Forms Large Pores in Phospholipid Bilayer Membranes." *Proceedings of the National Academy of Sciences* 78 (8): 4950–54. https://doi.org/10.1073/pnas.78.8.4950.

Kakita, M., T. Takahashi, T. Komiya, Y. Iba, T. Tsuji, Y. Kurosawa, and M. Takahashi. 2006. "Isolation of a Human Monoclonal Antibody with Strong Neutralizing Activity against Diphtheria Toxin." *Infection and Immunity* 74 (6): 3682–83. https://doi.org/10.1128/IAI.01731-05.

Kniker, W. T. 1968. "THE LOCALIZATION OF CIRCULATING IMMUNE COMPLEXES IN EXPERIMENTAL SERUM SICKNESS: THE ROLE OF VASOACTIVE AMINES AND HYDRODYNAMIC FORCES." *Journal of Experimental Medicine* 127 (1): 119–36. https://doi.org/10.1084/jem.127.1.119.

Köhler, G., and C. Milstein. 1975. "Continuous Cultures of Fused Cells Secreting Antibody of Predefined Specificity." *Nature* 256 (5517): 495–97. https://doi.org/10.1038/256495a0.

Krebs, Barbara, Robert Rauchenberger, Silke Reiffert, Christine Rothe, Michael Tesar, Elisabeth Thomassen, Manqiu Cao, et al. 2001. "High-Throughput Generation and Engineering of Recombinant Human Antibodies." *Journal of Immunological Methods* 254 (1–2): 67–84. https://doi.org/10.1016/S0022-1759(01)00398-2.

Kügler, Jonas, Sonja Wilke, Doris Meier, Florian Tomszak, André Frenzel, Thomas Schirrmann, Stefan Dübel, et al. 2015. "Generation and Analysis of the Improved Human HAL9/10 Antibody Phage Display Libraries." *BMC Biotechnology* 15 (1): 10. https://doi.org/10.1186/s12896-015-0125-0.

Kwaśnikowski, Piotr, Peter Kristensen, and Wojciech T. Markiewicz. 2005. "Multivalent Display System on Filamentous Bacteriophage PVII Minor Coat Protein." *Journal of Immunological Methods* 307 (1–2): 135–43. https://doi.org/10.1016/j.jim.2005.10.002.

Lin, Pei, Rebecca Owens, Guido Tricot, and Carla S. Wilson. 2004. "Flow Cytometric Immunophenotypic Analysis of 306 Cases of Multiple Myeloma." *American Journal of Clinical Pathology* 121 (4): 482–88. https://doi.org/10.1309/74R4TB90BUWH27JX.

Malito, Enrico, Badry Bursulaya, Connie Chen, Paola Lo Surdo, Monica Picchianti, Enrico Balducci, Marco Biancucci, et al. 2012. "Structural Basis for Lack of Toxicity of the Diphtheria Toxin Mutant CRM197." *Proceedings of the National Academy of Sciences of the United States of America* 109 (14): 5229–34. https://doi.org/10.1073/pnas.1201964109.

Mansur, H. S., R. L. Oréfice, W. L. Vasconcelos, Z. P. Lobato, and L. J. C. Machado. 2005. "Biomaterial with Chemically Engineered Surface for Protein Immobilization." *Journal of Materials Science: Materials in Medicine* 16 (4): 333–40. https://doi.org/10.1007/s10856-005-0632-y.

McCafferty, John, Andrew D. Griffiths, Greg Winter, and David J. Chiswell. 1990. "Phage Antibodies: Filamentous Phage Displaying Antibody Variable Domains." *Nature* 348 (6301): 552–54. https://doi.org/10.1038/348552a0.

Metz, Bernard, Wim Jiskoot, Wim E. Hennink, Daan J. A. Crommelin, and Gideon F. A. Kersten. 2003. "Physicochemical and Immunochemical Techniques Predict the Quality of Diphtheria Toxoid Vaccines." *Vaccine* 22 (2): 156–67.

Mills, Alan E., Rodney D. Mitchell, and Ernest K. Lim. 1997. "Corynebacterium Pseudotuberculosis Is a Cause of Human Necrotising Granulomatous Lymphadenitis." *Pathology* 29 (2): 231–33. https://doi.org/10.1080/00313029700169944.

Moghaddam, Amir, Tine Borgen, John Stacy, Louise Kausmally, Bjørg Simonsen, Ole J Marvik, Ole Henrik Brekke, and Michael Braunagel. 2003. "Identification of ScFv Antibody Fragments That Specifically Recognise the Heroin Metabolite 6-Monoacetylmorphine but Not Morphine." *Journal of Immunological Methods* 280 (1–2): 139–55. https://doi.org/12972195.

Montecucco, Cesare, Maurizio Tomasi, Giampietro Schiavo, and Rino Rappuoli. 1986. "Hydrophobic Photolabelling of Pertussis Toxin Subunits Interacting with Lipids." *FEBS Letters* 194 (2): 301–4. https://doi.org/10.1016/0014-5793(86)80105-3.

Moon, Sung Ah, Min Kyung Ki, Sungyoung Lee, Mi-Lim Hong, Misook Kim, Sungsub Kim, Junho Chung, Sue Goo Rhee, and Hyunbo Shim. 2011. "Antibodies against Non-Immunizing Antigens Derived from a Large Immune ScFv Library." *Molecules and Cells* 31 (6): 509–13. https://doi.org/10.1007/s10059-011-2268-8.

Morris, Randal E, and Alan S Gerstein. 1985. "Receptor-Mediated Entry of Diphtheria Toxin into Monkey Kidney (Vero) Cells: Electron Microscopic Evaluation." *INFECT. IMMUN.* 50: 7.

Moskaug, J. O., K. Sandvig, and S. Olsnes. 1988. "Low PH-Induced Release of Diphtheria Toxin A-Fragment in Vero Cells. Biochemical Evidence for Transfer to the Cytosol." *The Journal of Biological Chemistry* 263 (5): 2518–25.

Murphy, Kenneth P., Paul Travers, Mark Walport, Charles Janeway, Lothar(Übers) Seidler, Michael Ehrenstein, and Ingrid(Übers) Haußer-Stiller. 2009. *Janeway Immunologie*. 7. Auflage. Heidelberg: Spektrum Akademischer Verlag.

Ngundi, Miriam M., Bruce D. Meade, Stephen F. Little, Conrad P. Quinn, Cindi R. Corbett, Rebecca A. Brady, and Drusilla L. Burns. 2012. "Analysis of Defined Combinations of Monoclonal Antibodies in Anthrax Toxin Neutralization Assays and Their Synergistic Action." *Clinical and Vaccine Immunology* 19 (5): 731–39. https://doi.org/10.1128/CVI.05714-11.

Osada, Naoki, Arihiro Kohara, Toshiyuki Yamaji, Noriko Hirayama, Fumio Kasai, Tsuyoshi Sekizuka, Makoto Kuroda, and Kentaro Hanada. 2014. "The Genome Landscape of the African Green Monkey Kidney-Derived Vero Cell Line." *DNA Research* 21 (6): 673–83. https://doi.org/10.1093/dnares/dsu029.

Pappenheimer Jr, A. M. 1977. "Diphtheria Toxin." *Annual Review of Biochemistry* 46 (1): 69–94. https://doi.org/10.1146/annurev.bi.46.070177.000441.

Parmley, S F, and G P Smith. 1988. "Antibody-Selectable Filamentous Fd Phage Vectors: Affinity Purification of Target Genes." *Gene* 73 (2): 305–18.

Peel, M. M., G. G. Palmer, A. M. Stacpoole, and T. G. Kerr. 1997. "Human Lymphadenitis Due to Corynebacterium Pseudotuberculosis: Report of Ten Cases from Australia and Review." *Clinical Infectious Diseases* 24 (2): 185–91. https://doi.org/10.1093/clinids/24.2.185.

Porter, R. R. 1959. "The Hydrolysis of Rabbit Y-Globulin and Antibodies with Crystalline Papain." *The Biochemical Journal* 73 (September): 119–26.

Pyun, J. C., M. Y. Cheong, S. H. Park, H. Y. Kim, and J. S. Park. 1997. "Modification of Short Peptides Using Epsilon-Aminocaproic Acid for Improved Coating Efficiency in Indirect Enzyme-Linked Immunosorbent Assays (ELISA)." *Journal of Immunological Methods* 208 (2): 141–49.

Ratts, Ryan C., and John R. Murphy. 2012. "Diphtheria Toxin and Cytosolic Translocation Factors." In *Insight and Control of Infectious Disease in Global Scenario*, edited by Roy Priti. InTech. http://www.intechopen.com/books/insight-and-control-of-infectious-disease-in-global-scenario/diphtheria-toxin-and-cytosolic-translocation-factors.

Retter, I. 2004. “VBASE2, an Integrative V Gene Database.” *Nucleic Acids Research* 33 (Database issue): D671–74. https://doi.org/10.1093/nar/gki088.

Rondot, S., J. Koch, F. Breitling, and S. Dübel. 2001. “A Helper Phage to Improve Single-Chain Antibody Presentation in Phage Display.” *Nature Biotechnology* 19 (1): 75–78. https://doi.org/10.1038/83567.

Russo, Giulio, Ulrike Theisen, Wieland Fahr, Saskia Helmsing, Michael Hust, Reinhard W. Köster, and Stefan Dübel. 2018. “Sequence Defined Antibodies Improve the Detection of Cadherin 2 (N-Cadherin) during Zebrafish Development.” *New Biotechnology* 45 (October): 98–112. https://doi.org/10.1016/j.nbt.2017.12.008.

Sandvig, K. 1980. “Diphtheria Toxin Entry into Cells Is Facilitated by Low PH.” *The Journal of Cell Biology* 87 (3): 828–32. https://doi.org/10.1083/jcb.87.3.828.

Sangal, Vartul, Andreas Burkovski, Alison C. Hunt, Becky Edwards, Jochen Blom, and Paul A. Hoskisson. 2014. “A Lack of Genetic Basis for Biovar Differentiation in Clinically Important Corynebacterium Diphtheriae from Whole Genome Sequencing.” *Infection, Genetics and Evolution* 21 (January): 54–57. https://doi.org/10.1016/j.meegid.2013.10.019.

Schofield, Darren J, Anthony R Pope, Veronica Clementel, Jenny Buckell, Susan DJ Chapple, Kay F Clarke, Jennie S Conquer, et al. 2007. “Application of Phage Display to High Throughput Antibody Generation and Characterization.” *Genome Biology* 8 (11): R254. https://doi.org/10.1186/gb-2007-8-11-r254.

Schütte, Mark, Philippe Thullier, Thibaut Pelat, Xenia Wezler, Philip Rosenstock, Dominik Hinz, Martina Inga Kirsch, et al. 2009. “Identification of a Putative Crf Splice Variant and Generation of Recombinant Antibodies for the Specific Detection of Aspergillus Fumigatus.” Edited by Jörg Hermann Fritz. *PLoS ONE* 4 (8): e6625. https://doi.org/10.1371/journal.pone.0006625.

Schwimmer, Lauren J., Betty Huang, Hoa Giang, Robyn L. Cotter, David S. Chemla-Vogel, Francis V. Dy, Eric M. Tam, et al. 2013. “Discovery of Diverse and Functional Antibodies from Large Human Repertoire Antibody Libraries.” *Journal of Immunological Methods* 391 (1–2): 60–71. https://doi.org/10.1016/j.jim.2013.02.010.

Sevigny, L. M., B. J. Booth, K. J. Rowley, B. A. Leav, P. S. Cheslock, K. A. Garrity, S. E. Sloan, W. Thomas, G. J. Babcock, and Y. Wang. 2013. “Identification of a Human Monoclonal Antibody To Replace Equine Diphtheria Antitoxin for Treatment of Diphtheria Intoxication.” *Infection and Immunity* 81 (11): 3992–4000. https://doi.org/10.1128/IAI.00462-13.

Shinefield, Henry R. 2010. “Overview of the Development and Current Use of CRM197 Conjugate Vaccines for Pediatric Use.” *Vaccine* 28 (27): 4335–39. https://doi.org/10.1016/j.vaccine.2010.04.072.

Siegrist, Claire-Anne. 2013. “Vaccine Immunology.” In *Vaccines*, edited by Stanley A. Plotkin, Walter A. Orenstein, and Paul A. Offit, Sixth edition. Philadelphia, Pa.: Elsevier Saunders.

Smith, W. P., P. C. Tai, J. R. Murphy, and B. D. Davis. 1980. “Precursor in Cotranslational Secretion of Diphtheria Toxin.” *Journal of Bacteriology* 141 (1): 184–89.

Thie, Holger, Lars Toleikis, Jiandong Li, Reinhard von Wasielewski, Gunther Bastert, Thomas Schirrmann, Isabel Tourais Esteves, et al. 2011. “Rise and Fall of an Anti-MUC1 Specific Antibody.” *PloS One* 6 (1): e15921. https://doi.org/10.1371/journal.pone.0015921.

Uchida, Tsuyoshi, D. Michael Gill, and A. M. Pappenheimer Jr. 1971. “Mutation in the Structural Gene for Diphtheria Toxin Carried by Temperate Phage β.” *Nature New*

Biology 233 (September): 8.

Uchida, Tsuyoshi, A. M. Pappenheimer, and A. A. Harper. 1973. "Diphtheria Toxin and Related Proteins. II. Kinetic Studies on Intoxication of HeLa Cells by Diphtheria Toxin and Related Proteins." *The Journal of Biological Chemistry* 248 (11): 3845–50.

Varshney, Avanish K., Xiaobo Wang, Emily Cook, Kaushik Dutta, Matthew D. Scharff, Michael J. Goger, and Bettina C. Fries. 2011. "Generation, Characterization, and Epitope Mapping of Neutralizing and Protective Monoclonal Antibodies against Staphylococcal Enterotoxin B-Induced Lethal Shock." *Journal of Biological Chemistry* 286 (11): 9737–47. https://doi.org/10.1074/jbc.M110.212407.

"Venezuela Diphtheria Case Tally Hits 800 in 2018." 2018. *Outbreak News Today* (blog). October 30, 2018. http://outbreaknewstoday.com/venezuela-diphtheria-case-tally-hits-800-2018/.

Vieira, J., and J. Messing. 1987. "Production of Single-Stranded Plasmid DNA." *Methods in Enzymology* 153: 3–11.

"WHO | Diphtheria." 2018. WHO. September 20, 2018. http://www.who.int/immunization/diseases/diphtheria/en/.

"WHO World Health Organization: Immunization, Vaccines And Biologicals. Vaccine Preventable Diseases Vaccines Monitoring System 2018 Global Summary Reference Time Series: DIPHTHERIA." 2018. 2018. http://apps.who.int/immunization_monitoring/globalsummary/timeseries/tsincidencediphtheria.html.

Wild, Martha A, Hong Xin, Toshiaki Maruyama, Mary Jean Nolan, Peter M Calveley, John D Malone, Mark R Wallace, and Katherine S Bowdish. 2003. "Human Antibodies from Immunized Donors Are Protective against Anthrax Toxin in Vivo." *Nature Biotechnology* 21 (11): 1305–6. https://doi.org/10.1038/nbt891.

Winter, Greg, and César Milstein. 1991. "Man-Made Antibodies." *Nature* 349 (6307): 293–99. https://doi.org/10.1038/349293a0.

"Yemen Diphtheria and Cholera Update." 2018. *Outbreak News Today* (blog). April 26, 2018. http://outbreaknewstoday.com/yemen-diphtheria-cholera-update-10360/.

6 List of Figures

7 List of Tables

Acknowledgments

Good times, bad times, I know you've had your share! (inspired by Led Zepplin).
Eine gute Zeit ist zu Ende und ich möchte nichts aus dieser Zeit missen. Es gibt viele Wegbegleiter, denen ich auf diesen Weg danken möchte.

Ein ganz besonderer Dank gilt meinem Mentor **Prof. Dr. Michael Hust** für seine große Hilfe und enorme Unterstützung bei dem Projekt. Danke das du immer da warst und zu jeder Zeit ein offenes Ohr hattest.

Vielen Dank an **Prof. Dr. Stefan Dübel** für die Möglichkeit der Promotion in seiner Arbeitsgruppe und für die Übernahme des Zweitgutachtens.

Danke an **Prof. Dr. Michael Steinert** für die Übernahme des Prüfungsvorsitzes.

A big thank to my cooperation partners **Dr. Paul Stickings**, **Dr. Jeffrey Brown**, **Dr. Thea Sesardic** and **Dr. Androulla Efstratiou** for the support during the DATMAB project.

Danke an „Der Bsrest“. Danke für unsere regelmäßigen Treffen. Unvergessen bleibt „And an angle said – it is not logic it is BIOlogic“ (inspired by **Christina Engel**, 2018). Und besonders danke an **Franzi**, dass du mit soviel Sorgfalt durch meine Arbeit gegangen bist und sogar die kleinsten Fehler gefunden hast. Ebenso Danke an die LLL-Gang das ihr immer aufmunternde Worte und Bilder für jede Lebenslage für mich hattet.

Ein ganz großer Dank geht an die ganze Arbeitsgruppe der **Abteilung Biotechnologie** für eine tolle Arbeitsatmosphäre. Danke an **Viola** und **Jörn** für die vielen guten Gespräche und den immer hilfreichen input, vor allem in Kombination mit dem Genuss eines guten Kaffees. Thanks to **Gustavo** for a lot of really good discussions. Thanks to **Giulio** for always helping me with every question, no matter how difficult. Danke an **Wieland**, der mit seiner Musik immer die Ruhe zurück ins Labor gebracht hat. Danke an **Maren** für ihre große Hilfe bei meinen ersten Schreibversuchen.

Danke an meine Freunde und Familie für ihre Unterstützung. Ganz herzlich danken möchte ich meinem Lebensgefährten **Mario Schmid** für seine bedingungslose Unterstützung! Ohne dich wäre weder diese Arbeit, noch die letzten 8 Jahre möglich gewesen. Danke! Und Led Zepplin haben es schon sehr treffend formuliert:
And so today, my world it smiles! Your hand in mine, we walked the miles! Thanks to you it is done!

Supplemental Information

Table 31: Oligonucleotides used in this Study

Primer name	Sequence	Used for
MHLacZ-Pro_f	GGCTCGTATGTTGTGTGG	Colony PCR
MHgIII_r	CTAAAGTTTTGTCGTCTTTCC	Colony PCR
ToR-pCMV-mlgG01-Fc-seq-f	CACTTTGCCTTTCTCTCC	Colony PCR
ToR-pCMV-mlgG01-Fc-seq-r	CAGATGGCTGGCAACTAG	Colony PCR
CM2_f	CGCAAATGGGCGGTAGGCGTG	Sequencing
ToR-pCMV-Seq-f	TGGTAGCAACAGCTACAG	Sequencing
ewe_DT-C-Nhe_f	GCGTGGCTAGCGGCGCTGATGATG	DT cloning
ewe_DT-C-Not_r	GCACGCGGCCGCTCGCCTGACACG	DT cloning
ewe_DT-B-Nhe_f	GCGTGGCTAGCTCAGTAGGTAGCTCATTGTC	DT cloning
ewe_DT-T-Not_r	GCACGCGGCCGCGGGACGATTATACGAATTATG	DT cloning
ewe_DT-R-Nhe_f	GCGTGGCTAGCGCGTATTCTCCGGG	DT cloning
ewe_DT-B-Not_r	GCACGCGGCCGCGCTTTTGATTTCAAAAAATAGCG	DT cloning
EwC1+A6+E4+G12AgeI_f	AAAGCACCGGTGAAACGACACTCACGCAG	IgG subcloning
EWE_VH-4-BssHII_f	TGAGCGGCGCGCACTCCCAAATGCAGCTGGTGCAG	IgG subcloning
EWE_VH-5-NheI_r	TGAGCCGCTAGCTGCGGAGACGGTGACTGTG	IgG subcloning
EWE_VH-6-NheI_r	TGAGCCGCTAGCTGAGGAGATGGTGACCATTG	IgG subcloning
EWE_VL-5_BsiWI_r	TGAGCCCGTACGTCTAATCTCCAGCTTGGTCC	IgG subcloning
EWE_VL-6_BsiWI_r	TGAGCCCGTACGTCTGATTTCCACTTTGGTCC	IgG subcloning
AF_pCSL3_DraIII-rev	AGTGACACTTGGTGCAGCCTTGGGCTGACC	IgG subcloning
AF120.2-H2_LC_AgeI_f	TGAGCCACCGGTGAAATTGTGTTGACGCAG	IgG subcloning
AF165R4.2-G11-HC_BssHII_f	CACAGGCGCGCACTCCGAGGTGCAGCTGGTGC	IgG subcloning
AF311-G6-VH_BssHII_f	CCACAGGCGCGCACTCCCAGCTGCAGCTGCAGGAG	IgG subcloning
AF311-H7-VH_BssHII_f	CCACAGGCGCGCACTCCCAGGTGCAGCTGGT	IgG subcloning

Primer name	Sequence	Used for
AF312-G1VH_BssHII_f	CCACAGGCGCGCACTCCCAGGTCCAGCTGGTGCAG	IgG subcloning
ew191_2C1+B5_BsiWI_r	TGAGCCCGTACGTTTGATCTCCACCTTGGTCC	IgG subcloning
Ew191-C10_VL_AgeI_f	AAAGCACCGGTCAGCCAGTGCTAACTCAG	IgG subcloning
Ew191-C12_VL_AgeI_f	AAAGCACCGGTTCCTATGTGCTGACACAG	IgG subcloning
Ew191/2-A7+D8_AgeI_f	AAAGCACCGGTTCCTATGAGCTGACTCAG	IgG subcloning
ew191/2C1+B5_BsiWI_r	TGAGCCCGTACGTTTGATCTCCACCTTGGTCC	IgG subcloning
Ew191/2D1+F11_AgeI_f	AAAGCACCGGTCAGTCTGTGTTGACGCAG	IgG subcloning
ew191E12_VL_DraIII_r	AGTGACACTTGGTGCGGCCTTGGGCTGACCTAG	IgG subcloning
ew191F11_VL_DraIII_r	AGTGACACTTGGTGCGGCCTTGGGCTGACTTAG	IgG subcloning
Ew192-B5_VL_AgeI_f	AAAGCACCGGTGCCATCCAGATGACCCAG	IgG subcloning
Ew192-C11_VL_AgeI_f	AAAGCACCGGTCAGGCTGTGGTGACTCAG	IgG subcloning
Ew192-F6_VL_AgeI_f	AAAGCACCGGTGAAGTTGTGCTGACACAG	IgG subcloning
ew192-G12_VL_BsiWI_r	TGAGCCCGTACGTTTGATATCCACCTTGGTCC	IgG subcloning
EwC1+A6+E4+G12AgeI_f	AAAGCACCGGTGAAACGACACTCACGCAG	IgG subcloning
EWE_VH-1-BssHII_f	TGAGCGGCGCGCACTCCCAGGTGCAGCTGCAACAG	IgG subcloning
EWE_VH-1-NheI_r	TGAGCCGCTAGCTGAAGAGACGGTGACCAG	IgG subcloning
EWE_VH-2-BssHII_f	TGAGCGGCGCGCACTCCCAGGTGCAGCTACAACAG	IgG subcloning
EWE_VH-2-NheI_r	TGAGCCGCTAGCGGAGGAGACGGTGACCAG	IgG subcloning
EWE_VH-3-BssHII_f	TGAGCGGCGCGCACTCCCAAGTGCAGCTGGTGCAATC	IgG subcloning
EWE_VH-3-NheI_r	TGAGCCGCTAGCTGAGGAGACAGCGACCAG	IgG subcloning
EWE_VH-4-NheI_r	TGAGCCGCTAGCGGAGGCTGAGGAGACGGTG	IgG subcloning
EWE_VL-1-AgeI_f	AAAGCACCGGTGACATCCGGATGACCCAG	IgG subcloning
EWE_VL-1-BsiWI_r	TGAGCCCGTACGTTTGACGTCTACCTTGGTCC	IgG subcloning
EWE_VL-2-AgeI_f	AAAGCACCGGTGCCATCCGGTTGACCCAG	IgG subcloning

Primer name	Sequence	Used for
EWE_VL-2-BsiWI_r	TGAGCCCGTACGTTTGATGTCTACCTTGGTCC	IgG subcloning
EWE_VL-3-AgeI_f	AAAGCACCGGTGATGTTGTGCTGACTCAG	IgG subcloning
EWE_VL-3-BsiWI_r	TGAGCCCGTACGTTTGATATCCACTTTGGTCC	IgG subcloning
EWE_VL-4-AgeI_f	AAAGCACCGGTGAAATTGTGATGACACAG	IgG subcloning
EWE_VL-4-BsiWI_r	TGAGCCCGTACGCTTGATCTCTACCTTGGTCC	IgG subcloning
EWE_VL-5-AgeI_f	AAAGCACCGGTGACATCCAGATGACACAG	IgG subcloning
Ewe-B5P_VH_BssHIII_f	TGAGCGGCGCGCACTCCCAGGTGCAGCTGCAGCAG	IgG subcloning
ewe191_1_IgG-VH_r	TGAGCCGCTAGCTGAGGAGACGGTGACCAG	IgG subcloning
ewe191-A9_IgG-VH_r	TGAGCCGCTAGCTGAAGAGATGGTGACCATTG	IgG subcloning
ewe191-A9_VH_BssHIII_f	TGAGCGGCGCGCACTCCCAAGTCCAGCTGGTACAG	IgG subcloning
ewe191-C1_IgG-VH_r	TGAGCCGCTAGCTGAGGACACGGTGACCGTG	IgG subcloning
ewe191A7_VL_DraIII_r	AGTGACACTTGGTGCAGCCTTGGGCTGACGTAG	IgG subcloning
ewe191C/E12_IgG-VH_r	TGAGCCGCTAGCTGAGGAGACGGTGACCCG	IgG subcloning
ewe191D1_VL_DraIII_r	AGTGACACTTGGTGCAGCCTTGGACTGACCTAG	IgG subcloning
Ewe192_5_IgG-VH_r	TGAGCCGCTAGCTGAGGAGACGGTGACTGTG	IgG subcloning
Ewe192_7_IgG-VH_r	TGAGCCGCTAGCTGAAGAGATGGTGACGATTG	IgG subcloning
Ewe192_8_IgG-VH_r	TGAGCCGCTAGCTGAGGAGATGGTGACCATTG	IgG subcloning
ewe192-A6+H8_BsiWI_r	TGAGCCCGTACGTTTAATCTCCAGTCGTGTCC	IgG subcloning
ewe192-B5_IgG-VH_r	TGAGCCGCTAGCTGAGGAGACAGTGACTAG	IgG subcloning
ewe192-B5_VH_BssHIII_f	TGAGCGGCGCGCACTCCCAGGTGCAGCTATAGCAG	IgG subcloning
ewe192-E4_VL_BsiWI_r	TGAGCCCGTACGTCTGATCTCCACCTTGGTCC	IgG subcloning
ewe192-F6_VL_BsiWI_r	TGAGCCCGTACGTTTGATTTCCACCTTGGTCC	IgG subcloning
ewe192-H7_VH_BssHIII_f	TGAGCGGCGCGCACTCCGAAGTGCAGCTGGTGGAG	IgG subcloning
JOZ_AgeI_JOZ376-C5_f	GATCACCGGTGAAATTGTGCTGACTCAG	IgG subcloning

Primer name	Sequence	Used for
JOZ_AgeI_JOZ376E12_f	AAAGCACCGGTGATATTGTGATGACTCAG	IgG subcloning
MaK_9E10_VH_BssHII_f	CACAGGCGCGCACTCCCAGGTGCAGCTGCAGGAG	IgG subcloning
MHSH1684-C12-BssHII_f	GCGTGGCGCGCACTCCCAGGTTCAGCTGGTGCAG	IgG subcloning
MZI15_A2_AgeI_F	AAAGCACCGGTCAGTCTGTGCTGACGCAGCC	IgG subcloning
MZI8_1.2_D11_AgeI_F	AAAGCACCGGTCAGTCTGCCCTGACTCAGC	IgG subcloning
MZI8_1.2_D11_BssHII_F	CACAGGCGCGCACTCCCAGGTACAGCTGCAGCAGTC	IgG subcloning
MZI8_1.4_D1_AgeI_F	AAAGCACCGGTCAGGCTGTGCTGACTCAGC	IgG subcloning
SH1785-E8_NheI_r	TGAGCCGCTAGCTGAGGAGACAGTGACCAG	IgG subcloning
SoS-AgeI-SH83-A7VK-f	CATAACCGGTGACATCCAGATGACCCAGT	IgG subcloning
SoS-AgeI-SUW117-H2VL-f	CAATACCGGTCAGTCTGTGCTGACTCAGCCA	IgG subcloning
SoS-AgeI-SUW119-H2VL-f	GTACACCGGTCAGCCTGTGCTGACTCAGC	IgG subcloning
SoS-BssHII-SUW57-D11VH-f	CAAGGCGCGCACTCCCAGGTGCAACTGCAGGAGTCG	IgG subcloning
SUW_AgeI_313-B5_f	CAGCACCGGTCTGCCTGTGCTGACTCAGCC	IgG subcloning
SUW_BssHII_hMN-14VH_f	CACAGGCGCGCACTCCGAGGTGCAGCTGGTGGAG	IgG subcloning
MHVH1_f:	CAG GTB CAG CTG GTG CAG TCT GG	Library cloning
MHVH1/7_f:	CAR RTS CAG CTG GTR CAR TCT GG	Library cloning
MHVH2_f:	CAG RTC ACC TTG AAG GAG TCT GG	Library cloning
JokVH3_f1:	SAG GTG CAG CTG GTG GAG TCT GG	Library cloning
JokVH3_f2:	GAR GTG CAG CTG KTG GAG TCT GG	Library cloning
MHVH4_f1:	CAG GTG CAR CTG CAG GAG TCG GG	Library cloning
JokVH4_f2:	CAG GTG CAG CTA CAR CAG TGG GG	Library cloning
JokVH4_f2:	CAG CTG CAG CTG CAG GAG TCS GG	Library cloning
MHVH5_f:	GAR GTG CAG CTG GTG CAG TCT GG	Library cloning
MHVH6_f:	CAG GTA CAG CTG CAG CAG TCA GG	Library cloning
MHkappaCL_r:	ACA CTC TCC CCT GTT GAA GCT CTT	Library cloning
MHVL1_f1:	CAG TCT GTG CTG ACT CAG CCA CC	Library cloning

Primer name	Sequence	Used for
MHVL1_f2:	CAG TCT GTG YTG ACG CAG CCG CC	Library cloning
MHVL2_f:	CAG TCT GCC CTG ACT CAG CCT	Library cloning
MHVL3_f1:	TCC TAT GWG CTG ACW CAG CCA CC	Library cloning
MHVL3_f2:	TCT TCT GAG CTG ACT CAG GAC CC	Library cloning
MHVL4_f1:	CTG CCT GTG CTG ACT CAG CCC	Library cloning
MHVL4_f2:	CAG CYT GTG CTG ACT CAA TCR YC	Library cloning
MHVL5_f:	CAG SCT GTG CTG ACT CAG CC	Library cloning
MHVL6_f:	AAT TTT ATG CTG ACT CAG CCC CA	Library cloning
MHVL7/8_f:	CAG RCT GTG GTG ACY CAG GAG CC	Library cloning
MHVL9/10_f:	CAG SCW GKG CTG ACT CAG CCA CC	Library cloning
MHlambdaCL_r:	TGA ACA TTC TGT AGG GGC CAC TG	Library cloning
MHVK1_f1:	GAC ATC CAG ATG ACC CAG TCT CC	Library cloning
MHVK1_f2:	GMC ATC CRG WTG ACC CAG TCT CC	Library cloning
MHVK2_f:	GAT RTT GTG ATG ACY CAG WCT CC 3	Library cloning
MHVK3_f:	GAA ATW GTG WTG ACR CAG TCT CC	Library cloning
MHVK4_f:	GAC ATC GTG ATG ACC CAG TCT CC	Library cloning
MHVK5_f:	GAA ACG ACA CTC ACG CAG TCT CC	Library cloning
MHVK6_f:	GAW RTT GTG MTG ACW CAG TCT CC	Library cloning
MHkappaCL_r:	ACA CTC TCC CCT GTT GAA GCT CTT	Library cloning

Table 32: 130 scFv-Fc V gene information. Outcome of panning with immobilized a ntigen.

Antibody clones	VH			VL	
	V	D	J	V	J
ewe190-A11__f	IGHV1-69*01	IGHD3-22*01	IGHJ3*02	IGLV6-57*01	IGLJ3*02
ewe190-A2__f	IGHV3-30*18	IGHD1-26*01	IGHJ3*02	IGLV3-1*01	IGLJ1*01
ewe190-A3__f	IGHV3-9*01	IGHD1-26*01	IGHJ4*02	IGLV6-57*01	IGLJ3*02
ewe190-A6__f	IGHV4-4*02	IGHD1-26*01	IGHJ3*02	IGLV1-44*01	IGLJ3*02
ewe190-A9__f	IGHV4-4*02	IGHD3-16*01	IGHJ3*02	IGLV1-50*01	IGLJ3*02
ewe190-B10__f	IGHV3-30*18	IGHD3-3*01	IGHJ4*02	IGLV1-44*01	IGLJ1*01
ewe190-B1__f	IGHV3-23*04	IGHD3-16*01	IGHJ4*02	IGLV1-44*01	IGLJ3*02
ewe190-C10__f	IGHV3-23*04	IGHD3-22*01	IGHJ3*02	IGLV3-1*01	IGLJ3*01
ewe190-C11__f	IGHV3-30*18	IGHD1-26*01	IGHJ4*02	IGLV3-21*01	IGLJ3*02
ewe190-C2__f	IGHV1-46*03	IGHD3-22*01	IGHJ6*03	IGLV1-40*01	IGLJ3*02
ewe190-C5__f	IGHV6-1*01	IGHD5-12*01inv	IGHJ6*02	IGLV1-47*02	IGLJ3*02
ewe190-C6__f	IGHV5-51*01	IGHD3-22*01	IGHJ3*02	IGLV1-44*01	IGLJ3*01

Antibody clones	VH			VL	
	V	D	J	V	J
ewe190-D3__f	IGHV1-24*01	IGHD1-26*01	IGHJ4*02	IGLV6-57*01	IGLJ3*02
ewe190-D6__f	IGHV3-23*04	IGHD2-15*01inv	IGHJ4*02	IGLV1-44*01	IGLJ3*01
ewe190-D7__f	IGHV3-23*04	IGHD3-9*01	IGHJ4*02	IGLV1-44*01	IGLJ3*02
ewe190-D8__f	IGHV4-4*02	IGHD3-10*01	IGHJ3*02	IGLV1-44*01	IGLJ1*01
ewe190-D9__f	IGHV1-f*01	IGHD5-5*01	IGHJ4*02	IGLV3-19*01	IGLJ3*02
ewe190-E10__f	IGHV3-9*01	IGHD3-3*02	IGHJ4*02	IGLV1-44*01	IGLJ1*01
ewe190-E1__f	IGHV3-9*01	IGHD3-22*01	IGHJ4*02	IGLV2-8*01	IGLJ1*01
ewe190-E3__f	IGHV3-30*18	IGHD4-17*01	IGHJ4*02	IGLV6-57*01	IGLJ3*02
ewe190-E5__f	IGHV1-46*03	IGHD3-22*01	IGHJ6*03	IGLV1-40*01	IGLJ1*01
ewe190-E6__f	IGHV1-18*01	IGHD1-26*01	IGHJ4*02	IGLV1-44*01	IGLJ3*01
ewe190-G10__f	IGHV3-23*04	IGHD5-12*01	IGHJ6*02	IGLV1-44*01	IGLJ3*02
ewe190-G11__f	IGHV1-69*06	IGHD3-9*01	IGHJ3*02	IGLV1-47*01	IGLJ3*01
ewe190-G4__f	IGHV1-69*01	IGHD6-19*01	IGHJ5*02	IGLV1-40*01	IGLJ3*01
ewe190-H11__f	IGHV4-4*02	IGHD2-15*01inv	IGHJ4*02	IGLV1-44*01	IGLJ1*01
ewe190-H1__f	IGHV3-9*01	IGHD4-17*01	IGHJ6*02	IGLV3-19*01	IGLJ3*02
ewe190-E7__f	IGHV1-46*03	IGHD3-22*01	IGHJ6*03	IGLV1-40*01	IGLJ3*02
ewe190-H10__f	IGHV3-9*01	IGHD3-22*01	IGHJ4*02	IGLV2-8*01	IGLJ1*01
E09_4519__f	IGHV1-3*01	IGHD3-10*01	IGHJ6*02	IGLV1-44*01	IGLJ1*01
E10_4519__f	IGHV1-3*01	IGHD3-10*01	IGHJ6*02	IGKV1-16*02	IGKJ4*01
E11_4519__f	IGHV1-3*01	IGHD6-19*01	IGHJ4*02	IGKV3-15*01	IGKJ1*01
E12_4519__f	IGHV3-33*01	IGHD6-13*01	IGHJ4*02	IGLV1-47*01	IGLJ3*01
ewe191-G10__f	IGHV1-f*01	IGHD4-23*01	IGHJ6*02	IGLV1-40*01	IGLJ1*01
ewe191-G11__f	IGHV1-3*01	IGHD6-19*01	IGHJ4*02	IGLV1-40*01	IGLJ3*02
ewe191-G3__f	IGHV1-18*01	IGHD2-21*02	IGHJ4*02	IGLV2-14*04	IGLJ3*02
ewe191-G4__f	IGHV1-69*04	IGHD2-2*02inv	IGHJ4*02	IGKV3-11*01	IGKJ4*01
ewe191-G5__f	IGHV5-51*01	IGHD3-10*01	IGHJ5*02	IGLV8-61*01	IGLJ3*02
ewe191-G6__f	IGHV1-3*01	IGHD3-10*01	IGHJ6*02	IGLV1-44*01	IGLJ3*02
ewe191-G8__f	IGHV1-3*01	IGHD3-10*01	IGHJ6*02	IGKV1D-39*01	IGKJ5*01
ewe191-G9__f	IGHV1-18*01	IGHD2-21*02	IGHJ4*02	IGKV3-20*01	IGKJ3*01
ewe191-H10__f	IGHV3-21*01	IGHD2-21*02	IGHJ4*02	IGLV3-21*02	IGLJ3*02
ewe191-H11__f	IGHV3-21*01	IGHD6-6*01inv	IGHJ3*02	IGLV2-14*01	IGLJ3*01
ewe191-H1__f	IGHV1-69*06	IGHD2-15*01	IGHJ4*02	IGLV8-61*01	IGLJ3*02
ewe191-H8__f	IGHV3-23*04	IGHD3-10*01	IGHJ4*02	IGLV1-44*01	IGLJ3*02
F01_4519__f	IGHV3-21*01	IGHD6-6*01inv	IGHJ3*02	IGLV1-44*01	IGLJ3*01
F02_4519__f	IGHV1-f*01	IGHD3-22*01	IGHJ4*02	IGLV1-44*01	IGLJ3*02

Antibody clones	VH			VL	
	V	**D**	**J**	**V**	**J**
F03_4519__f	IGHV1-f*01	IGHD4-23*01	IGHJ6*02	IGLV3-19*01	IGLJ3*01
F04_4519__f	IGHV5-51*01	IGHD3-10*02	IGHJ5*02	IGLV1-44*01	IGLJ3*02
F05_4519__f	IGHV1-69*01	IGHD3-22*01	IGHJ6*02	IGLV3-21*02	IGLJ3*01
F06_4519__f	IGHV1-3*01	IGHD6-19*01	IGHJ4*02	IGLV2-8*01	IGLJ3*01
F08_4519__f	IGHV3-21*01	IGHD3-3*02	IGHJ3*02	IGLV6-57*01	IGLJ3*01
F09_4519__f	IGHV1-3*01	IGHD3-10*01	IGHJ6*02	IGLV1-44*01	IGLJ3*02
F10_4519__f	IGHV1-3*01	IGHD3-10*01	IGHJ6*02	IGKV3-15*01	IGKJ4*01
F12_4519__f	IGHV3-21*01	IGHD6-6*01inv	IGHJ3*02	IGLV1-44*01	IGLJ3*01
G01_4519__f	IGHV3-21*01	IGHD2-21*02	IGHJ4*02	IGLV6-57*01	IGLJ3*01
G02_4519__f	IGHV3-21*01	IGHD2-21*02	IGHJ4*02	IGLV3-21*02	IGLJ3*01
G03_4519__f	IGHV3-33*01	IGHD6-13*01	IGHJ4*02	IGLV1-47*01	IGLJ3*01
G04_4519__f	IGHV5-51*01	IGHD3-10*02	IGHJ5*02	IGLV1-44*01	IGLJ3*01
G05_4519__f	IGHV3-21*01	IGHD2-21*02	IGHJ4*02	IGLV1-47*02	IGLJ3*01
G06_4519__f	IGHV5-51*01	IGHD3-10*02	IGHJ5*02	IGLV3-19*01	IGLJ3*01
G07_4519__f	IGHV4-4*02	IGHD4-17*01	IGHJ4*02	IGLV1-44*01	IGLJ7*01
G08_4519__f	IGHV1-f*01	IGHD4-23*01	IGHJ6*02	IGLV3-1*01	IGLJ1*01
G09_4519__f	IGHV1-3*02	IGHD2-2*01	IGHJ5*02	IGLV2-14*04	IGLJ1*01
G10_4519__f	IGHV1-2*02	IGHD3-22*01	IGHJ6*02	IGLV1-44*01	IGLJ3*01
G11_4519__f	IGHV4-34*01	IGHD1-1*01	IGHJ6*02	IGLV1-44*01	IGLJ3*02
G12_4519__f	IGHV1-69*06	IGHD6-19*01	IGHJ6*02	IGKV2D-28*01	
H02_4519__f	IGHV5-51*01	IGHD3-10*02	IGHJ5*02	IGLV6-57*01	IGLJ3*01
H03_4519__f	IGHV3-33*02	IGHD6-13*01	IGHJ4*03	IGLV1-47*01	IGLJ3*01
H04_4519__f	IGHV5-51*01	IGHD3-16*01	IGHJ5*02	IGLV1-44*01	IGLJ1*01
H05_4519__f	IGHV3-21*01	IGHD6-6*01inv	IGHJ3*02	IGLV6-57*01	IGLJ3*01
H06_4519__f	IGHV3-21*01	IGHD2-21*02	IGHJ4*02	IGKV3-20*01	IGKJ1*01
H07_4519__f	IGHV1-69*04	IGHD4-17*01	IGHJ4*02	IGKV1D-39*01	IGKJ3*01
H08_4519__f	IGHV1-3*01	IGHD6-19*01	IGHJ4*02	IGLV1-44*01	IGLJ1*01
H09_4519__f	IGHV3-21*01	IGHD6-6*01inv	IGHJ3*02	IGLV2-14*04	IGLJ1*01
H10_4519__f	IGHV1-3*01	IGHD2-2*01	IGHJ6*02	IGLV3-21*02	IGLJ1*01
H11_4519__f	IGHV1-3*01	IGHD3-10*01	IGHJ6*02	IGLV1-44*01	IGLJ1*01
H12_4519__f	IGHV3-21*01	IGHD2-15*01	IGHJ4*02	IGKV1D-39*01	IGKJ2*01
F07_4519__f	IGHV1-3*01	IGHD6-19*01	IGHJ4*02	IGLV2-8*01	IGLJ3*01
H01_4519__f	IGHV1-3*01	IGHD3-10*01	IGHJ6*02	IGKV1D-39*01	IGKJ5*01
A01_4519__f	IGHV3-21*01	IGHD5-24*01	IGHJ3*02	IGKV1D-39*01	IGKJ4*01
A02_4519__f	IGHV3-21*01	IGHD6-6*01inv	IGHJ3*02	IGLV1-44*01	IGLJ3*01

Antibody clones	VH			VL	
	V	D	J	V	J
A03_4519__f	IGHV3-21*01	IGHD6-6*01inv	IGHJ3*02	IGLV1-40*01	IGLJ3*01
A04_4519__f	IGHV3-21*01	IGHD5-24*01	IGHJ3*02	IGLV2-8*01	IGLJ3*02
A05_4519__f	IGHV4-39*01	IGHD6-6*01	IGHJ6*02	IGKV3-15*01	IGKJ5*01
A06_4519__f	IGHV4-39*01	IGHD6-6*01	IGHJ6*02	IGKV3-15*01	IGKJ4*01
A07_4519__f	IGHV3-21*01	IGHD6-6*01inv	IGHJ3*02	IGLV1-44*01	IGLJ3*02
A08_4519__f	IGHV3-21*01	IGHD6-6*01inv	IGHJ3*02	IGLV1-47*01	IGLJ3*02
A09_4519__f	IGHV3-21*01	IGHD6-6*01inv	IGHJ3*02	IGLV1-44*01	IGLJ3*02
A10_4519__f	IGHV4-34*01	IGHD4-17*01	IGHJ2*01	IGKV1D-39*01	IGKJ4*01
A11_4519__f	IGHV4-39*01	IGHD6-6*01	IGHJ6*02	IGLV1-40*01	IGLJ3*01
A12_4519__f	IGHV3-21*01	IGHD6-6*01inv	IGHJ3*02	IGLV2-8*01	IGLJ3*01
B01_4519__f	IGHV4-39*01	IGHD6-6*01	IGHJ6*02	IGKV3-20*01	IGKJ5*01
B02_4519__f	IGHV3-21*01	IGHD5-24*01	IGHJ3*02	IGLV2-11*01	IGLJ3*02
B03_4519__f	IGHV4-30-2*01	IGHD3-22*01	IGHJ4*02	IGLV3-21*02	IGLJ3*01
B04_4519__f	IGHV3-21*01	IGHD5-24*01	IGHJ3*02	IGLV3-25*03	IGLJ3*01
B05_4519__f	IGHV3-21*01	IGHD5-24*01	IGHJ3*02	IGLV2-8*01	IGLJ3*01
B06_4519__f	IGHV3-21*01	IGHD5-24*01	IGHJ3*02	IGLV8-61*01	IGLJ3*01
B07_4519__f	IGHV3-21*01	IGHD6-6*01inv	IGHJ3*02	IGLV1-44*01	IGLJ3*02
B09_4519__f	IGHV4-39*01	IGHD6-6*01	IGHJ6*02	IGKV3-20*01	IGKJ4*01
B10_4519__f	IGHV3-21*01	IGHD5-24*01	IGHJ3*02	IGLV3-1*01	IGLJ3*01
B11_4519__f	IGHV3-21*01	IGHD5-24*01	IGHJ3*02	IGLV2-23*03	IGLJ3*02
B12_4519__f	IGHV4-39*01	IGHD6-6*01	IGHJ6*02	IGLV3-21*02	IGLJ3*02
C02_4519__f	IGHV3-21*01	IGHD6-6*01inv	IGHJ3*02	IGLV1-44*01	IGLJ3*02
C06_4519__f	IGHV4-39*01	IGHD6-6*01	IGHJ6*02	IGKV3-20*01	IGKJ4*01
C07_4519__f	IGHV3-21*01	IGHD6-6*01inv	IGHJ3*02	IGLV1-40*01	IGLJ1*01
C08_4519__f	IGHV3-21*01	IGHD5-24*01	IGHJ3*02	IGLV3-1*01	IGLJ3*01
C09_4519__f	IGHV3-21*01	IGHD5-24*01	IGHJ3*02	IGLV1-44*01	IGLJ3*01
C10_4519__f	IGHV3-21*01	IGHD5-24*01	IGHJ3*02	IGLV2-11*01	IGLJ3*02
C11_4519__f	IGHV3-21*01	IGHD6-6*01inv	IGHJ3*02	IGLV1-40*01	IGLJ3*01
D01_4519__f	IGHV1-18*01	IGHD3-10*01	IGHJ6*02	IGLV1-44*01	IGLJ1*01
D02_4519__f	IGHV3-21*01	IGHD6-6*01inv	IGHJ3*02	IGLV2-14*04	IGLJ3*01
D03_4519__f	IGHV4-39*01	IGHD6-6*01	IGHJ6*02	IGKV3-15*01	IGKJ1*01
D04_4519__f	IGHV4-39*01	IGHD6-6*01	IGHJ6*02	IGKV3-20*01	IGKJ1*01
D05_4519__f	IGHV3-21*01	IGHD5-24*01	IGHJ3*02	IGLV1-44*01	IGLJ3*02
D06_4519__f	IGHV4-39*01	IGHD6-6*01	IGHJ6*02	IGLV1-40*01	IGLJ3*01
D07_4519__f	IGHV3-21*01	IGHD6-6*01inv	IGHJ3*02	IGLV1-44*01	IGLJ3*02

Antibody clones	VH			VL	
	V	**D**	**J**	**V**	**J**
D09_4519__f	IGHV3-21*01	IGHD6-6*01inv	IGHJ3*02	IGLV1-47*02	IGLJ3*01
D11_4519__f	IGHV3-21*01	IGHD6-6*01inv	IGHJ3*02	IGLV1-44*01	IGLJ3*01
D12_4519__f	IGHV3-21*01	IGHD6-6*01inv	IGHJ3*02	IGLV6-57*01	IGLJ3*01
E01_4519__f	IGHV3-21*01	IGHD5-24*01	IGHJ3*02	IGLV3-1*01	IGLJ3*02
E02_4519__f	IGHV3-21*01	IGHD6-6*01inv	IGHJ3*02	IGLV1-47*01	IGLJ3*01
E03_4519__f	IGHV4-39*01	IGHD6-6*01	IGHJ6*02	IGKV3-15*01	IGKJ3*01
E04_4519__f	IGHV4-39*01	IGHD6-6*01	IGHJ6*02	IGKV3-15*01	IGKJ3*01
E05_4519__f	IGHV3-21*01	IGHD6-6*01inv	IGHJ3*02	IGLV1-44*01	IGLJ5*02
E06_4519__f	IGHV3-21*01	IGHD6-6*01inv	IGHJ3*02	IGLV2-23*03	IGLJ3*02
E07_4519__f	IGHV4-39*01	IGHD6-6*01	IGHJ6*02	IGKV3D-15*01	IGKJ5*01
E08_4519__f	IGHV3-21*01	IGHD6-6*01inv	IGHJ3*02	no family assigned: humIGLV114	IGLJ3*02
B08_4519__f	IGHV3-21*01	IGHD6-6*01inv	IGHJ3*02	IGLV1-44*01	IGLJ3*01
C01_4519__f	IGHV4-39*01	IGHD6-6*01	IGHJ6*02	IGKV3-20*01	IGKJ5*01
C04_4519__f	IGHV4-39*01	IGHD6-6*01	IGHJ6*02	IGKV3-15*01	IGKJ4*01
C05_4519__f	IGHV4-39*01	IGHD6-6*01	IGHJ6*02	IGKV3-15*01	IGKJ5*01
D08_4519__f	IGHV3-21*01	IGHD6-6*01inv	IGHJ3*02	IGLV2-14*04	IGLJ3*01
D10_4519__f	IGHV3-21*01	IGHD6-6*01inv	IGHJ3*02	IGLV1-47*01	IGLJ3*02
C12_4519__f	IGHV3-21*01	IGHD6-6*01inv	IGHJ3*02	IGLV1-44*01	IGLJ3*01

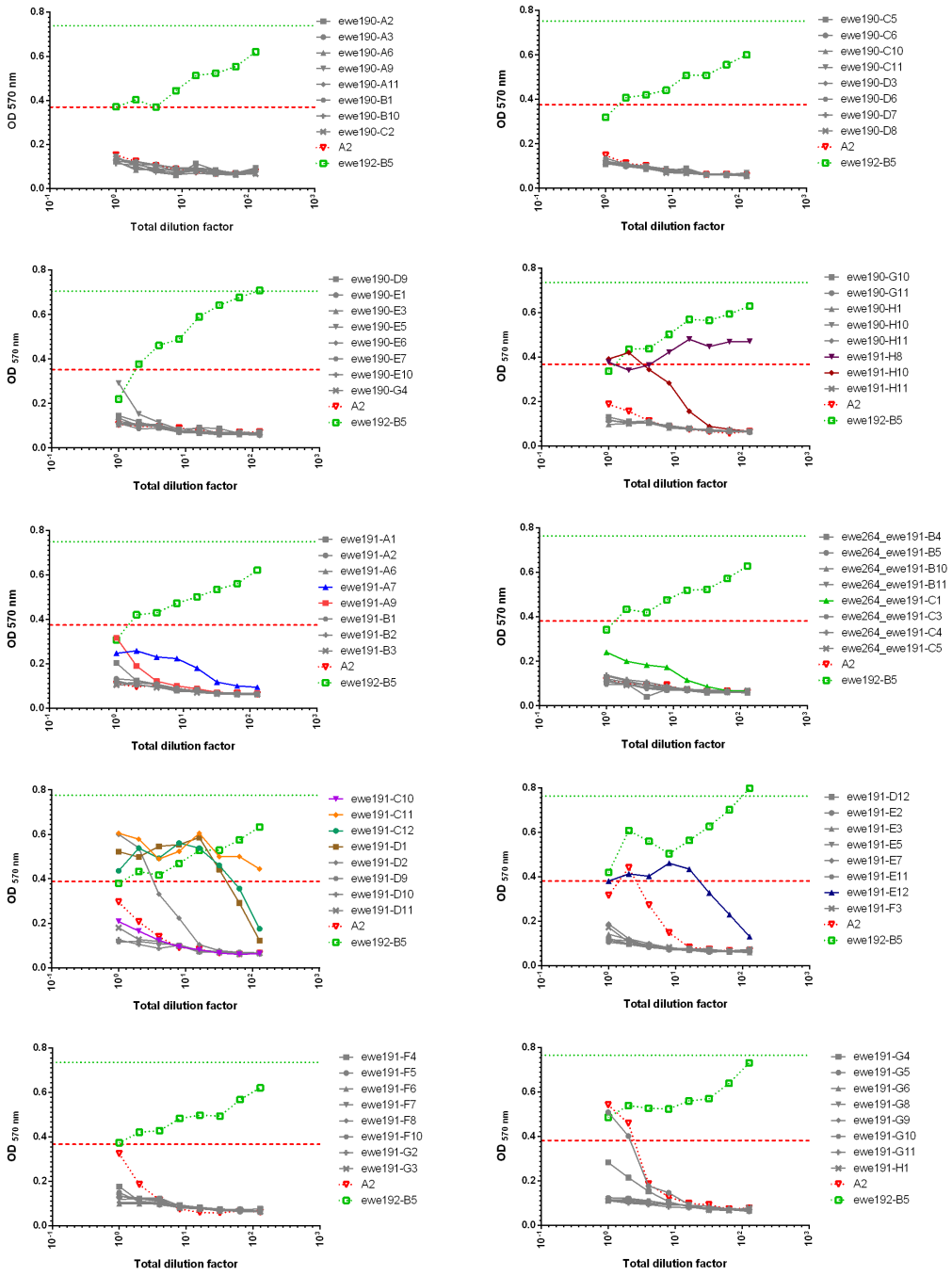

Figure 25: Neutralization assay of scFv-Fc in supernatant for screening. Untreated Vero cells are given as green dotted line. The threshold for neutralization is given as red dotted line (50 % of untreated Vero cells). The antibodies TM43-E10 and JöJ58B9 (red, open symbol and dotted line) are considered as negative control, ewe192-B5 (green, open symbol and dotted line) as positive control. All shown scFv-Fc antibodies were further analyzed. Mitochondrial activity was measured with an MTT assay after 6 days at OD_{570nm}.

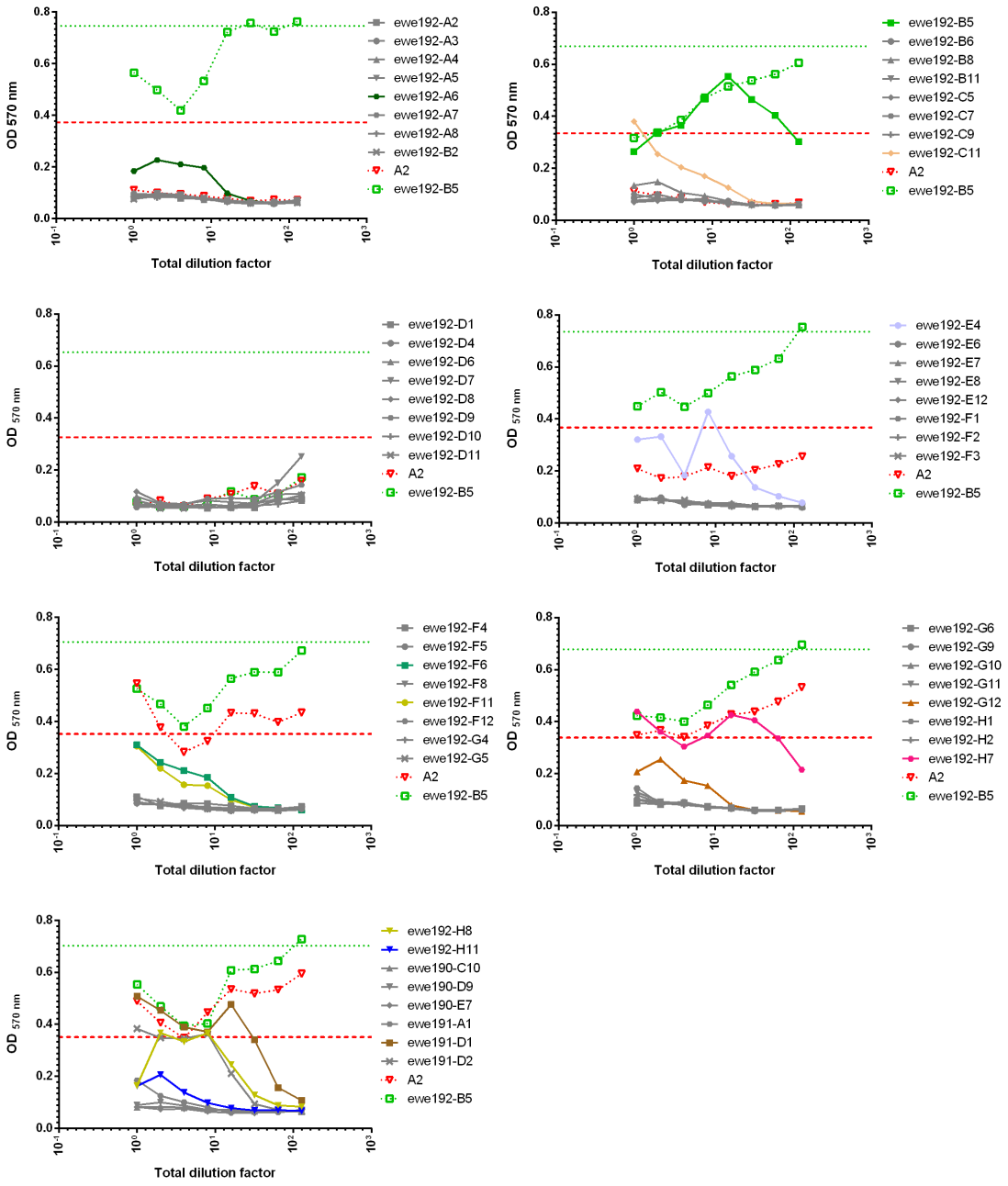

Figure 26: Neutralization assay of scFv-Fc in supernatant for screening. Untreated Vero cells are given as green dotted line. The threshold for neutralization is given as red dotted line (50 % of untreated Vero cells). The antibodies TM43-E10 and JöJ58B9 (red, open symbol and dotted line) are considered as negative control, ewe192-B5 (green, open symbol and dotted line) as positive control. All shown scFv-Fc antibodies were further analyzed. Mitochondrial activity was measured with an MTT assay after 6 days at OD_{570nm}.

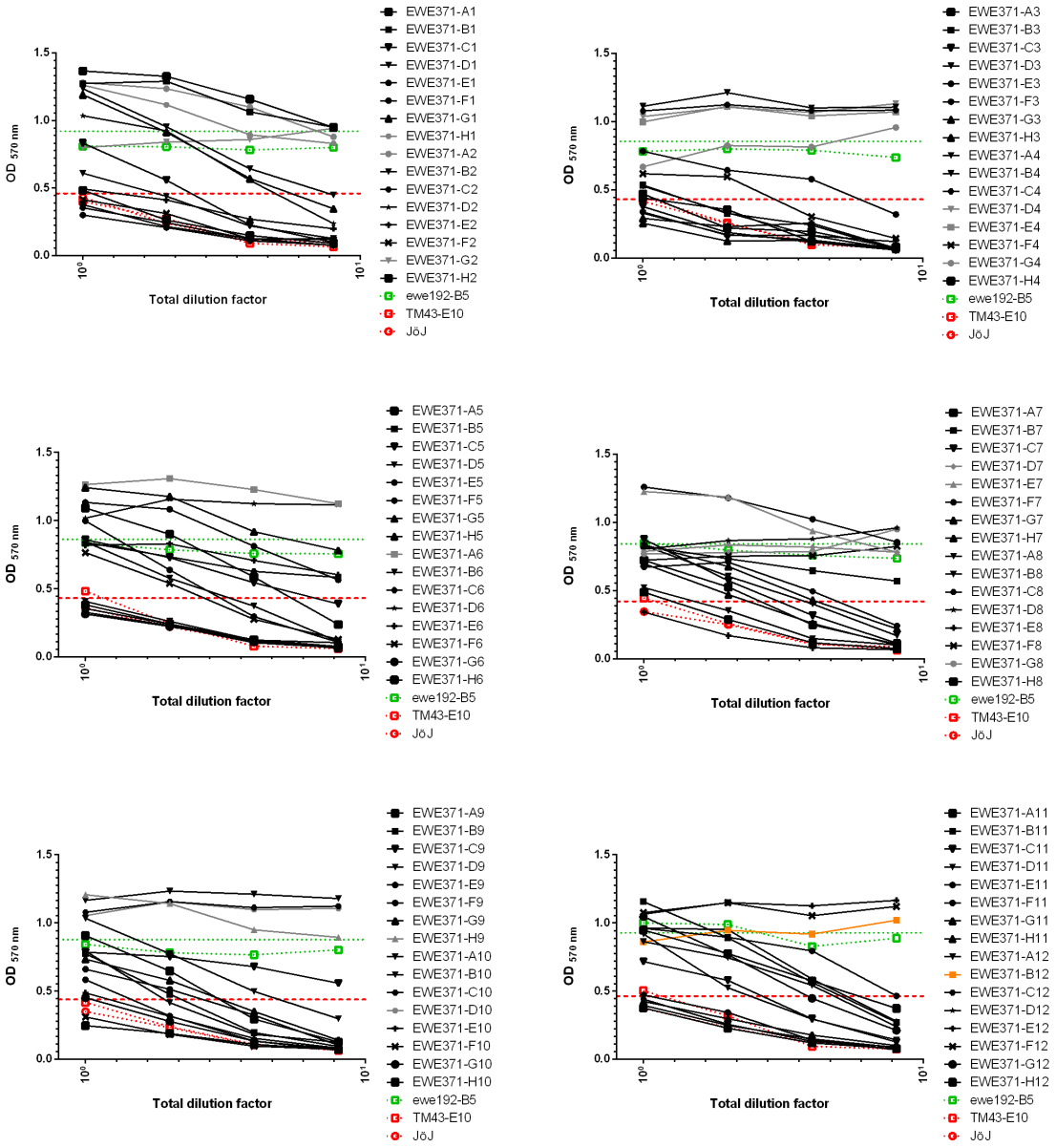

Figure 27: Neutralization assay of scFv-Fc in supernatant for screening. Untreated Vero cells are given as green dottet line. The threshold for neutralization is given as red dotted line (50 % of untreated Vero cells). The antibodies TM43-E10 and JöJ58B9 (red, open symbol and dotted line) are considered as negative control, ewe192-B5 (green, open symbol and dotted line) as positive control. Samples with gray or colored symbols were further analyzed, samples with black symbols not. Mitochondrial activity was measured with an MTT assay after 6 days at OD_{570nm}.

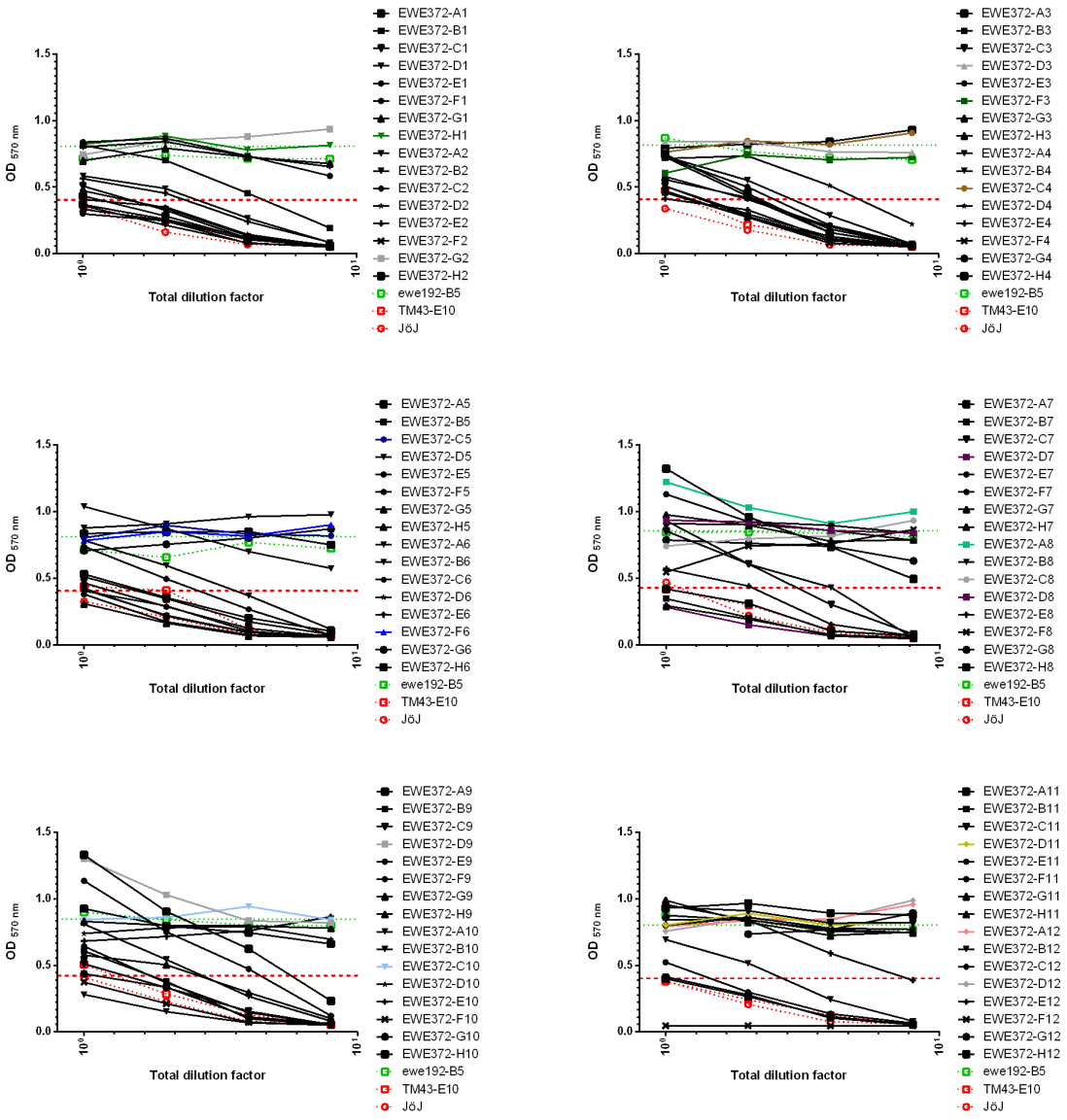

Figure 28: Neutralization assay of scFv-Fc in supernatant for screening. Untreated Vero cells are given as green dottet line. The threshold for neutralization is given as red dotted line (50 % of untreated Vero cells). The antibodies TM43-E10 and JöJ58B9 (red, open symbol and dotted line) are considered as negative control, ewe192-B5 (green, open symbol and dotted line) as positive control. Samples with gray or colored symbols were further analyzed, samples with black symbols not. Mitochondrial activity was measured with an MTT assay after 6 days at OD_{570nm}.

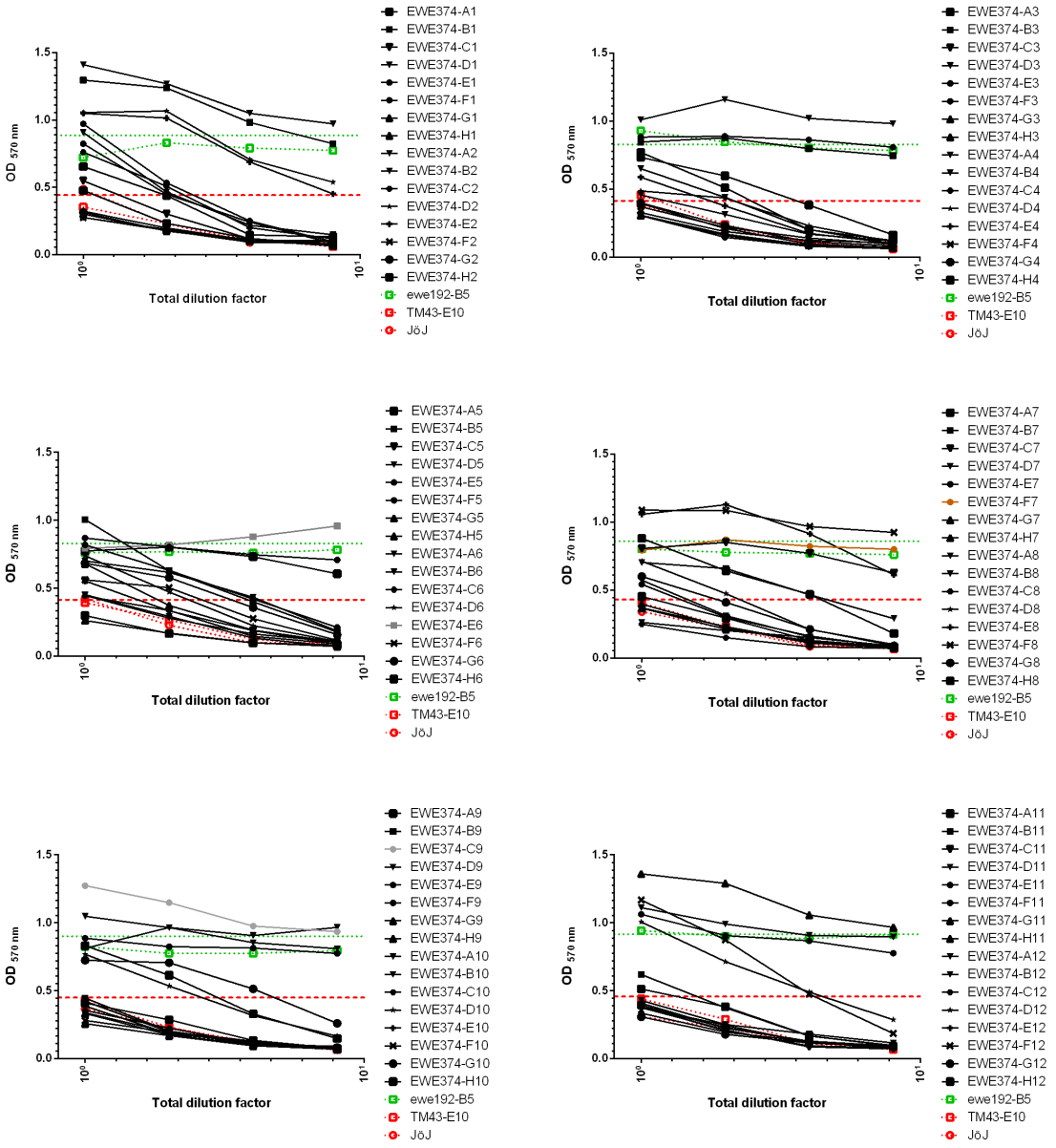

Figure 29: Neutralization assay of scFv-Fc in supernatant for screening. Untreated Vero cells are given as green dottet line. The threshold for neutralization is given as red dotted line (50 % of untreated Vero cells). The antibodies TM43-E10 and JöJ58B9 (red, open symbol and dotted line) are considered as negative control, ewe192-B5 (green, open symbol and dotted line) as positive control. Samples with gray or colored symbols were further analyzed, samples with black symbols not. Mitochondrial activity was measured with an MTT assay after 6 days at OD_{570nm}.

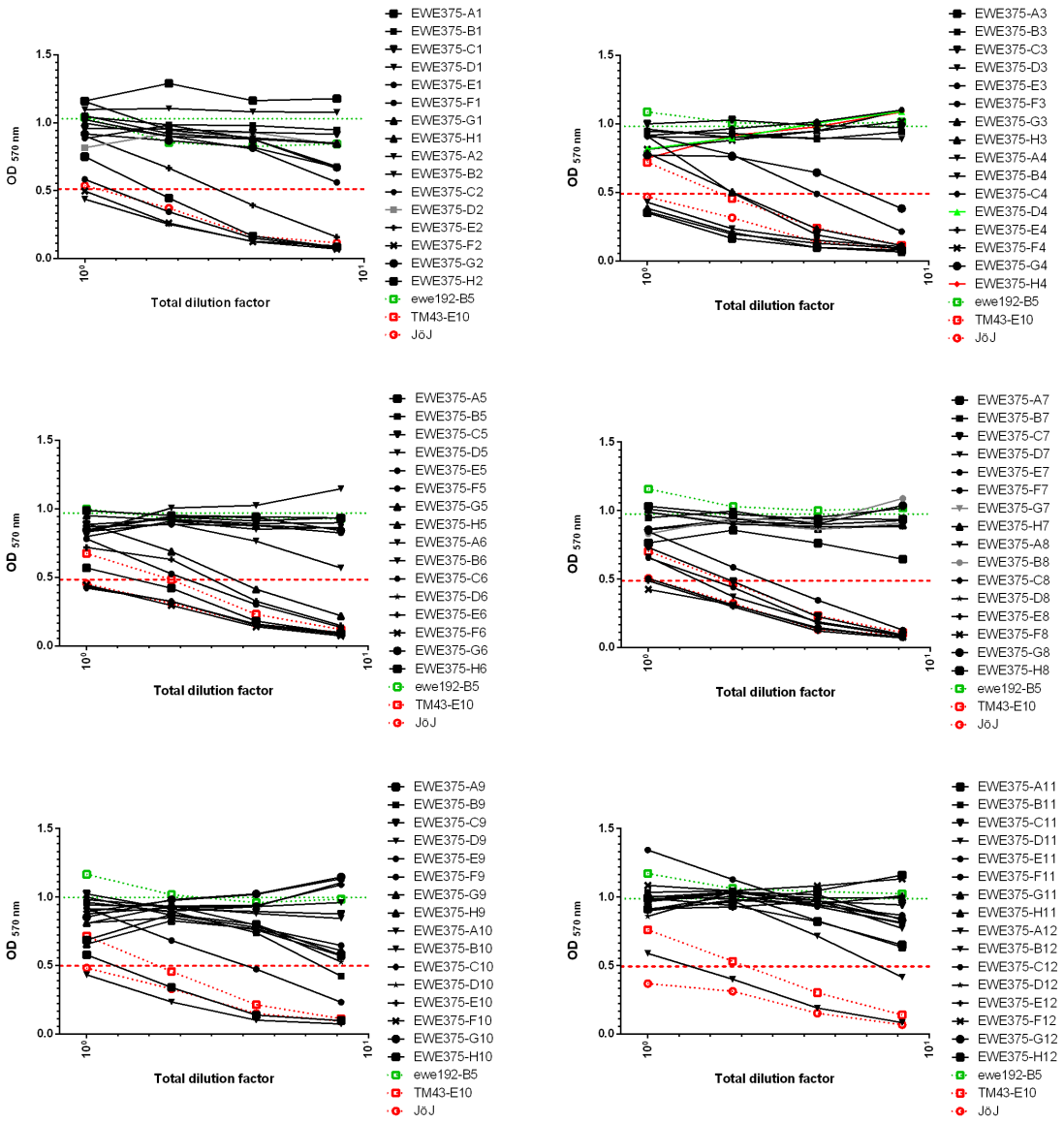

Figure 30: Neutralization assay of scFv-Fc in supernatant for screening. Untreated Vero cells are given as green dottet line. The threshold for neutralization is given as red dotted line (50 % of untreated Vero cells). The antibodies TM43-E10 and JöJ58B9 (red, open symbol and dotted line) are considered as negative control, ewe192-B5 (green, open symbol and dotted line) as positive control. Samples with gray or colored symbols were further analyzed, samples with black symbols not. Mitochondrial activity was measured with an MTT assay after 6 days at OD_{570nm}.

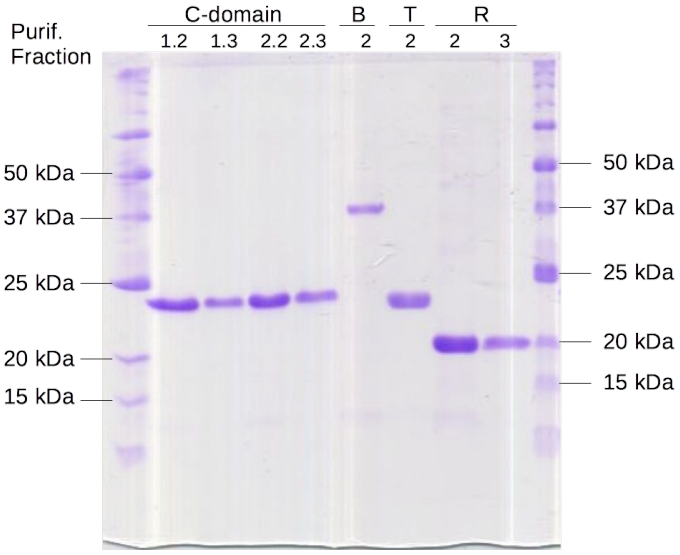

Figure 31: SDS-PAGE followed by Coomassie staining of purified domains and fragments of diphtheria toxin produced in BLR(DE3).

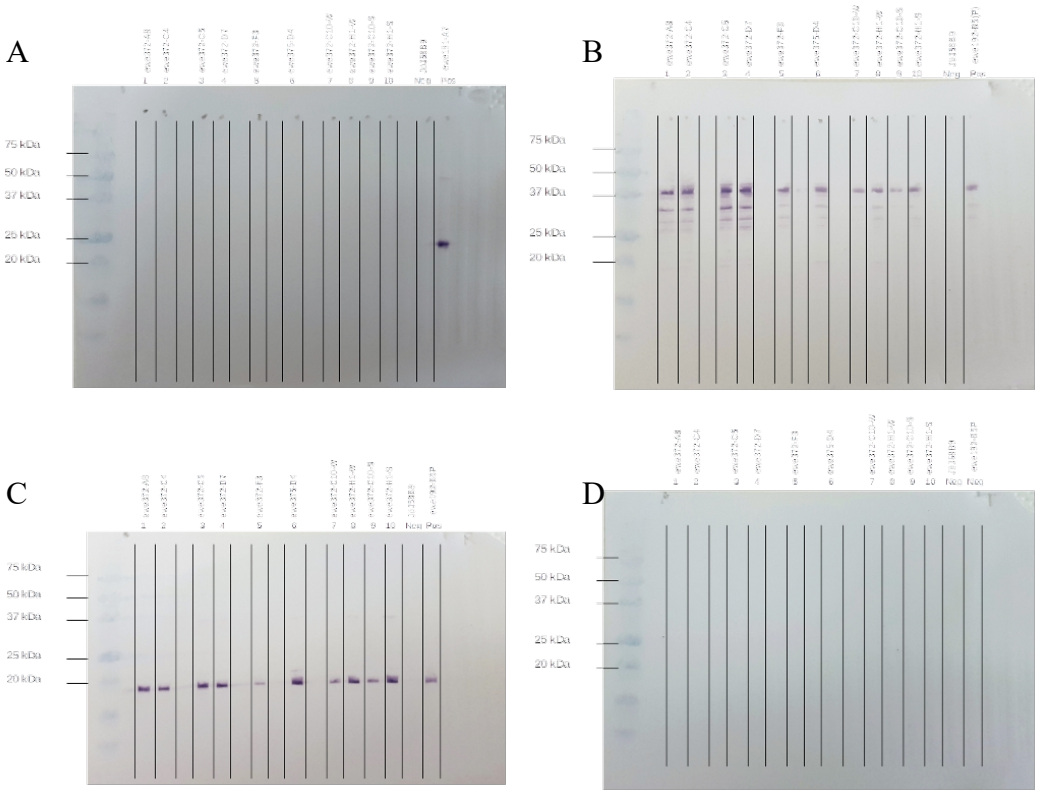

Figure 32: Western Blot after SDS-PAGE for domain mapping of scFv-Fc antibodies derived from panning with antigen in solution. All scFv-Fc antibodies are tested on fragments and domains of diphtheria toxin: A-fragment (A), B-fragment (B), R-domain (C) and T-domain (D).

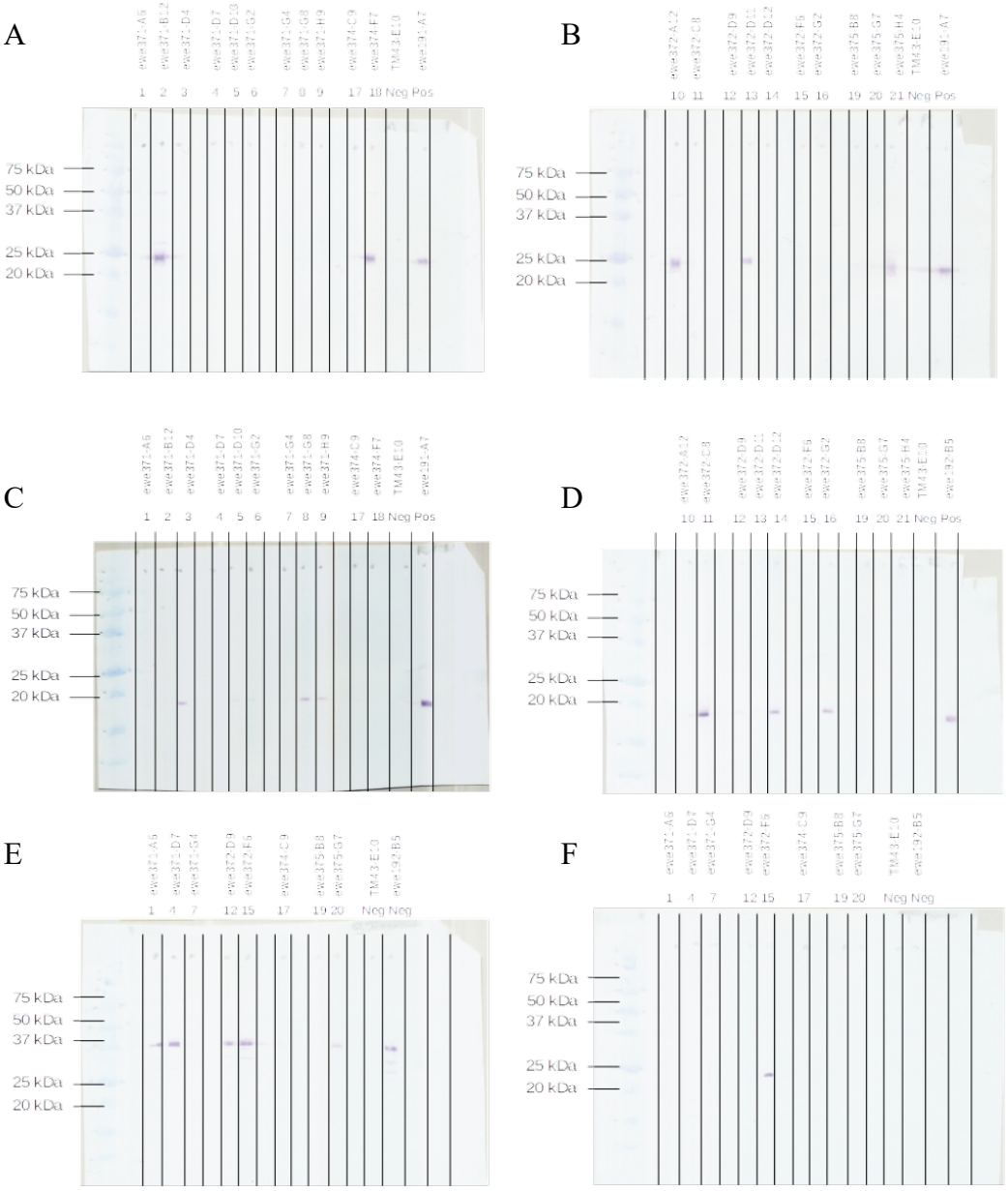

Figure 33: Western Blot after SDS-PAGE for domain mapping of scFv-Fc antibodies derived from panning with antigen in solution. All scFv-Fc antibodies are tested on fragments and domains of diphtheria toxin: A-fragment (A and B) and R-domain (C & D), B-fragment (E) and T-domain (F).

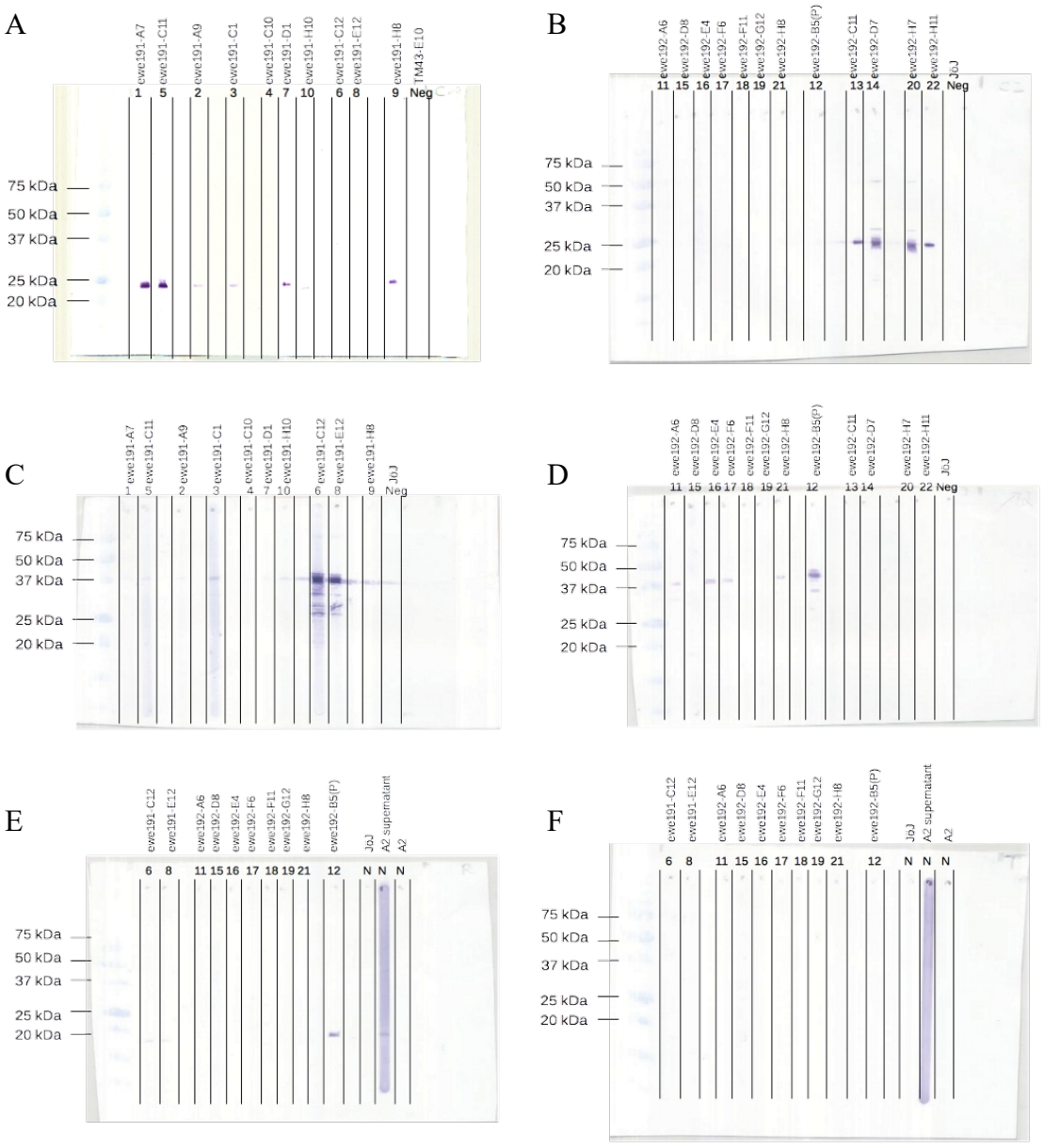

Figure 34: Western Blot after SDS-PAGE and immunostain for domain mapping of scFv-Fc antibodies derived from panning with immobilized antigen. All scFv-Fc antibodies are tested on the two fragments of diphtheria toxin: A-fragment (A and B) and B-fragment (C & D). The antibodies with positive reaction against B-fragment are further tested on the R-domain (E) and T-domain (F).

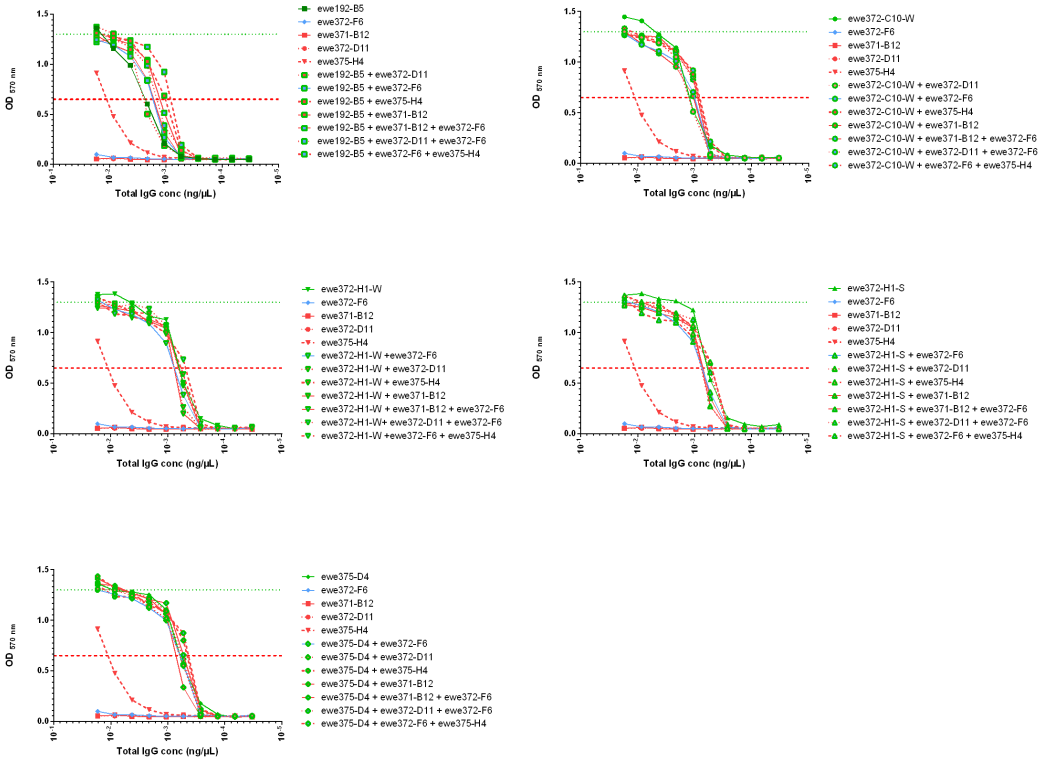

Figure 35: Cell-based combination, neutralization assay of IgG antibodies. Untreated Vero cells are given as green dotted line. The threshold for neutralization is given as red dotted line (50% of untreated Vero cells). Single antibodies are given in a single color (full symbol, solid line), combinations of antibodies are given in the colors the domain is binding against (red = C-doamin, green = R-domain and blue = T-domain; filling of symbol and color of line variates). Mitochondrial activity was measured with an MTT assay after 6 days at OD_{570nm}.

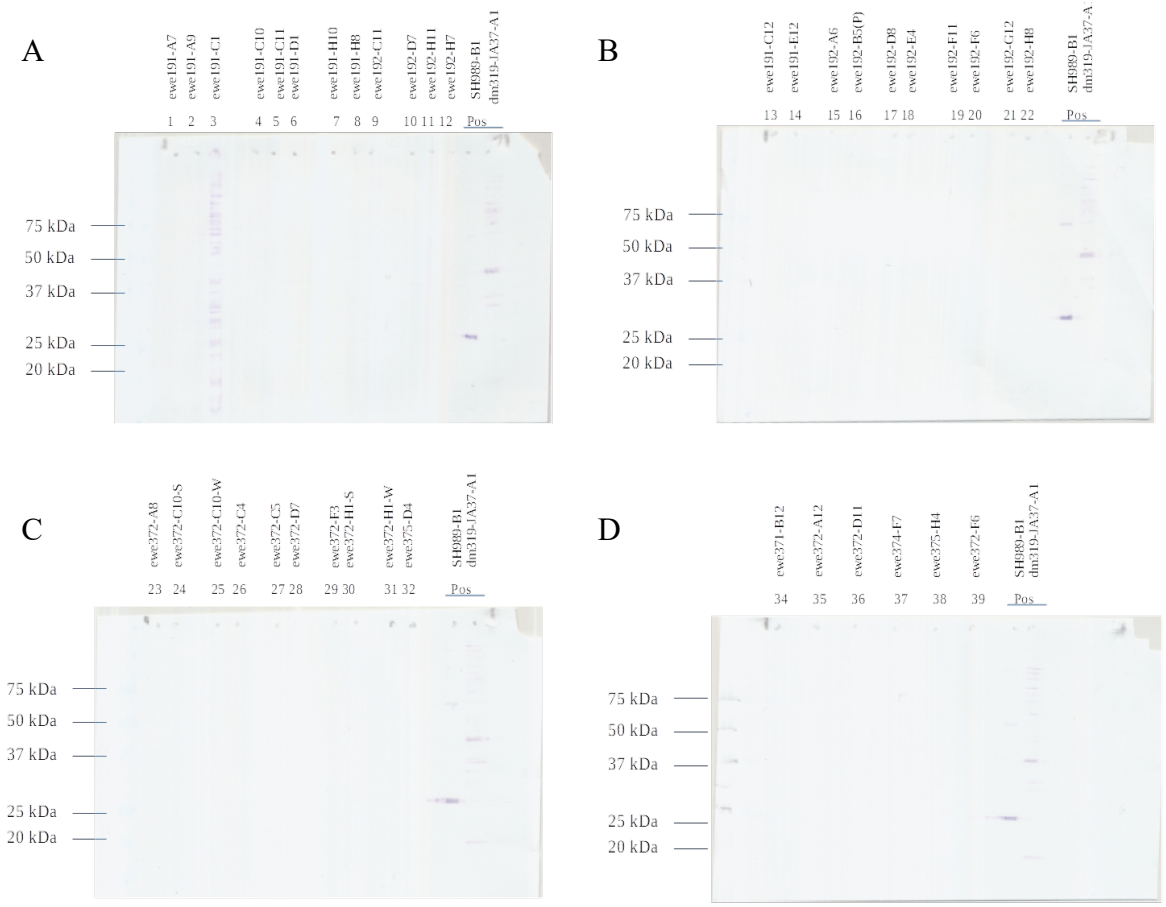

Figure 36: Specificity Immuno Blot. Western blot after SDS-PAGE of EXPI293F cell lysate and stained with DT neutralizing IgG antibodies. Detection with goat α-human Fc secondary antibody conjugated with AP and colored with AP substrate + NBT/BCIP.